# The Bedford Catchments. An Introduction to their Physical and Hydrological Characteristics

**Denis A. Hughes and Karim Sami**

**WRC Report No.235/2/93**

# THE BEDFORD CATCHMENTS. An Introduction to their Physical and Hydrological Characteristics.

**Final report to the Water Research Commission for the project :**

**"Hydrological Modelling Studies in the Eastern Cape".**

**by the**

**Institute for Water Research**
**Rhodes University**
**Grahamstown, South Africa**

**Denis A. Hughes and Karim Sami**

**November 1993**

IWR Report No. 1/93
WRC Report No. 235/2/93
ISBN

**TABLE OF CONTENTS**

**LIST OF FIGURES**

## LIST OF TABLES

## ACKNOWLEDGEMENTS

The authors would like to thank their colleagues in the Institute for Water Research for their assistance and support during the work undertaken for this report. Dr John Herald played a major role in the initial selection of the Bedford catchments and the design of the basic hydrometeorological gauging network. He is also to be thanked, together with Mr Colin Hobson of the Department of Geography at Rhodes, for advice on several aspects of GIS. Ms Anne Beater and Ms Merryl Pearce both worked as Junior Research Officers on the project and made valuable contributions. Stanley Kara and John Landman, the present and former technical officers have shared the responsibility for network maintenance and other fieldwork, while the secretarial staff of the IWR and former HRU have contributed to data processing. Mr Andrew Murdoch has to be thanked for his assistance with computer programs and sorting out problems with proprietary software packages. He was also responsible for creating most of the graphs contained within the report. Ms Deidre Watkins (a Masters student in the Department of Geography) was responsible for capturing most of the GIS coverages.

The fieldwork would never have been completed without the assistance of a number of Rhodes students (many from the Department of Geography) who helped out during the vacations. Some of these students have used the information collected for undergraduate and postgraduate projects (Maclear, 1989; Kent, 1990; Engelbrecht, 1991).

We are also greatly indebted to the farming community and landowners of the Bedford area who have allowed the project staff to install instrumentation and carry out fieldwork on their property. It should be noted that, should any other group wish to carry out research in the Bedford area, they should seek permission from the landowners directly.

We would also like to thank Professors John McI Daniel and Colin Lewis, former and present heads of the Department of Geography for their support during the time that the former Hydrological Research Unit was part of that department.

The project staff are very grateful to the Department of Water Affairs personnel who were involved in the planning and implementation of the move away from the former research catchments in the Ecca valley to the Bedford catchments. The flow measurement structures were all designed and constructed by the Department of Water Affairs.

The whole project would, have course, not been possible without the funding provided to Rhodes University by the Water Research Commission. The following people comprised the Water Research Commission Steering Committee for this project and the authors would like to acknowledge their contributions to this report and the project in general. Special thanks are due to Mr Hugo Maaren for his guidance as the responsible WRC Research Manager for this project and Dr Malcolm Hensley for his contribution to defining the soil characteristics of the area.

Mr J M Bosch : FORESTEK.
Mr H C Chapman : Water Research Commission.
Dr M Hensley : Department of Agricultural Development.
Dr J J Lambourne : University of the Witwatersrand.

Prof. C A Lewis : Rhodes University.
Mr H Maaren : Water Research Commission (Chairman)
Prof. R E Schulze : University of Natal, Pietermaritzburg.
Dr A Seed : Department of Water Affairs.
Mr P J Strumpher : Department of Agriculture and Water Supply.
Mr P W Weideman : Water Research Commission.

Thanks are also due to Mr Dave Cousens, a former member of the WRC, who played a major role in establishing the Bedford catchments and getting the current project started.

# 1. INTRODUCTION

The Institute for Water Research (formerly the Hydrological Research Unit) of Rhodes University began work in the Bedford catchments in 1988. This took place as a result of the loss of the Ecca catchments as a semi-arid hydrology 'field laboratory' due to the construction of a major water scheme to supply Grahamstown and the Lower Fish River valley. The Ecca catchments had been monitored for some 15 years and it was considered necessary to replace them with an area where semi-arid hydrological processes could be studied over the long term. The initial project in the Bedford catchments was partly designed to set up a hydrometeorological network as well as to determine some of the basic physiographic characteristics of the area. It was believed that this baseline project would then establish the catchments as an area where future studies of semi-arid hydrology could take place against a background of a growing database of information.

This report covers the work that has been undertaken, and the information collected over the period of 1988 to 1992. The chapters of the report include information on the basic hydrometeorological gauging network, climate, surface and subsurface hydrology, soils, vegetation and land use, topography and drainage. An attempt has been made to cover the whole area, although in some instances at a relatively low level of detail. Where more detailed studies of some specific aspects of the hydrology or physical characteristics of the catchments have been studied this information is summarised in the report, or in more detail in the appendices. Where possible an attempt has been made to extrapolate to the whole area.

There is inevitably more detailed data available at the IWR than can be completely reported on here. This information is freely available to anyone who wishes to carry out further research in the Bedford projects and can be obtained by contacting the Director of the IWR, or the research officer in charge of the Bedford catchments. In certain cases the data are stored in a format specific to the IWR and the relevant data analysis or extraction programs are also available.

The total area covered by the catchments is about 670 km$^2$ and they are situated (figure 1.1) in the eastern Cape Province, some 150km inland from the coast and about 90km north west of Grahamstown. They lie at the foot of the Winterberg escarpment and are so called due to the location of the town of Bedford close to the northern boundary. The main river draining the catchments is the eNyara River, a tributary of the Koonap River, which is tributary to the Great Fish River.

There was very little formal information available for this area before the project began. There were the usual 1:50 000 topographic maps as well as some black and white aerial photography flown in 1976 at a similar scale. The latter was supplemented in 1990 by colour aerial photography specially flown for the project at a scale of 1:20 000. The complete aerial survey (flying and photo production) was carried out by the Department of Surveying and Mapping of Natal University, Durban. A set of black and white diapositives have also been produced to allow for future photogrammetric mapping where and when required. The only available geology map is at a scale of 1:250 000, very generalised and does not cover the whole area. During the course of the project the SIRI (Soils and Irrigation Research Institute) land type map (also 1:250 000) information became available. The following section lists the previously available hydrometeorological data and need not be referred to separately here.

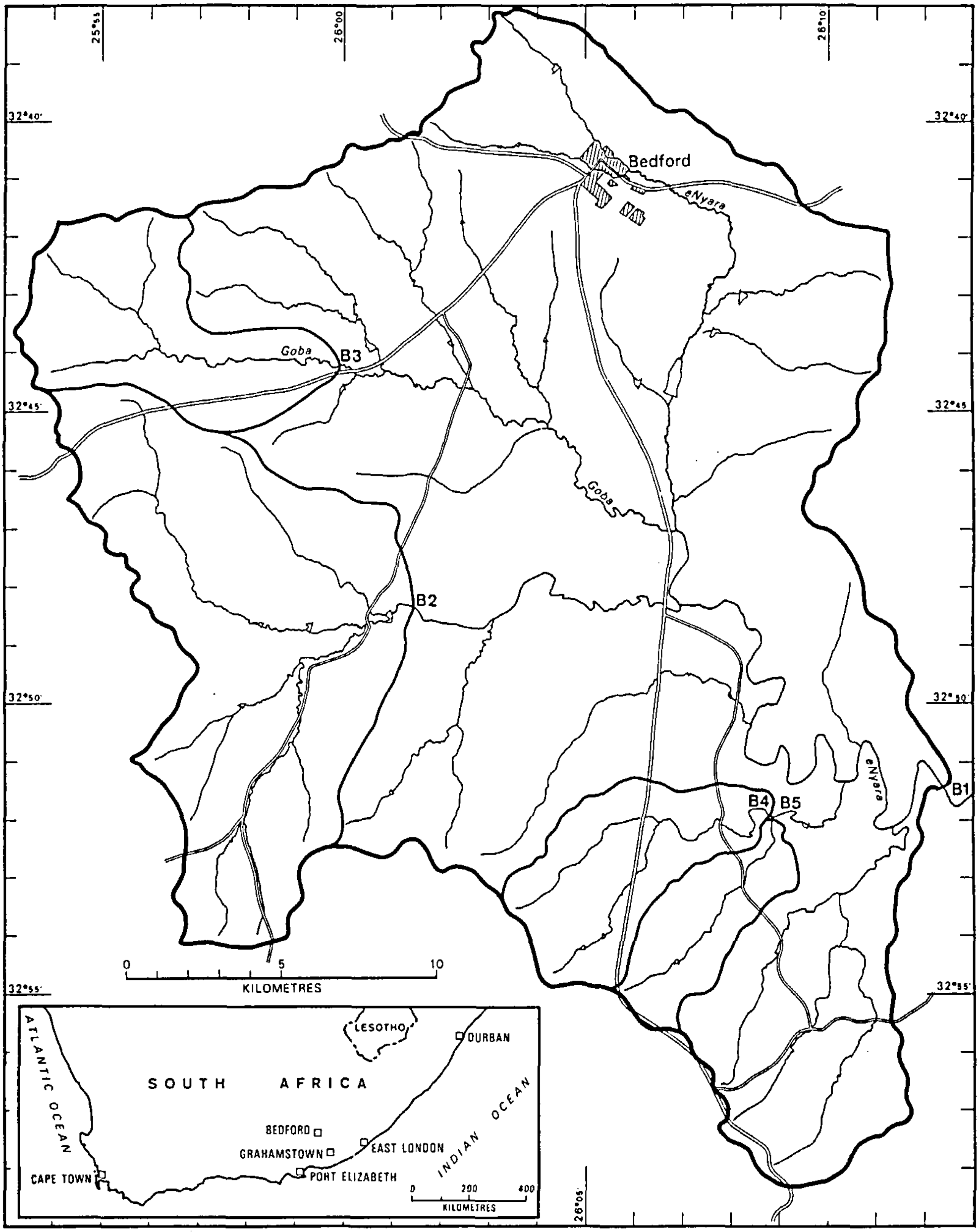


Figure 1.1 Location of the Bedford catchments.

The majority of the information contained within this report has therefore been collected since the start of the project by staff employed on the project or by students of the Department of Geography. Fieldwork has obviously played a major role in data collection and the analysis and interpretation of the data has been assisted by proprietary PC software packages (spreadsheet, database programs, etc.) as well as some software specially written by IWR staff. Some of this software has been designed for more generally applicable use than just in the Bedford catchments.

The project that was initiated to establish the Bedford catchments was also designed to develop and improve certain aspects of hydrological models. One of the areas of hydrological modelling considered to require further work was the soil moisture budgeting and groundwater recharge components of models. It was considered important to review our understanding of these processes, specifically in semi-arid environments, and attempt to develop improved algorithms for simulating them within practically applicable models.

Consequently, a large part of the fieldwork programme that the IWR has carried out within the Bedford area over the period 1989 to 1993 has concentrated on these aspects. Inevitably, the degree to which a better understanding of any hydrological process can be achieved in a semi-arid environment depends upon the number of events that occur which cause some measurable response in other processes. Typically, studies of this nature undertaken in semi-arid areas can take quite some time before enough data are collected to be able to substantiate theories or hypotheses.

Notwithstanding the above comments, the Bedford catchments have proved to be useful experimental areas for studying the following aspects of semi-arid hydrology and have contributed to the development of improved modelling approaches.

* Short term temporal and spatial distributions of rainfall amounts and intensities during different types of storms.

* Infiltration rates on different soil types and under different vegetation covers.

* Rainfall/runoff dynamics associated with soil moisture content and rainfall intensities.

* Channel transmission losses to areas of deep alluvial or colluvial material.

* Groundwater recharge processes as well as the estimation of long term average rates of recharge.

These examples are used to illustrate the nature of the hydrological research activities that can be carried out within the Bedford catchments, but are far from being the only types of research that could prove worthwhile in this area. In retrospect, the choice of this area to establish monitoring sites has been justified. The catchments are accessible, reasonably representative of large areas of semi-arid South Africa and can be used to study processes at a variety of scales.

# 2. HYDROMETEOROLOGICAL GAUGING NETWORK.

## 2.1 Raingauge network.

Prior to the involvement of the IWR in the area, the only official rainfall monitoring station was a Weather Bureau daily gauge (076/884) located at Albertvale Farm (32°00'S 26°00'E). There are now some 80 years of record available for this station. However, many of the local farmers also have records of varying length, quality and time intervals (daily, monthly or annual). Some of these have been collected and stored by the IWR as well as being passed on to the Computing Centre for Water Research (CCWR) at the University of Natal, Pietermaritzburg. In this report eight of these farm records have been used as well as one from the Bedford Municipality. Table 2.1 summarises the availability of rainfall records.

Table 2.1 Availability of rainfall records (see figure 2.2 for farm locations).

| Station name. | Lat | Long | Period of record | Data resolution | Data quality |
|---|---|---|---|---|---|
| Albertvale | 3244 | 2601 | 1904-1989 | Daily | Good |
| Bedford Mun. | 3241 | 2605 | 1972-1988 | Monthly | Unsure |
| Van Wyks Kraal | 3244 | 2556 | 1942-1988 | Daily | Unsure |
| Elizabeth Farm | 3244 | 2608 | 1932-1982 | Monthly | Unsure |
| Klipfontein (S) | 3247 | 2557 | 1933-1987 | Daily | Unsure |
| Klipfontein (N) | 3246 | 2556 | 1906-1990 | Daily | Unsure |
| Havelock Home | 3241 | 2607 | 1950-1962 | Monthly | Unsure |
| Blakesley | 3249 | 2609 | 1971-1988 | Monthly | Unsure |
| Request | 3242 | 2559 | 1916-1989 | Annual | Unsure |
| IWR Gauges 1-23 | | | 1988-now | 5 mins | Good |
| IWR Gauges 24-28 | | | 1989-now | 5 mins | Good |

The IWR initially installed 23 electronic data logging raingauges during the months of March and April 1988 and added a further 5 during October 1989. The data is collected at a minimum time resolution of 5 min and stored as breakpoint data in the IWR's database as well as being periodically passed on to the CCWR. The location of the 28 gauges is illustrated in figure 2.1. It should be noted that gauge 15 was moved some 2km east to it's present location during July 1991. While there are some gaps in the records for individual gauges, the network as a whole has operated at better than a 90% success (based on the number of gauge-days of completely recorded data) rate since it was started.

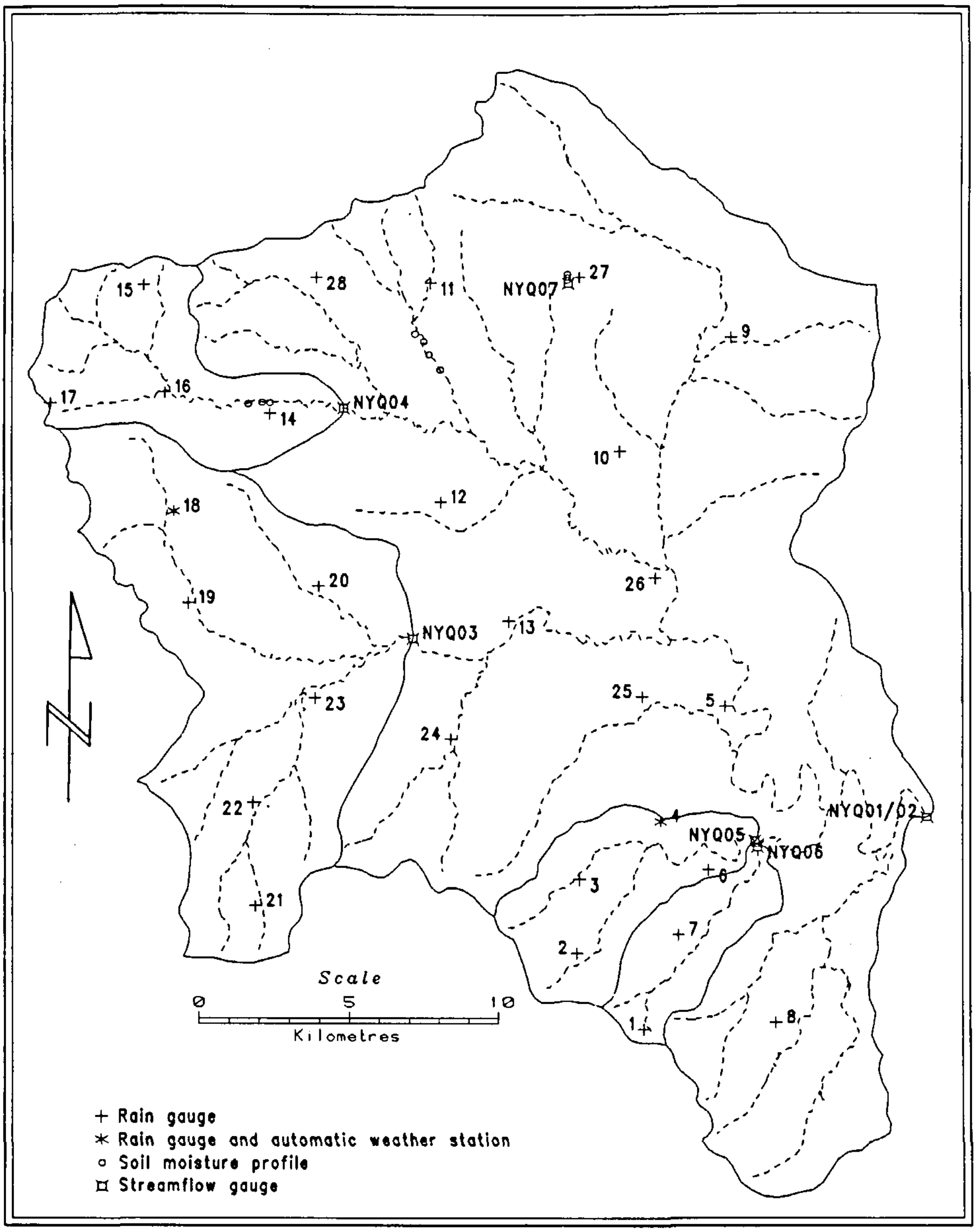


Figure 2.1 Instrumentation in the Bedford catchments.

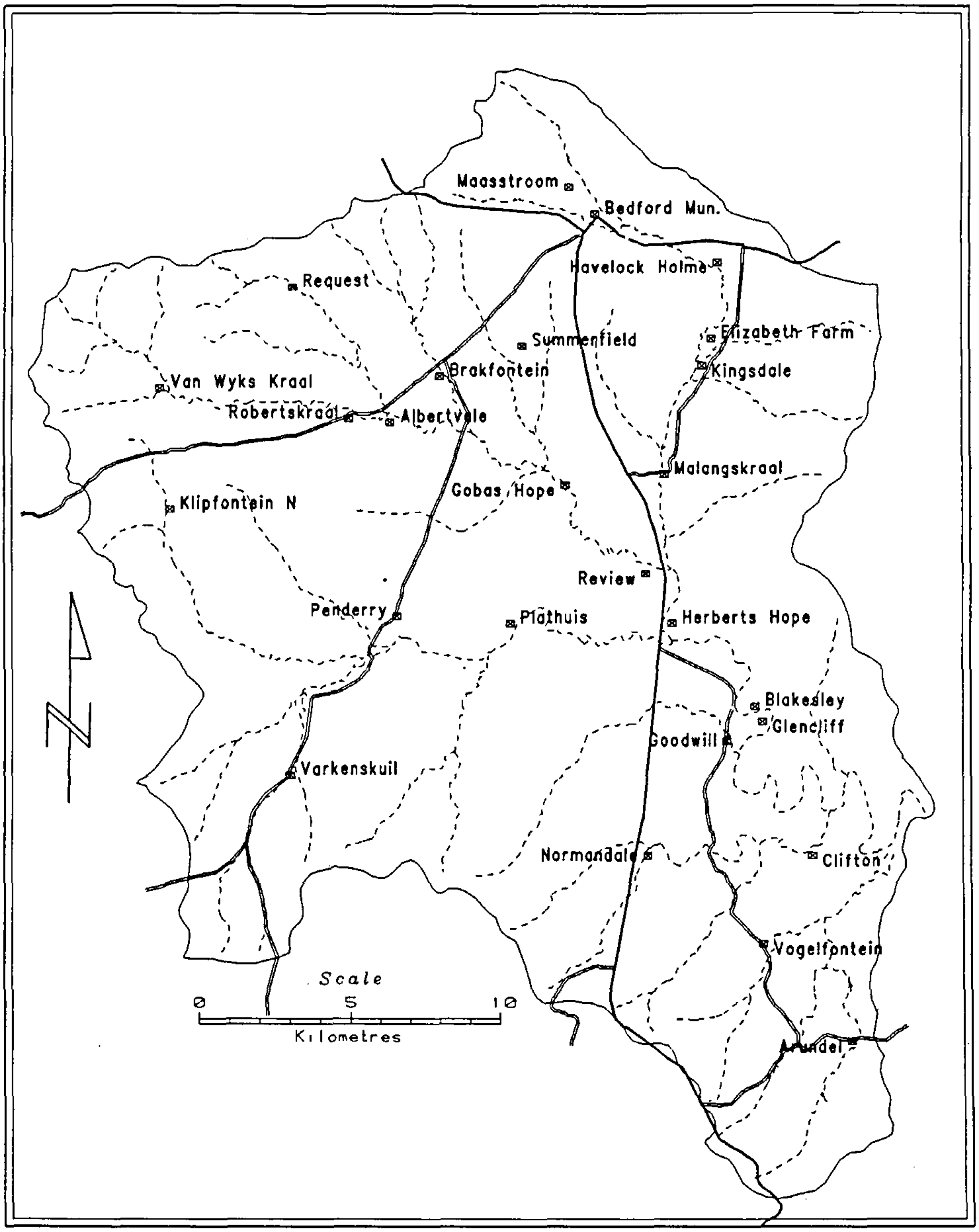


Figure 2.2 Location of farms in the Bedford catchments.

## 2.2 Streamflow gauging network.

Five flat-vee Crump weirs were constructed by Water Affairs during 1988 and electronic data logging water level recorders installed soon after (figure 2.1). They are located at the outlet of the total catchment as well as four sub-catchments of varying size. A further streamflow monitoring gauge was installed on a small first order catchment during January 1991. This consists of an H-flume constructed by the IWR and is also monitored by an electronic water level recorder. Table 2.2 lists the gauge numbers, gauging structure type, upstream catchment area and structure capacity for the six sites.

Table 2.2 Details of the gauging structures in the Bedford catchments.

| Catchment | Catchment area ($km^2$) | Recording station | Structure type | Capacity ($m^3 s^{-1}$) |
|---|---|---|---|---|
| B1 | 656.6 | NYQ01 | Flat-V Crump | 69.8 |
| B1 | 656.6 | NYQ02 | Downstream level | 69.8 |
| B2 | 111.8 | NYQ03 | Flat-V Crump | 33.5 |
| B3 | 40.3 | NYQ04 | Flat-V Crump | 17.8 |
| B4 | 31.1 | NYQ05 | Flat-V Crump | 35.5 |
| B5 | 17.7 | NYQ06 | Flat-V Crump | 32.9 |
| B6 | 0.18 | NYQ07 | H-Flume | 0.86 |

The water level data are recorded using a level change threshold procedure and are stored as breakpoint values in the IWR's database. The IWR have experienced a number of problems with the recording instruments which have been difficult to isolate due to the infrequency of flow events. Consequently, of the few events that have occurred during the period of observation, not all of them have been completely recorded.

## 2.3 Automatic Weather Station network.

Two automatic weather stations were installed during late 1988 (figure 2.1). The sensors attached are three temperature sensors (2 air and 1 soil), one relative humidity sensor, wind speed and direction sensors, two soil moisture sensors (nylon blocks) and a solar radiation sensor. The data are recorded at 1 hour intervals and stored on the IWR's database.

Power supply problems experienced during their operation means that the records are not complete for the whole period. In addition major problems have been experienced with the soil moisture sensors as well as the relative humidity sensor, such that all the data from these is of very limited value.

**2.4 Groundwater monitoring network.**

As most of the catchment is dependent on groundwater for household, stock watering and irrigation purposes, a large number of boreholes are present. Interviews with the farmers during 1988/89 provided some approximate information on rest water levels and yields for 282 of the existing boreholes in the catchment. In addition, water levels in 6 boreholes have been monitored monthly since mid-1989. Four more boreholes have been monitored since mid-1990, and an additional 10 boreholes were added to the monthly survey in 1991. Further borehole logging is severely hampered by the presence of windmills or monopumps which deny access to boreholes.

Groundwater dissolved salt concentrations are monitored from actively pumping boreholes. Cation concentrations are obtained using atomic absorbtion spectrophotometry, while anion concentrations are determined by titration methods. All analyses are performed by the IWR staff. Twenty-seven boreholes were sampled intensively on a monthly basis, of which 10 continue to be sampled. An additional 43 boreholes have been tested at infrequent intervals in order to obtain a more detailed survey of spatial water quality variations. Selected samples have also been sent to the CSIR in Pretoria for isotopic analysis (deuterium and oxygen-18). The location of these boreholes is shown in figure 2.4.

**2.5 Soil moisture content network.**

Three groups (figure 2.1) of neutron probe access tubes were established during 1989, two situated in the soils and alluvial material of valley bottoms and one in the small gauged first order sub-catchment (B6) referred to in section 2.2. The depths of the access tube holes varies from close to 0.3m (on the slopes of the first order catchment) to over 5.0m (in the deeper alluvial deposits) and neutron probe readings are taken at depths of 0.15, 0.3, 0.5, 0.75, 1.0, 1.5 and 2.0m and thereafter at 1m intervals where possible. The access tube sites are routinely visited twice a month, but more frequent readings are taken when the rate of change of moisture status is perceived to warrant the extra visits.

The first site (tubes NYN01/1 - NYN03/4) is situated on the farm Van Wyks Kraal and consists of at least four tubes in each of three valley floor cross-sections (Hughes and Sami, 1991). The maximum depth of the alluvial material here is in excess of 6.0m, while the tubes only extend down to just over 5.0m (table 2.3). The second (tubes NYN04/1 to NYN07/4) is on the farm Brakfontein and consists of four tubes in each of five valley floor cross-sections. The alluvial material at this site tends to be somewhat shallower than the first site and the tubes extend to it's base. The third site (tubes NYN08/1 to NYN10/4) consists of three sections across the lower, middle and upper parts of the whole sub-catchment. The valley bottom soils are up to 2.0m deep, while the slope soils vary from very shallow to little over 0.5m deep.

During the installation of the tubes a reasonably wide range of moisture conditions were encountered. This meant that the neutron probe calibration data could be collected at the same time (through measurement of bulk density and gravimetric analysis of samples at the different depths) as the tubes were installed. An attempt to calibrate the probe separately for different soil textures or depths did not prove to be statistically significant and consequently a single calibration equation is used for all samples (figure 2.3).

Table 2.3 Depths of the neutron probe access tubes in the Bedford catchments.

| Site | Tube depth in metres | | | | | |
|---|---|---|---|---|---|---|
| | 1 | 2 | 3 | 4 | 5 | 6 |
| NYN01 | 5.8 | 5.0 | 5.0 | 2.5 | | |
| NYN02 | 1.0 | 2.5 | 2.9 | 0.9 | 5.9 | 1.0 |
| NYN03 | 1.9 | 4.4 | 5.9 | 2.5 | | |
| NYN04 | 1.9 | 1.5 | 2.0 | 2.5 | | |
| NYN05 | 2.0 | 2.5 | 2.0 | 1.0 | | |
| NYN06 | 2.0 | 1.0 | 1.5 | 2.5 | | |
| NYN07 | 1.5 | 2.0 | 2.5 | 2.5 | | |
| NYN08 | 0.3 | 0.3 | 1.5 | 0.5 | | |
| NYN09 | 0.5 | 0.5 | 1.0 | 0.7 | | |
| NYN10 | 0.3 | 2.0 | 1.5 | 1.5 | 0.5 | |

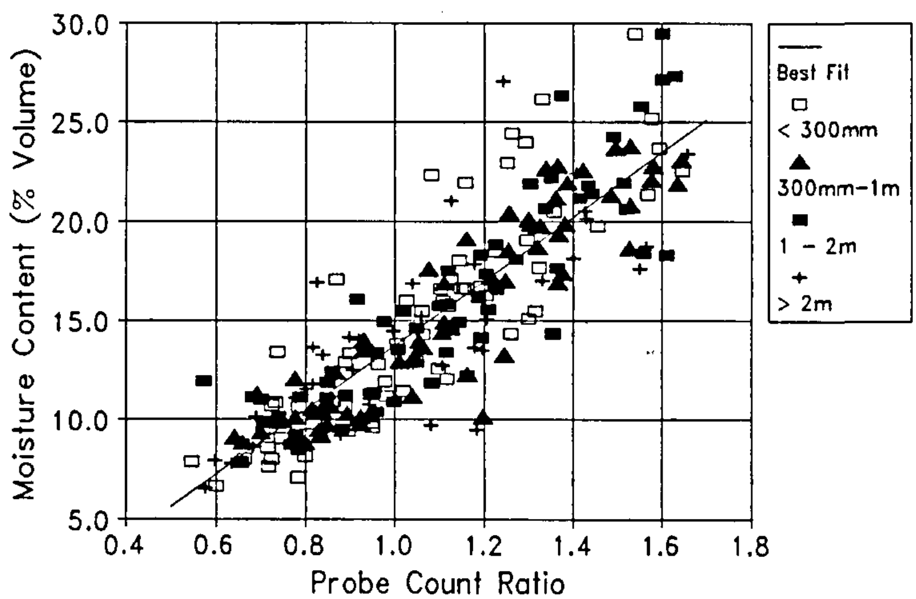


Figure 2.3 Neutron probe calibration data.

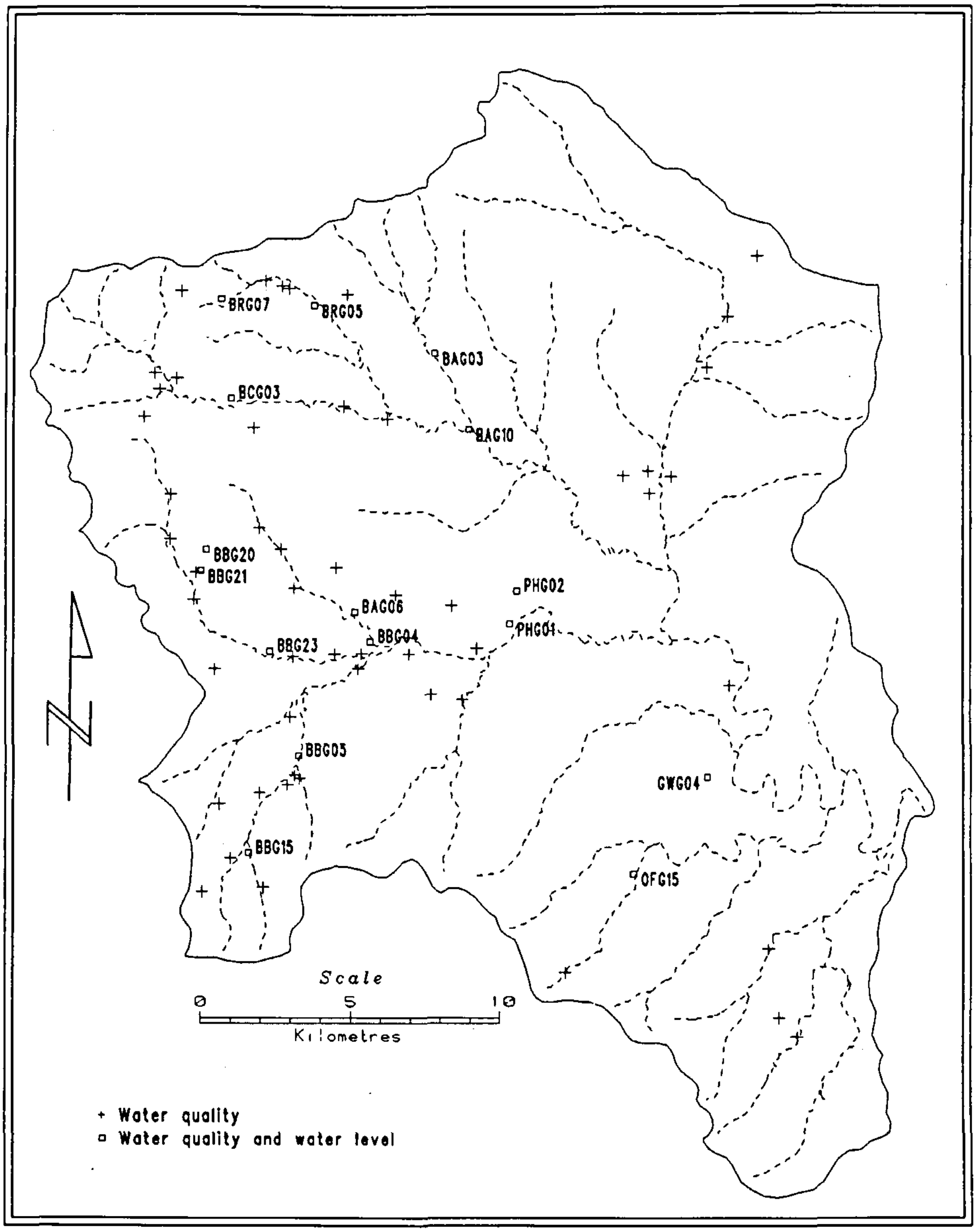


Figure 2.4 Location of monitored boreholes.

## 3. CLIMATE.

The climate data in this section include information on temperature, radiation, wind speed and direction and rainfall. There are no evaporation measurement stations in the immediate vicinity and anyone requiring such information will have to consult alternative sources (such as national data banks on regional pan evaporation estimates).

### 3.1 Temperature.

The data used to describe the general climatic conditions prevailing over the area are drawn from one of the IWR's weather stations (NYW02), for which approximately two years of data are available. It is difficult to make any statements about the representativeness of these records as there are no others for comparison purposes.

Figure 3.1 illustrates the annual air and soil (depth of 0.2m) temperature regimes based on data collected from August 1989 to July 1992. The figures for the July data are based on only several days of data and should be treated with some caution. The same problem applies to the solar radiation figure for July (figure 3.2).

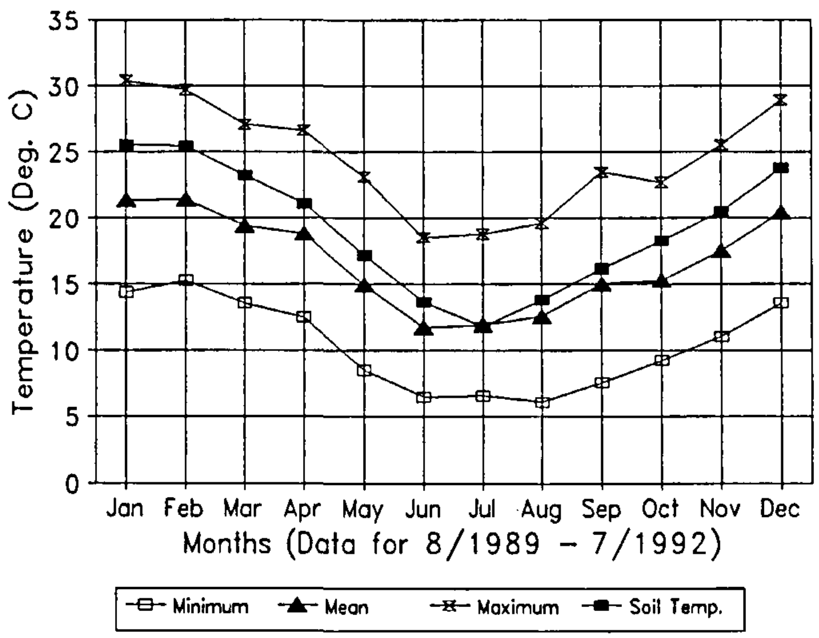


Figure 3.1 Seasonal distribution of monthly mean daily temperature characteristics.

### 3.2 Wind patterns.

The available wind direction data have been plotted as 'direction vectors' based upon a mean hourly wind speed (km $hr^{-1}$) weighting of mean hourly recorded directions. This method of calculating an index of wind direction favours the directions when the wind speed is greater and is designed to offset the influence of light winds when the vane may lie in any direction.

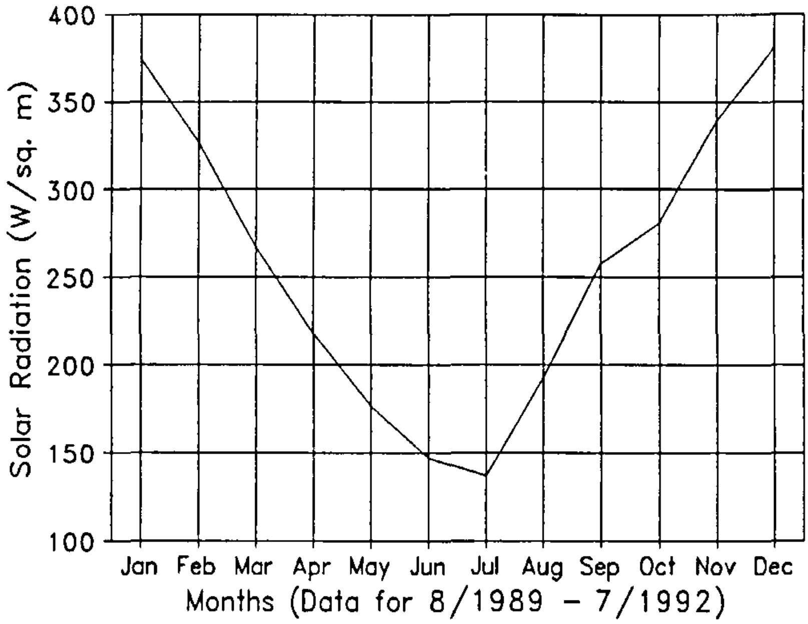


Figure 3.2 Seasonal distribution of mean total daily solar radiation.

Figures 3.3 to 3.6 illustrate the percentage of each month when the hourly wind vector lay in eight direction groups. The data for July should be treated with caution as they are based on relatively few observations. The summer months seem to be dominated by westerly winds and the winter months by easterly winds. October, November and March appear to group closely with the summer months, while May is more typical of winter. April and September seem therefore to be the only transitional months where the spread of wind direction vector is more even over all directions.

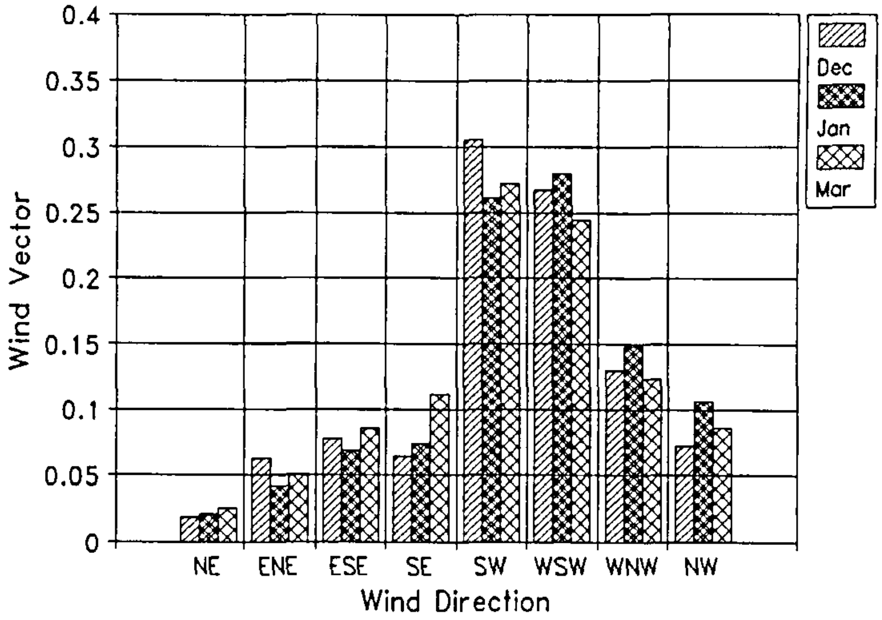


Figure 3.3 Wind direction vectors for Summer.

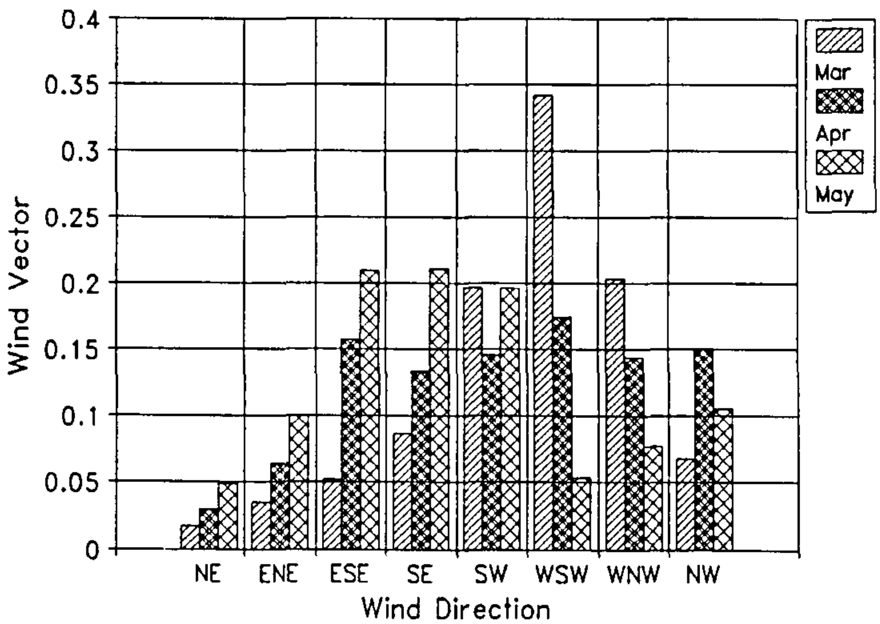


Figure 3.4 Wind direction vectors for Autumn.

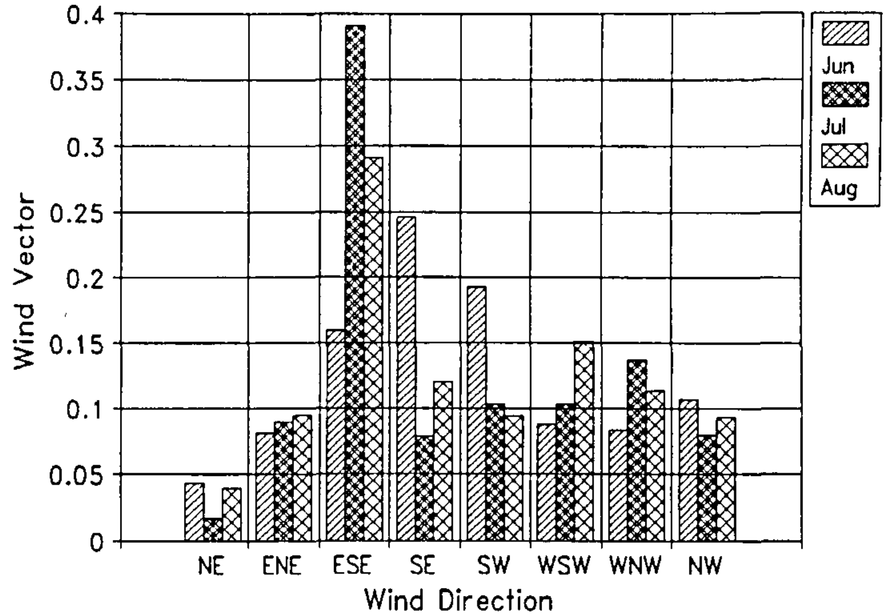


Figure 3.5 Wind direction vectors for Winter.

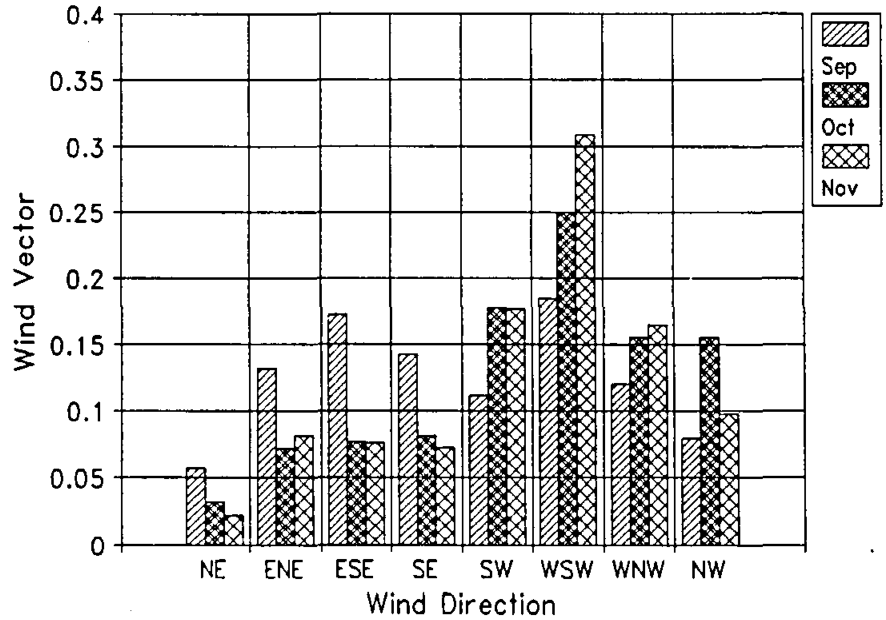


Figure 3.6 Wind direction vectors for Spring.

## 3.3 Rainfall.

### 3.3.1 Annual and Seasonal.

Time series plots of annual rainfall totals for Albertvale and several other stations are given in figures 3.7 to 3.9. These demonstrate the high degree of variability in the annual series, which is typical of the semi-arid areas of South Africa. It is difficult to visualise any trend in this data as the dominant pattern is one of large fluctuations from one year to the next (see 1949 to 1954 for example). Table 3.1 lists the mean annual rainfall (and standard deviations) for all the relatively long record stations available at present (i.e. excluding the IWR stations). It is apparent that the biggest difference is between the Bedford station (located immediately against the escarpment) and the others in the catchment.

This feature is also clearly demonstrated by figures 3.10 to 3.12 which illustrate the mean monthly distributions for eight stations. The small differences between all the stations except Bedford are difficult to attribute to real spatial differences due to the unknown accuracy of the data and the fact that the data are based on different lengths of record. However, there is a suggestion of a trend of decreasing rain away from the northern and western edges of the catchment (Van Wyks Kraal does not fit this trend). The variability of monthly rainfalls is illustrated in figure 3.13 for stations Bedford and Albertvale (both quite long records). There is a clear seasonal pattern of lowest rainfall in the winter months and the highest in the late summer months of February and March. However, the variability of monthly rainfalls suggests that all months can experience low rainfalls at some time. This has very important implications for farming activities in the area, which predominantly rely upon the growth of natural veld from rainfall inputs. If the late summer rain period is below average, the condition of the veld is inadequate for stock feeding over winter.

Table 3.1 Mean annual rainfall characteristics (see table 2.1 for record lengths).

| Station | Mean Annual rainfall (mm) | St. Dev. of Annual rainfalls (mm) |
|---|---|---|
| Albertvale | 469.6 | 120.7 |
| Bedford Mun. | 669.9 | 162.4 |
| Van Wyks Kraal | 435.2 | 164.8 |
| Elizabeth Farm | 422.8 | 108.5 |
| Klipfontein (S) | 489.1 | 129.6 |
| Klipfontein (N) | 477.3 | 162.9 |
| Havelock Home | 480.0 | 125.0 |
| Blakesley | 435.2 | 164.8 |
| Request | 491.9 | 132.3 |

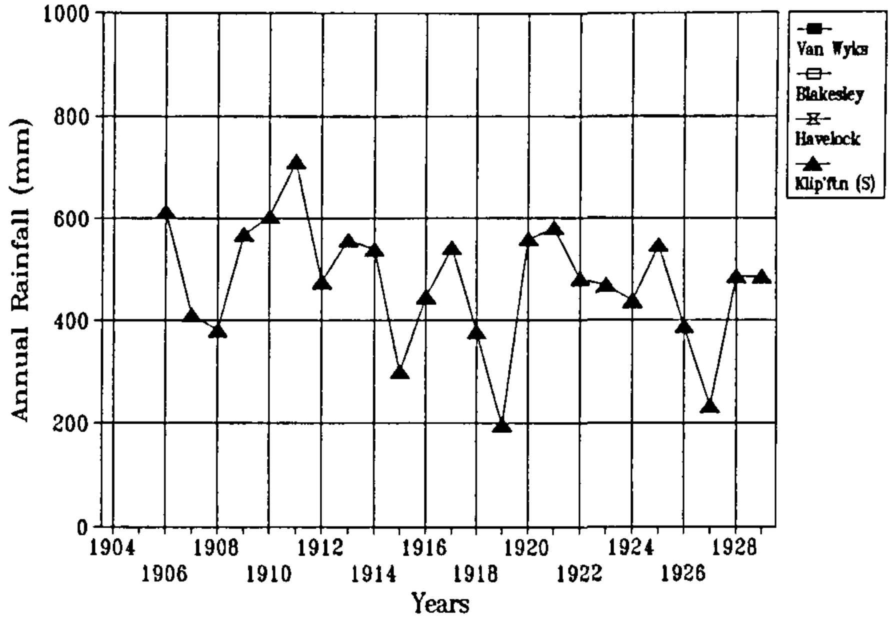


Figure 3.7a Annual rainfall totals, 1906 - 1929.

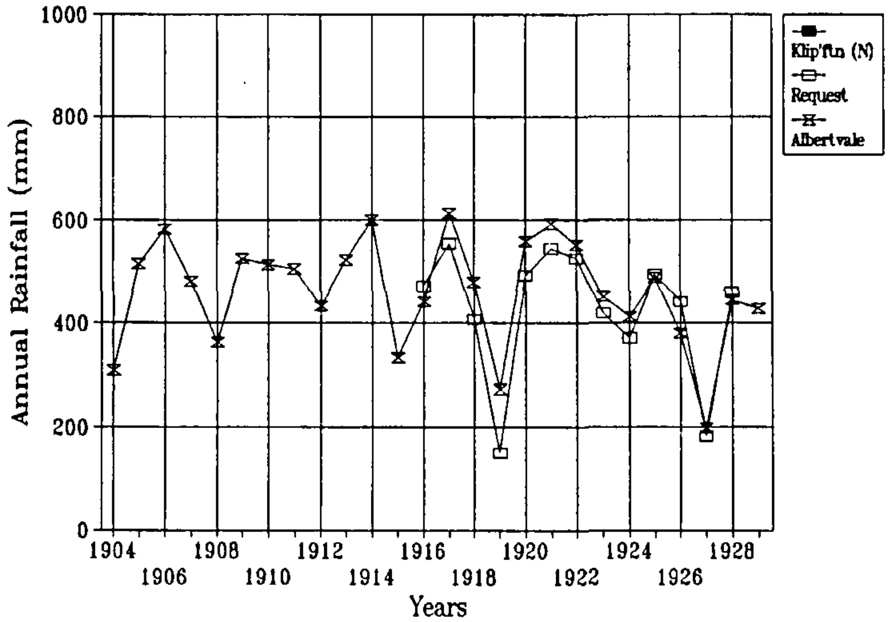


Figure 3.7b Annual rainfall totals, 1906 - 1929.

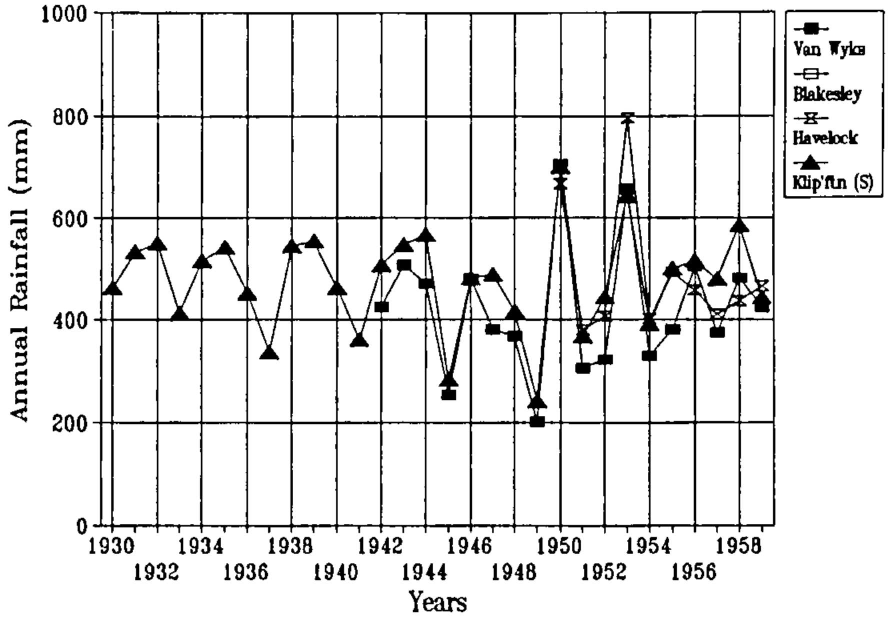


Figure 3.8a Annual rainfall totals, 1930 - 1959.

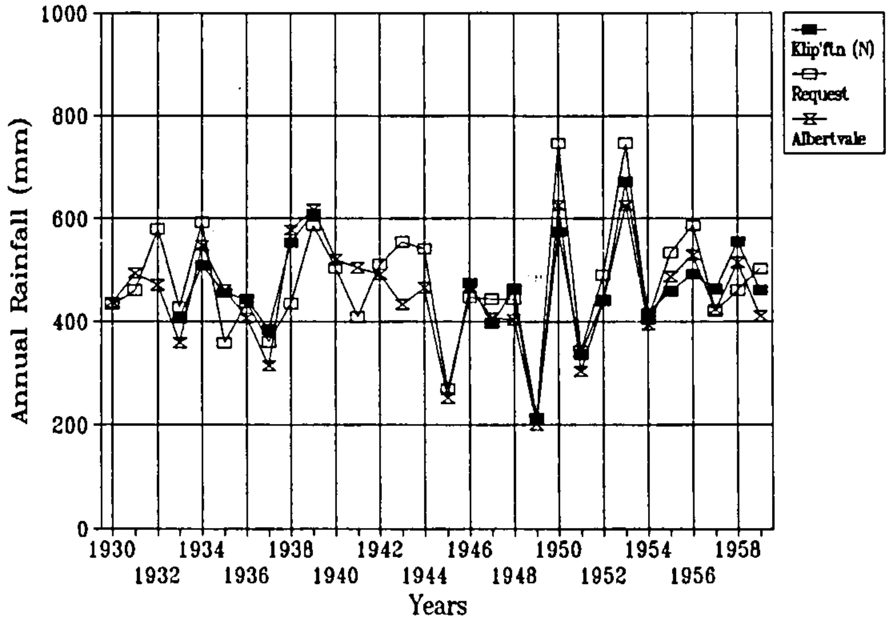


Figure 3.8b Annual rainfall totals, 1930 - 1959.

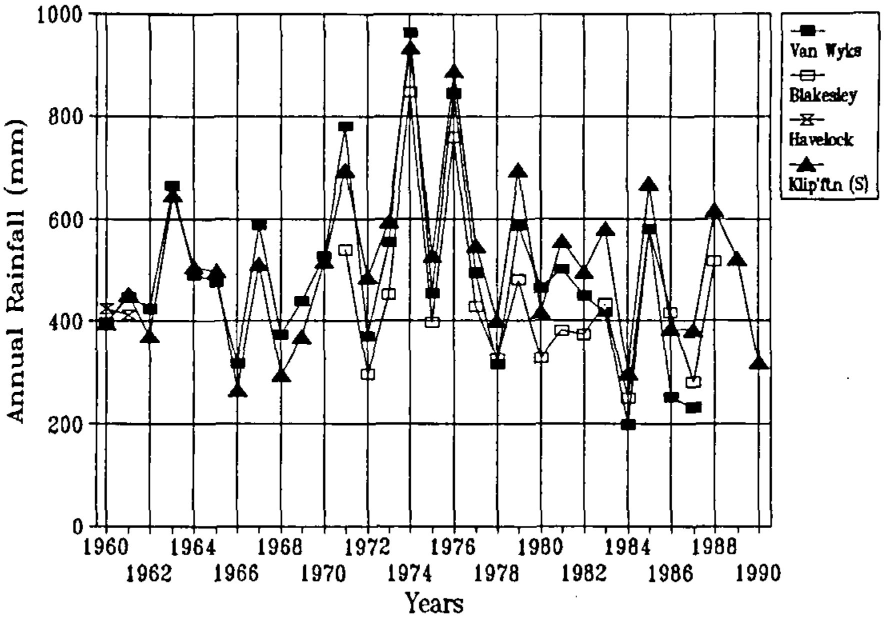


Figure 3.9a Annual rainfall totals, 1960 - 1990.

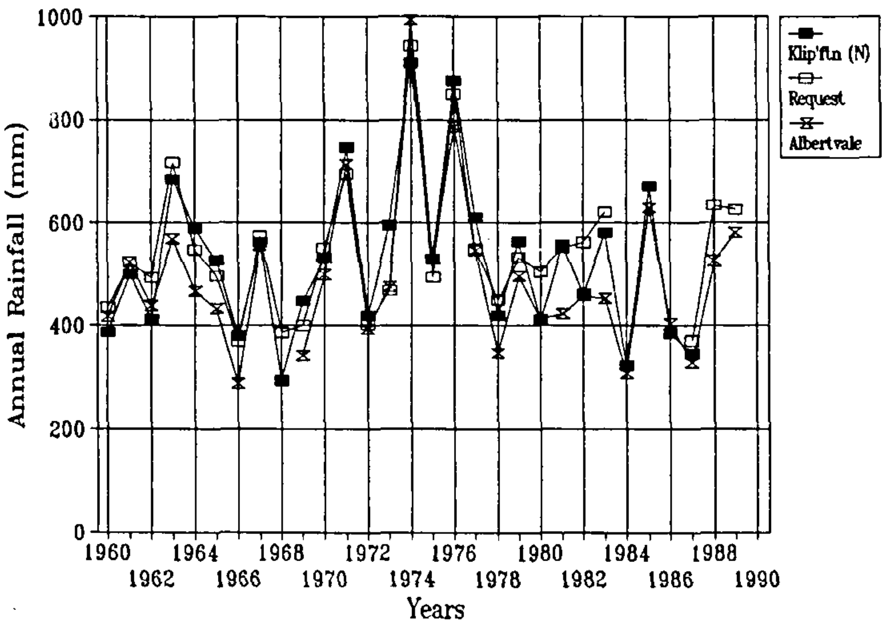


Figure 3.9b Annual rainfall totals, 1960 - 1990.

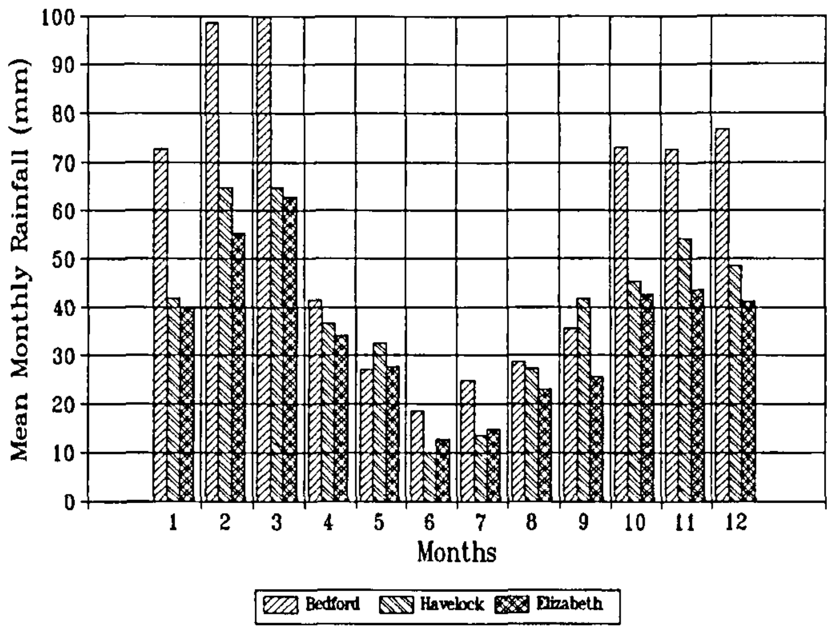


Figure 3.10 Mean monthly rainfall for stations in the north and east.

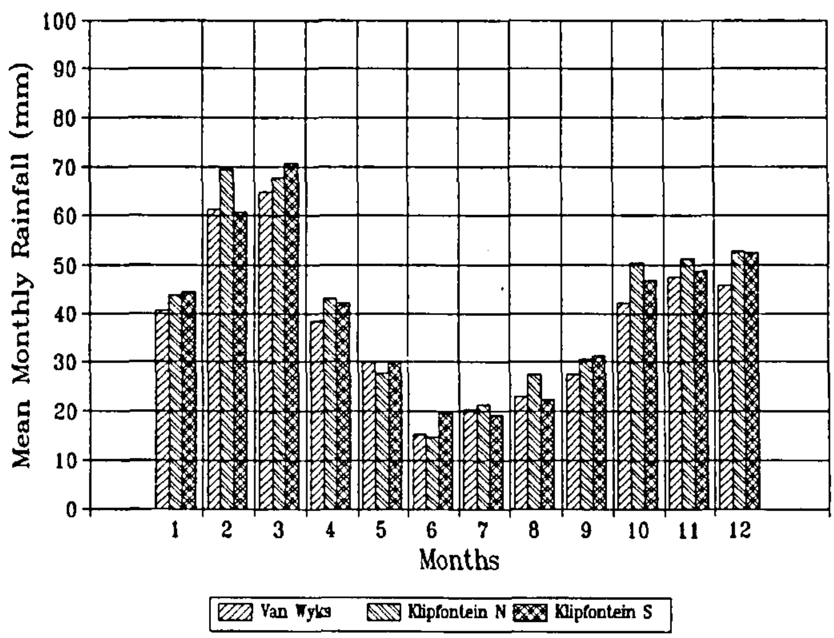


Figure 3.11 Mean monthly rainfall for stations in the west.

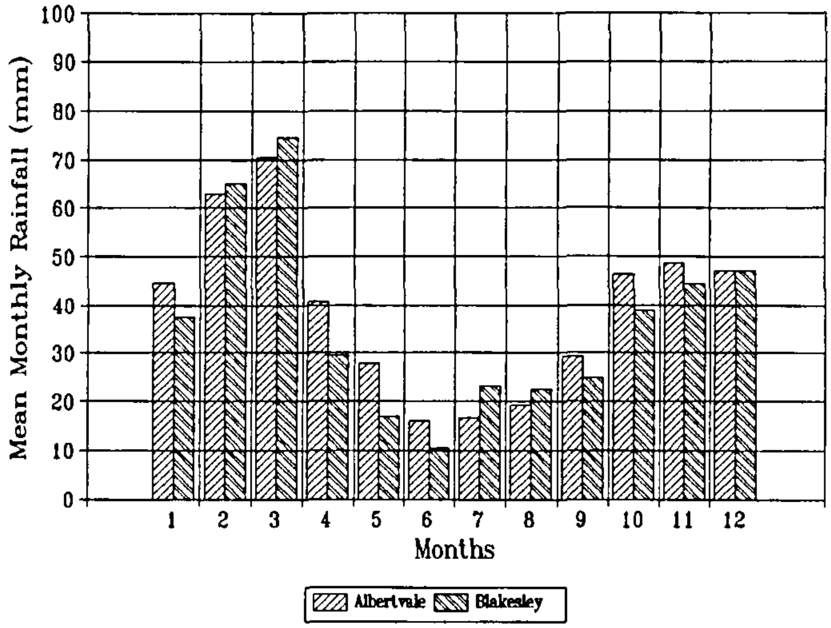


Figure 3.12 Mean monthly rainfall for Albertvale and Blakesley (south).

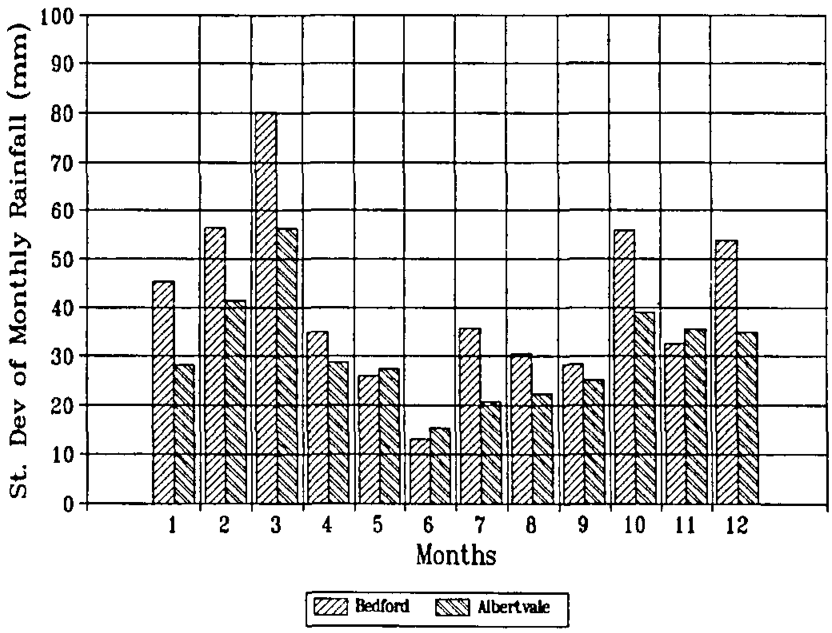


Figure 3.13 Standard deviations of monthly rainfalls for Bedford and Albertvale.

**3.3.2 Short term rainfall variations.**

Figures 3.14 to 3.19 illustrate the depth-duration-frequency relationships for rainfall in the Bedford area based on data collected over the period April 1988 to July 1991. Three stations have been used, one on the north western border (NYP15), one close to the southern border (NYP01) and one in the east central part of the catchment. The patterns for all three stations are broadly similar, with station NYP15 experiencing slightly higher rains and NYP05 slightly lower. For example, NYP15 has 124 days/year experiencing at least 0.2mm rain, while the equivalent for stations NYP01 and NYP05 are 98 and 78 days respectively. For daily rainfalls of 50mm or higher, the mean number of days/year are 0.8 for NYP15 and 0.7 for the other two stations.

The 5 min rainfall database for the 28 stations of the IWR gauge network has been used to evaluate the patterns of spatial variation in rainfall for storms occurring during different synoptic situations. Much of this work was carried out as a student project by a Geography honours student (Kent, 1990). The techniques used involved extracting rainfall for short time periods (usually 5 or 10 min) over the storm duration as well as the total storm depth and interpolating for the equivalent period rainfalls over a fixed 1 x 1 km grid. The total number of grid elements in the catchment is 672 and the interpolation method used is the inverse distance squared approach, which has been demonstrated to be a suitable method (Patrick, 1989).

The computer software generates a screen graphics image of each period within the storm and these can be saved, then recalled sequentially to obtain an impression of the concentration and movement of rain cells within a storm. Summary statistics of the spatial characteristics of the storm rainfall are also computed. Table 3.2 lists some of the mean statistics for the storms grouped into five types. Columns 5 to 7 refer to the distribution statistics for each short period within the storms and the values listed are averaged for all the periods and all the storms within the type category. The last column lists the mean number of grids (out of 672) that have a rainfall greater than 0.8 of the maximum grid rainfall value for that period.

The tabulated values indicate that there are distinct differences between the first two types and the last three. The values indicate that the cumulus (thunderstorm), and to a degree the advection, events have smaller and more concentrated cell sizes (higher coefficients of variation, skewness and kurtosis and lower number of grids > 0.8 x maximum rain). If individual storm periods are studied more closely, then the differences are even more apparent. For example, the coefficients of variation and kurtosis values for the peak intensity periods of cumulus events can exceed 3.0 and 30.0 respectively. The equivalent values for the cut-off low events are likely to be closer to 1.0 and 5.0. The differences between the other events are not always as clear.

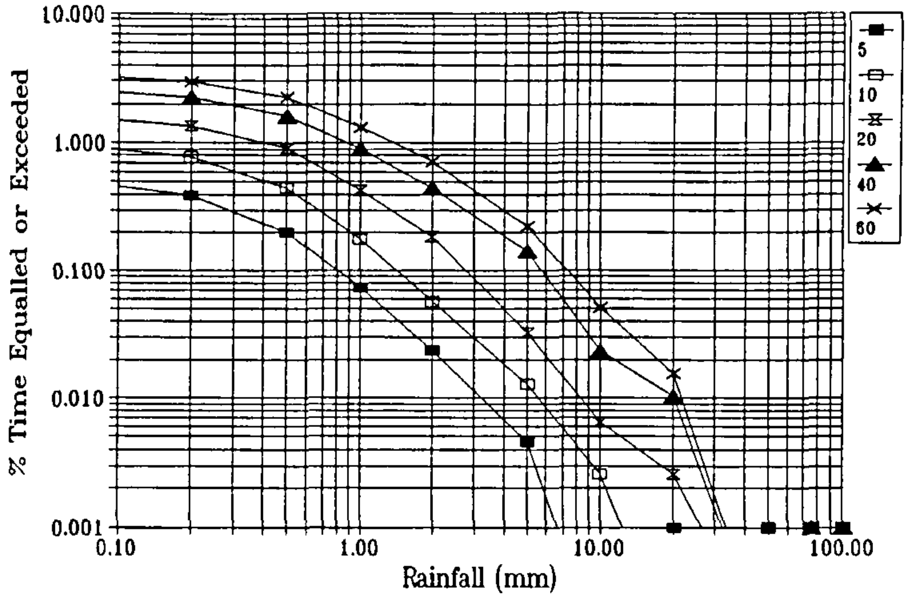


Figure 3.14 Depth-duration-frequency curves, NYP01, 5 - 60 minutes (1989 - 1991 data).

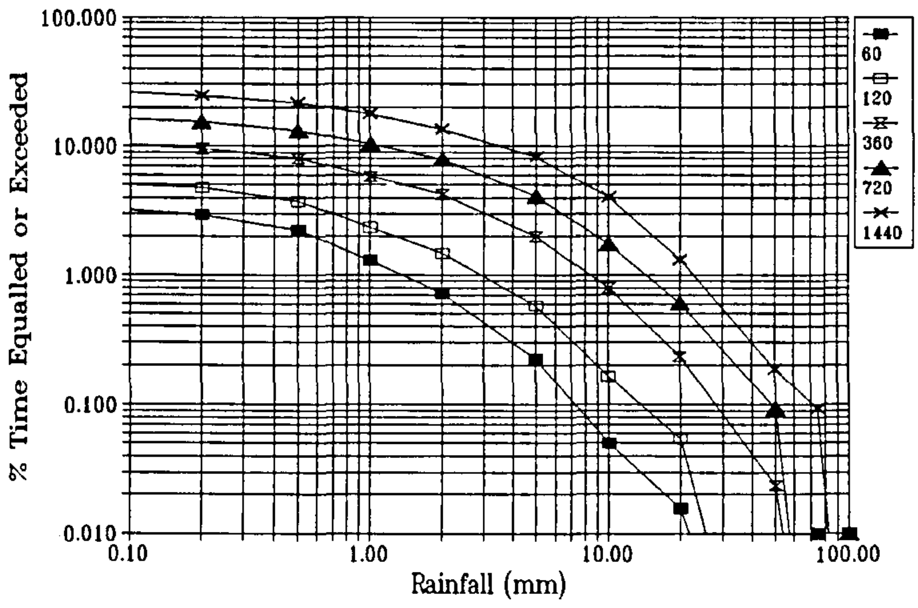


Figure 3.15 Depth-duration-frequency curves, NYP01, 1 - 24 hours (1989 - 1991 data).

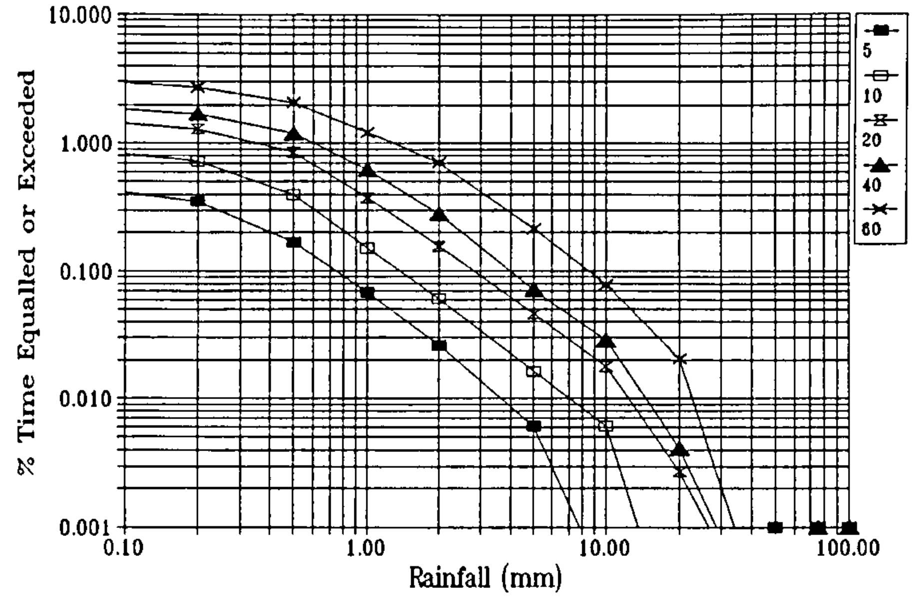


Figure 3.16 Depth-duration-frequency curves, NYP05, 5 - 60 minutes (1989 - 1991 data).

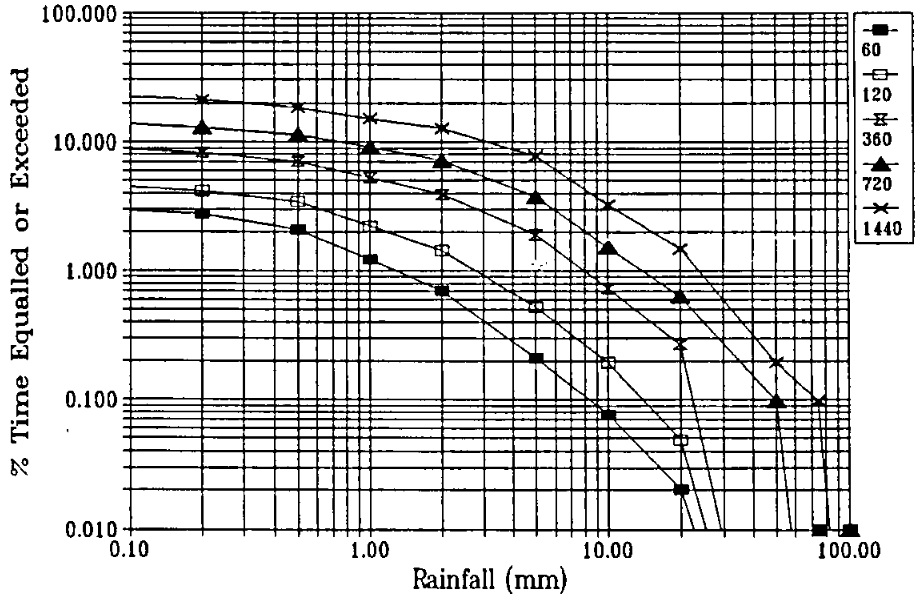


Figure 3.17 Depth-duration-frequency curves, NYP05, 1 - 24 hours (1989 - 1991 data).

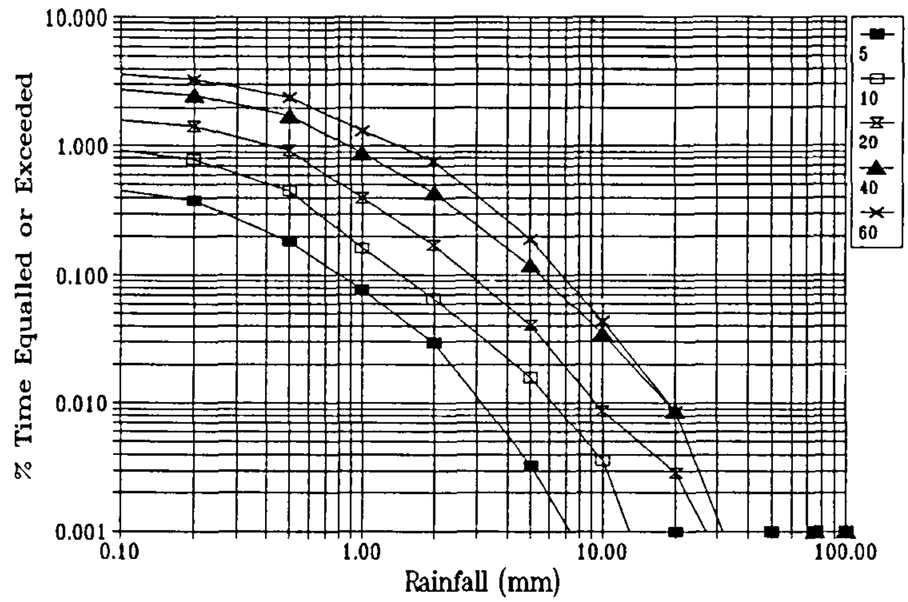


Figure 3.18 Depth-duration-frequency curves, NYP015, 5 - 60 minutes (1989 - 1991 data).

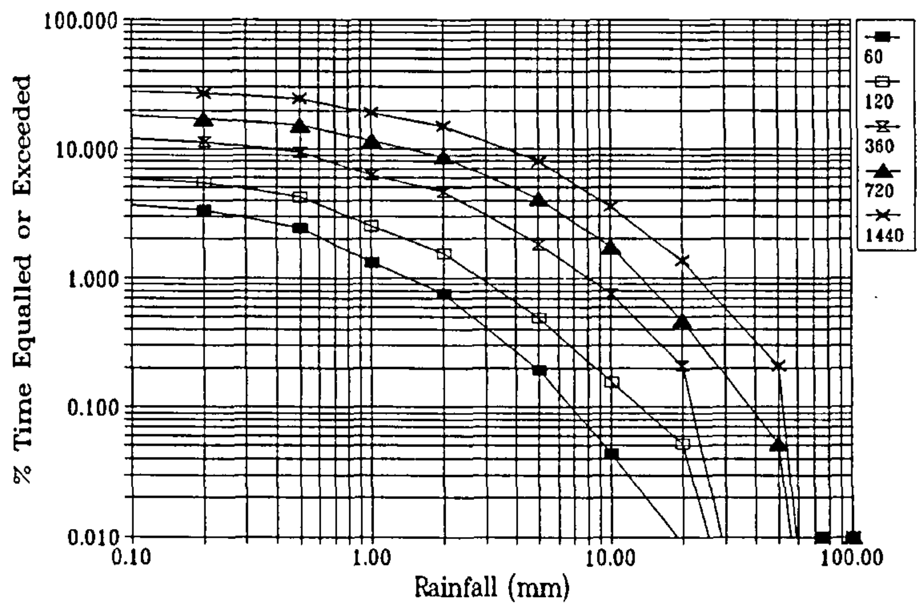


Figure 3.19 Depth-duration-frequency curves, NYP015, 1 - 24 hours (1989 - 1991 data).

Table 3.2 Summary statistics for 46 storms based on the distribution characteristics of short period rain depth for 672 1km² grids during the storms.

| Event type | No. of events | Mean duration (min) | Mean depth (mm) | Coef. of variation | Skewness | Kurtosis | Mean no. of grids |
|---|---|---|---|---|---|---|---|
| Cumulus | 18 | 668 | 10.6 | 0.43 | 0.71 | 4.33 | 8.1 |
| Advection | 9 | 707 | 8.9 | 0.37 | 0.62 | 3.86 | 11.3 |
| Coastal low | 10 | 1241 | 18.2 | 0.33 | 0.38 | 2.94 | 7.2 |
| Frontal | 6 | 688 | 17.3 | 0.18 | 0.39 | 3.25 | 21.1 |
| Cut-off low | 3 | 1570 | 66.5 | 0.11 | -0.03 | 2.54 | 69.6 |

With respect to the spatial positioning of rain cells and their movement during events, there are some trends which emerge. There is a higher frequency of cell development over the western border and northern area around Bedford for all of the storm types. The initial cell development is usually followed by movement to either the north-east or south-east. A decrease in rainfall as the cells move, followed by the development of a new cell, spatially removed from the last, is common for the thunderstorm events. Multiple cells, occurring simultaneously, are also a relatively common feature. While the size and intensity characteristics of the rain cells appear to vary between storm types, the patterns of movement do seem to be the same.

The patterns of short time period rainfall variations broadly agree with the monthly and annual statistics presented in section 3.3.1 in that there seems to be a higher likelihood of rainfall (or higher rainfall) over the western boundaries of the catchment and close to Bedford mountain. The influence of the local topography is therefore evident. The high proportion of thunderstorms that are generated on the western boundaries and their patterns of movement are suggested to be a combined effect of the generation of these events in the Great Fish River valley to the west and the prevailing westerly winds during summer. The orographic effects of the escarpments on the western boundaries as well as to the north (Bedford mountain) are also evident. While the number of events analysed is probably insufficient to draw final conclusions about the spatial patterns of rainfall, the techniques used do seem to be appropriate and can therefore be applied again at a later date when more rainfall data are available.

Figures 3.20 and 3.24 illustrate storm profiles for three convective rainfall events and the two parts of the large cut-off low event which caused the highest levels of streamflow in the area. The choice of which gauges to include in the plots has been determined to a large extent by the patterns of spatial rainfall distribution for the storms. During the cut-off low event (figures 3.23 and 3.24) the spatial variations are relatively small and the timing of the rainfall broadly similar throughout the catchment.

The convective storms (figures 3.20 to 3.22) exhibit much greater degrees of variation in rainfall amount and timing. The storms of 9/12/88 and 14/2/89 demonstrate quite concentrated rainfall cells while the storm of 2/1/89 appears to more widespread. The latter also shows some fairly complex patterns of movement and multiple cell development which is not all that clearly demonstrated in the figure given the limitation of only plotting six gauges.

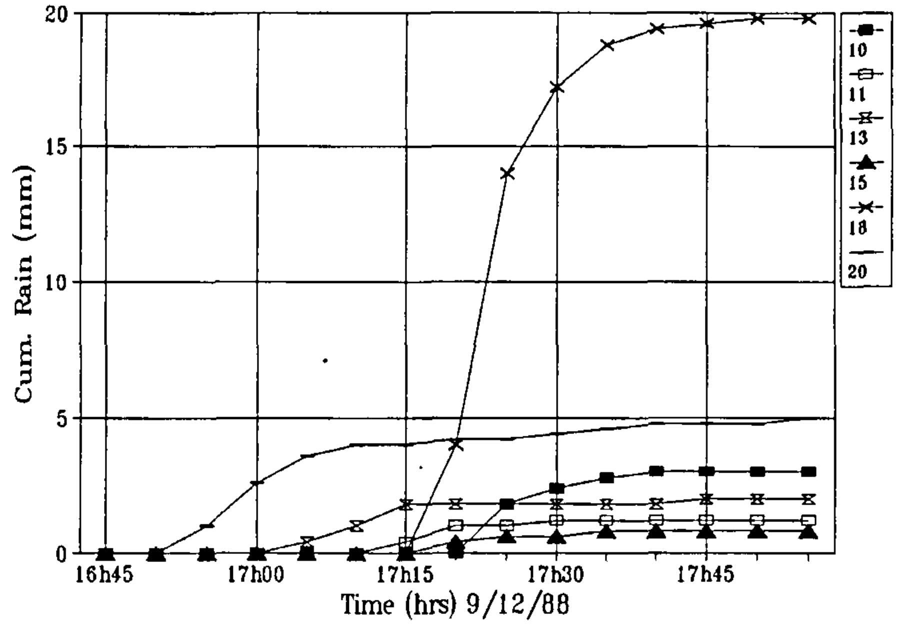


Figure 3.20 Storm distribution plots for 6 gauges, 9 December 1988.

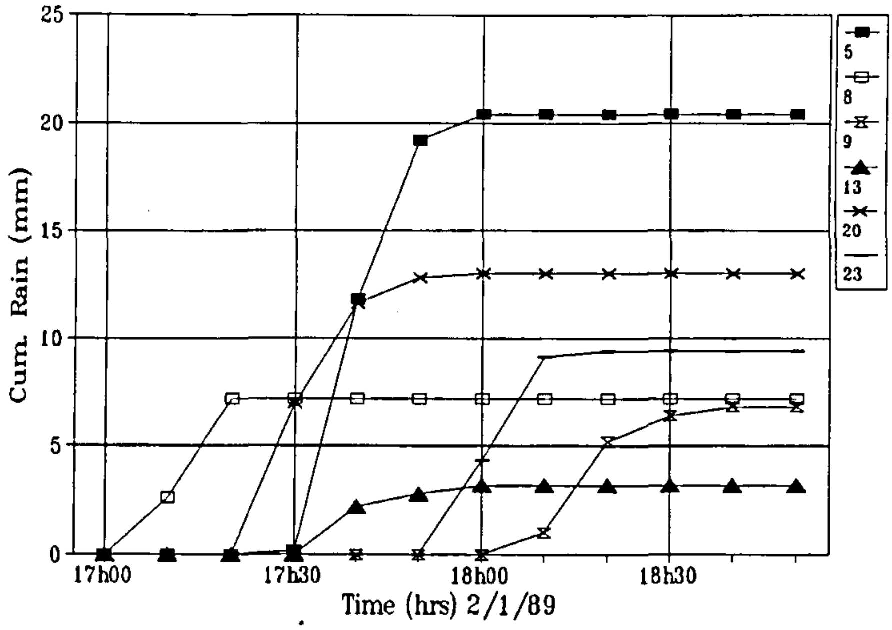


Figure 3.21 Storm distribution plots for 6 gauges, 2 January 1989.

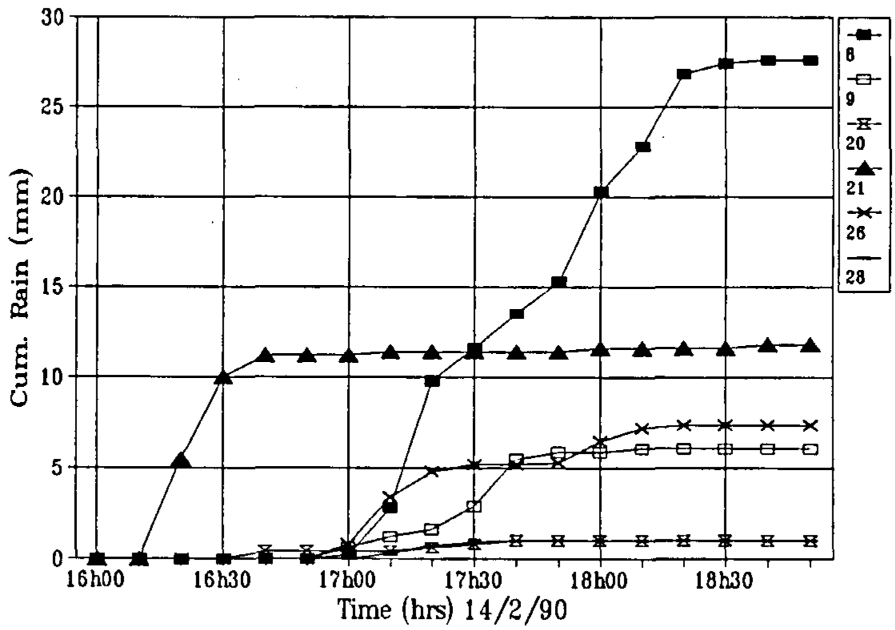


Figure 3.22 Storm distribution plots for 6 gauges, 14 February 1990.

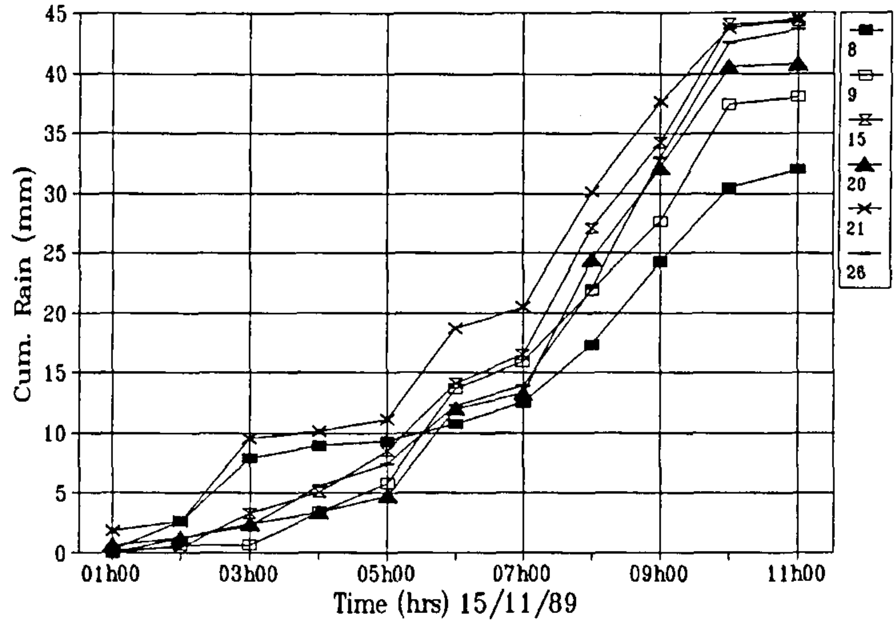


Figure 3.23 Storm distribution plots for 6 gauges, 15 November 1989.

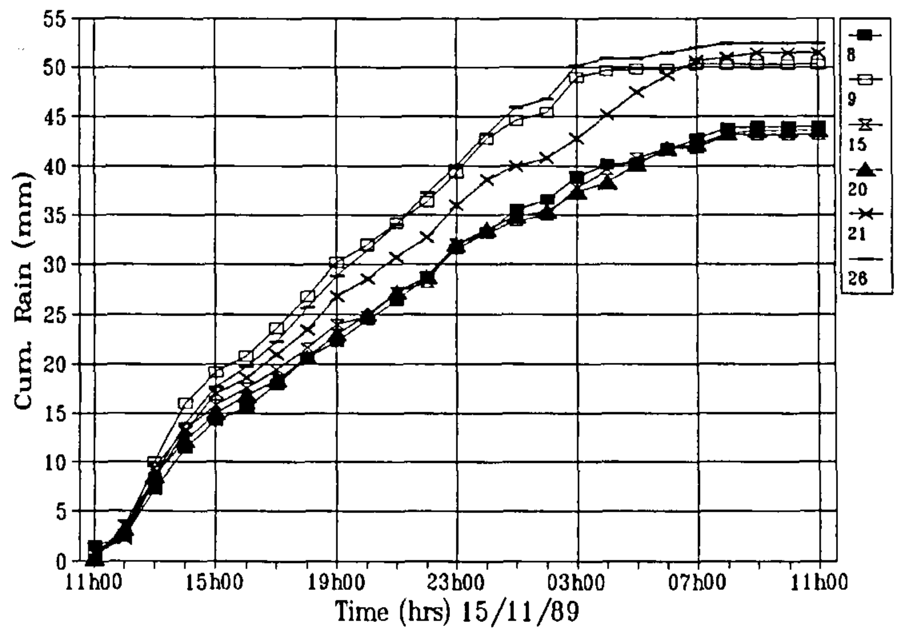


Figure 3.24 Storm distribution plots for 6 gauges, 15/16 November 1989.

# 4. GEOLOGY

The catchment is underlain by upper Permian age sandstones and mudstones of the Middleton Formation, as well as by subsequent intrusions of Jurassic dolerites. The southern edge lies near the approximate northern boundary of the underlying Koonap Formation, while the northern boundary is located in the transition to the Balfour Formation. Together these 3 Formations make up the Adelaide Sub-Group of the Beaufort Group of sediments in the Karoo Sequence. Roughly 60% of the catchment has not yet been mapped by the Geological Survey of South Africa and rock exposures and outcrops are generally sporadic and fragmentary, making geological observation difficult. As a result, available geological information is of a generalized nature, or based on interpretation from the 1:20 000 air photos.

## 4.1 Lithology

The Middleton Formation consists of alternating beds of fine-grained, massively bedded, lithofeldspathic sandstone and mudstone lithosomes which form upward fining cycles varying in thickness from a few meters to tens of meters in depth. Between Cookhouse and Middleton, sandstone was found to constitute between 20-25% of the total 2200-2900 m thickness of the Formation (Johnson 1976). Sandstone lithosomes vary from less than 1 m to 7 m in thickness, with thinner beds being more abundant. Occasional beds up to 15 m thick may also be encountered (Johnson 1976). These lithosomes are moderately lenticular to subtabular in shape (width/thickness = 30 to 1000), generally thickening and wedging out along an East-West strike. Because of the lack of outcrops, quantitative data on the lateral extent of sandstone lithosomes are not available, however, Johnson (1976) infers that widths vary from tens of meters to a few hundred meters. Sandstones are light grey to greenish grey in colour and begin with a sharp and uneven lower boundary, locally showing the development of erosive pre-depositional channels cutting into the underlying material. They gradually fine upward into greenish-grey mudstones with subordinate greyish-red mudstone beds.

## 4.2 Composition

The sediments which make up the Middleton Formation are derived from the weathering of andesitic and felsic volcanic rocks from the Cape Sequence to the south. The sediments therefore consist of minerals which have been previously weathered and which were resistant to breakdown. The composition of Middleton Formation rocks in the Great Fish River basin is given by Tordiffe (1978). Sandstones consist of quartz (19%), feldspars (29%), rock fragments (35%), cement (2%) and a mostly illite matrix (14%). The rock fragments are mainly felsite, micaceous and schistose fragments, chert, granite or gneiss. The mudstones consist of quartz (15-25%) and a matrix of illite and chlorite.

## 4.3 Depositional environment

The Karoo sediments represent the clastic infilling of a deep linear trough following a transition from shallow marine conditions to intracratonic basin sedimentation (Kingsley, 1981). The upward fining sedimentary sequences in the Middleton Formation, as well as the presence of erosive channels, trough cross bedding and micro cross-laminations indicate a continental fluviatile environment of deposition with a northwesterly paleocurrent (Johnson, 1976). Sandstone units represent stream channel deposits, whereas the finer sediments were deposited on a floodplain after overbank flooding. The incision of channels into previously deposited sediments, the lateral accretion of sandstone units and the upward fining cycles suggest that the Formation was deposited by meandering channels with varying flow conditions which wandered across a broad, essentially flat alluvial plain (Tankard et al., 1982).

## 4.4 Structural Geology

The Cape Orogeny which began in the early Triassic subjected the Middleton Formation to a directed stress from the south. The stress was insufficient to cause significant deformation and only minor folding and faulting are evident in the catchment (figure 4.1). This tectonic uplift gave the strata a gentle dip to the North of less than 3° in the northern half of the catchment and between 4-20° in the southern half.

During the Jurassic period, the sediments were intruded by East-West trending basaltic dolerite dykes (figure 4.1) which exploited zones of weakness in the sedimentary structure (Truswell, 1977). Because of the brittle deformation which often results from such intrusions, it is likely that fracture zones exist in the vicinity of these dykes. A magnetometer and electrical resistivity survey conducted by Maclear (1987) was able to trace the previously unknown westward extent of the central dyke and confirm the existence of a fracture zone running parallel to this dyke.

## 4.5 Topographical Influence

Although rock outcrops are rare, bedding planes are readily observed on the aerial photos. Due to its more resistant nature, sandstone often dominates the topography. The aerial photos show that where the sandstone lenses pinch out, the underlying mudstone has been eroded away. As the result, the topography is dominated by gently sloping hills and ridges capped by sandstone lens, with underlying sandstone beds creating breaks in the slope. On the farm Van Wyk's Kraal in the northwest corner, a cycle composed predominantly of many thin horizontal sandstone lenses has resulted in two large hills which dominate the area. The high sandstone composition has also permitted steep valley slopes to develop, resulting in a narrow gorge cut by the Goba River.

The two major dolerite dykes have a poor surface expression in the catchment. In places, however, they create small escarpments or ridges where the adjacent mudstones have been weathered away. Where the adjacent country rock consists of sandstone, the influence of dolerite is not as distinct.

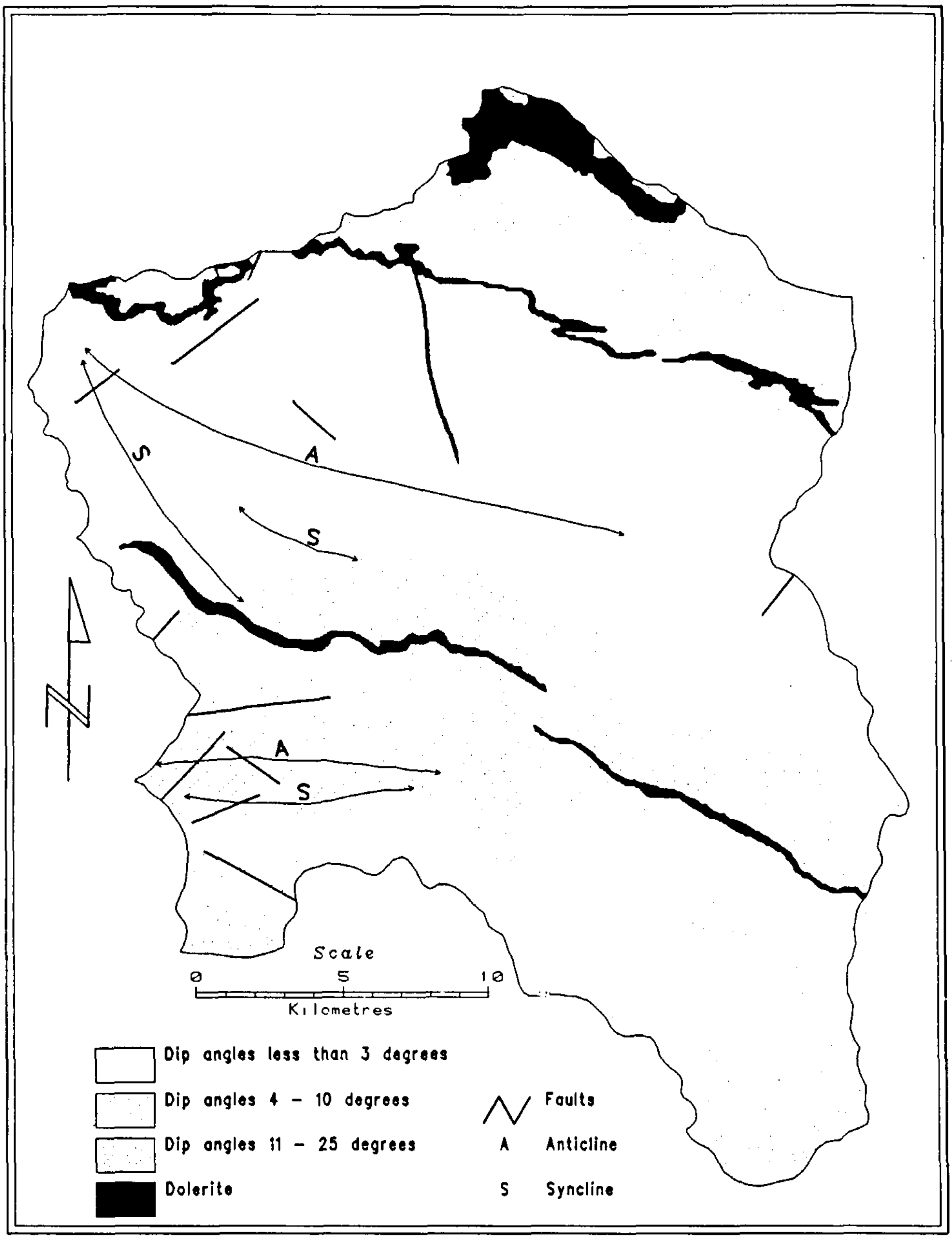


Figure 4.1 Dip angles and location of dolerite dykes.

# 5. TOPOGRAPHY AND DRAINAGE

Except for the small proportion of the area to the north of Bedford, which is very steeply sloping and mountainous, the majority of the area has relatively low relief and gentle slopes. The total relief in the gauged sub-areas is between 210m and 320m, the latter referring to sub-catchment B3 in the north west of the area. The relief of the total catchment is 890m but if the mountain area above Bedford is excluded this figure reduces to 510m. Figure 5.2 illustrates the topography of the area using a contour interval of 20m.

Figure 5.1 illustrates the range of slopes found in the catchments and the histogram has been compiled from a combination of the information supplied with the SIRI Land Type maps and data collected during a soil survey carried out by project staff.

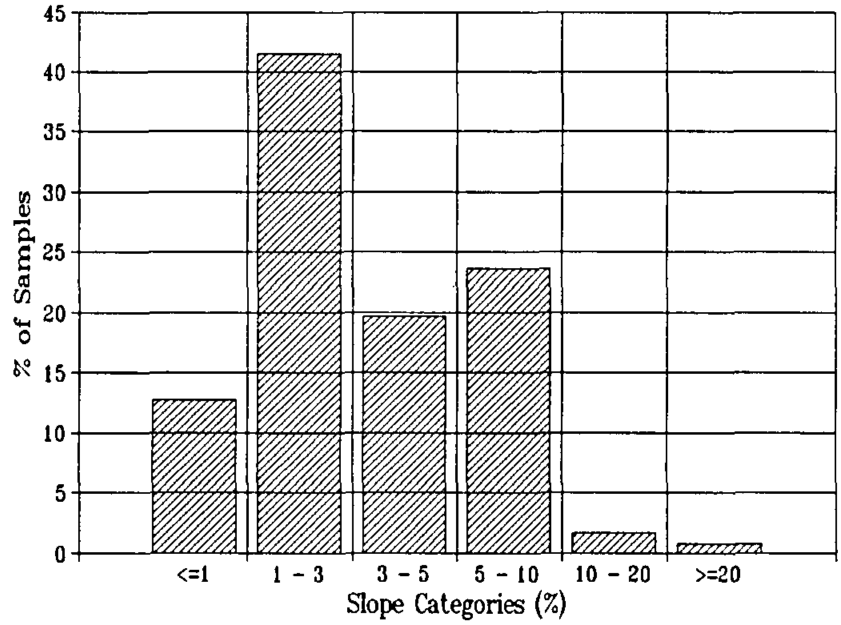


Figure 5.1 Estimated frequency of slopes (%), excluding the steep mountain area to the north of Bedford.

## 5.1 Channel characteristics

There is a great deal of variation in the channel characteristics within the Bedford catchments, largely dependent upon the degree of local incision which has taken place. A survey of 51 channel cross-sections (figure 5.3) was carried towards the end of 1989, which involved surveying the channel dimensions and local slope as well collecting photographic records of the characteristics of the bed and banks. From these data, estimates of the bankfull dimensions and Mannings 'n' values for each site have been made and used to calculate estimates of bankfull discharge (table 5.1). It was found to be rarely straightforward to define what constitutes the 'bankfull' channel as many are overdeepened with steep alluvial banks. To assume that the top of these banks constitute the present day bankfull channel would produce discharge values which are far in excess of realistic values.

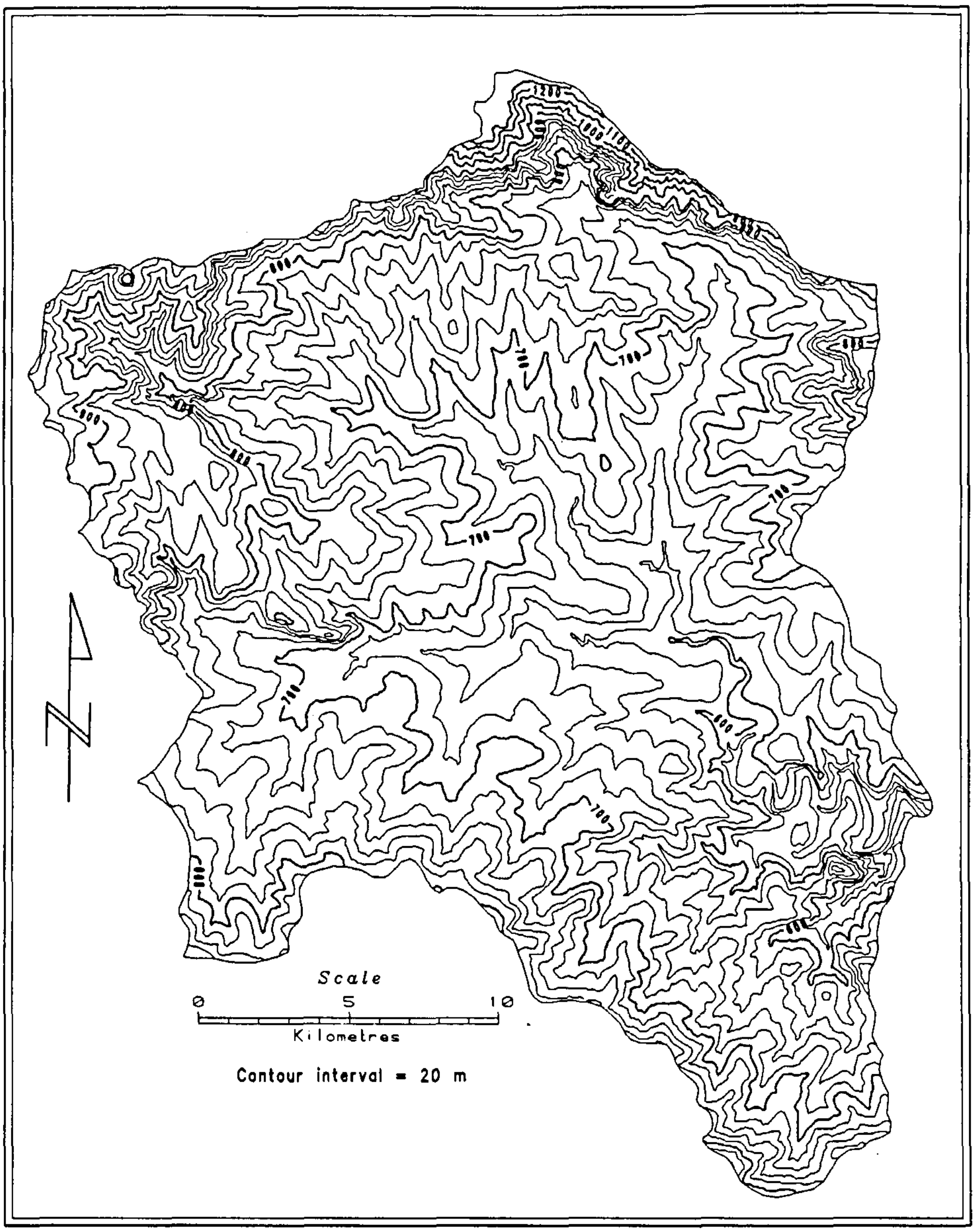


Figure 5.2 Topography of the Bedford catchment (contour interval is 20m).

The low order channels are generally poorly defined with shallow V-sections and barely distinguishable from the valley side slopes. Moving downstream, intermittent evidence of true channel beds developed on bedrock begins. Eventually, this gives way to better defined channels. In situations where the valley bottom consists of relatively deep infills of alluvial or colluvial material, the downstream trend of increasing channel size is often reversed and a well defined channel gives way to a series of laterally displaced unconnected channel features. This evidence of the effects of transmission losses is best seen in the area close to sections X28 and X30 as well as between X39 and X47 (figure 5.3).

Figure 5.4 illustrates a relatively strong relationship between Shreve channel order and cross-sectional area, while figures 5.5 and 5.6 illustrate the relationships between Shreve channel order and catchment area with estimated bankfull discharge. Both demonstrate a trend which could be useful for deriving first estimates of channel discharge capacity. However, they should be treated with caution owing to the inherent simplicity of the techniques used to derive the discharges. No statements can of course be made about the likely frequency of occurrence of these discharge values except that accepted geomorphological theory (Langbein and Leopold, 1964) suggests that the frequency should be similar for the values given for all the channel cross-section sites.

Table 5.1 Channel cross-section characteristics.

| Section | Shreve order | Drainage area ($km^2$) | Section area ($m^2$) | Wetted perimeter (m) | Mannings 'n' | Slope (m/m) | Velocity ($m\ s^{-1}$) | Discharge ($m^3\ s^{-1}$) |
|---|---|---|---|---|---|---|---|---|
| X01 | 3 | 2.77 | 0.83 | 8.83 | 0.040 | 0.0303 | 0.900 | 0.75 |
| X02 | 62 | 172.61 | 51.41 | 25.05 | 0.085 | 0.0020 | 0.850 | 43.68 |
| X03 | 210 | 292.11 | 22.35 | 17.10 | 0.075 | 0.0084 | 1.458 | 32.59 |
| X04 | 78 | 153.59 | 18.34 | 16.29 | 0.075 | 0.0120 | 1.582 | 29.01 |
| X05 | 57 | 154.54 | 15.64 | 17.52 | 0.070 | 0.0092 | 1.268 | 19.84 |
| X06 | 45 | 117.01 | 14.99 | 23.86 | 0.070 | 0.0077 | 0.920 | 13.79 |
| X07 | 80 | 164.99 | 24.33 | 20.81 | 0.050 | 0.0057 | 1.676 | 40.77 |
| X08 | 275 | 486.51 | 43.38 | 20.25 | 0.065 | 0.0072 | 2.168 | 94.04 |
| X09 | 36 | 49.44 | 7.69 | 9.10 | 0.050 | 0.0036 | 1.068 | 8.21 |
| X10 | 40 | 51.22 | 10.38 | 18.53 | 0.070 | 0.0162 | 1.234 | 12.81 |
| X11 | 17 | 26.87 | 6.66 | 8.73 | 0.060 | 0.0044 | 0.926 | 6.17 |
| X12 | 1 | 0.87 | 3.55 | 21.42 | 0.040 | 0.0675 | 1.960 | 6.96 |
| X13 | 5 | 9.29 | 5.79 | 13.28 | 0.090 | 0.0110 | 0.669 | 3.87 |
| X14 | 7 | 12.23 | 9.73 | 12.05 | 0.090 | 0.0278 | 1.607 | 15.63 |
| X15 | 15 | 15.21 | 4.79 | 11.10 | 0.060 | 0.0098 | 0.942 | 4.51 |
| X16 | 1 | 0.36 | 0.57 | 3.20 | 0.090 | 0.0174 | 0.464 | 0.26 |
| X17 | 3 | 0.40 | 1.76 | 11.67 | 0.085 | 0.0416 | 0.679 | 1.20 |
| X18 | 21 | 6.44 | 3.55 | 12.01 | 0.045 | 0.0088 | 0.927 | 3.29 |

| Section | Shreve order | Drainage area ($km^2$) | Section area ($m^2$) | Wetted perimeter (m) | Mannings 'n' | Slope (m/m) | Velocity ($m\ s^{-1}$) | Discharge ($m^3\ s^{-1}$) |
|---|---|---|---|---|---|---|---|---|
| X19 | 71 | 31.32 | 8.15 | 14.10 | 0.045 | 0.0087 | 1.440 | 11.73 |
| X20 | 123 | 103.15 | 14.72 | 10.84 | 0.095 | 0.0057 | 0.975 | 14.35 |
| X21 | 107 | 73.11 | 10.39 | 9.83 | 0.085 | 0.0173 | 1.607 | 16.70 |
| X22 | 14 | 10.20 | 2.22 | 6.48 | 0.075 | 0.0091 | 0.623 | 1.38 |
| X23 | 85 | 47.74 | 12.94 | 14.71 | 0.080 | 0.0061 | 0.893 | 11.56 |
| X24 | 7 | 8.78 | 2.07 | 9.78 | 0.050 | 0.0104 | 0.725 | 1.50 |
| X25 | 2 | 1.32 | 1.69 | 6.26 | 0.065 | 0.0130 | 0.731 | 1.24 |
| X26 | 3 | 3.97 | 2.59 | 10.82 | 0.065 | 0.0306 | 1.038 | 2.69 |
| X27 | 18 | 17.66 | 3.77 | 6.97 | 0.030 | 0.0046 | 1.501 | 5.66 |
| X28 | 22 | 28.36 | 7.71 | 9.22 | 0.050 | 0.0044 | 1.182 | 9.11 |
| X29 | 21 | 25.32 | 5.03 | 17.64 | 0.075 | 0.0209 | 0.834 | 4.19 |
| X30 | 24 | 32.55 | 9.13 | 9.73 | 0.055 | 0.0070 | 1.455 | 13.28 |
| X31 | 27 | 39.72 | 8.07 | 8.60 | 0.060 | 0.0090 | 1.515 | 12.23 |
| X32 | 8 | 3.78 | 1.33 | 10.37 | 0.045 | 0.0159 | 0.713 | 0.95 |
| X33 | 12 | 16.17 | 3.21 | 8.01 | 0.060 | 0.0136 | 1.058 | 3.39 |
| X34 | 13 | 21.34 | 4.66 | 11.75 | 0.055 | 0.0051 | 0.702 | 3.27 |
| X35 | 50 | 83.84 | 10.02 | 10.94 | 0.050 | 0.0087 | 1.754 | 17.58 |
| X36 | 63 | 107.56 | 18.79 | 15.00 | 0.060 | 0.0078 | 1.715 | 32.22 |
| X37 | 1 | 4.59 | 0.57 | 8.04 | 0.045 | 0.0186 | 0.519 | 0.30 |
| X38 | 7 | 17.17 | 6.24 | 9.87 | 0.065 | 0.0061 | 0.887 | 5.53 |
| X39 | 14 | 25.97 | 4.08 | 15.08 | 0.040 | 0.0042 | 0.680 | 2.77 |
| X40 | 7 | 15.80 | 2.27 | 7.94 | 0.040 | 0.0144 | 1.304 | 2.96 |
| X41 | 4 | 8.81 | 2.30 | 11.34 | 0.060 | 0.0216 | 0.847 | 1.95 |
| X42 | 37 | 90.17 | 14.48 | 14.54 | 0.060 | 0.0065 | 1.338 | 19.37 |
| X43 | 18 | 44.28 | 9.03 | 15.67 | 0.060 | 0.0094 | 1.117 | 10.08 |
| X44 | 12 | 27.64 | 7.10 | 8.82 | 0.070 | 0.0084 | 1.132 | 8.04 |
| X45 | 1 | 1.06 | 0.62 | 11.95 | 0.040 | 0.0310 | 0.612 | 0.38 |
| X46 | 2 | 4.09 | 1.36 | 11.78 | 0.060 | 0.0228 | 0.597 | 0.81 |
| X47 | 18 | 37.01 | 7.76 | 14.25 | 0.045 | 0.0052 | 1.068 | 8.28 |
| X48 | 1 | 5.87 | 1.22 | 9.80 | 0.045 | 0.0132 | 0.636 | 0.78 |
| X49 | 416 | 665.02 | 48.96 | 22.92 | 0.060 | 0.0020 | 1.236 | 60.53 |
| X50 | 336 | 590.09 | 46.98 | 26.80 | 0.070 | 0.0022 | 0.974 | 45.77 |
| X51 | 292 | 529.60 | 49.81 | 29.78 | 0.050 | 0.0021 | 1.288 | 64.173 |

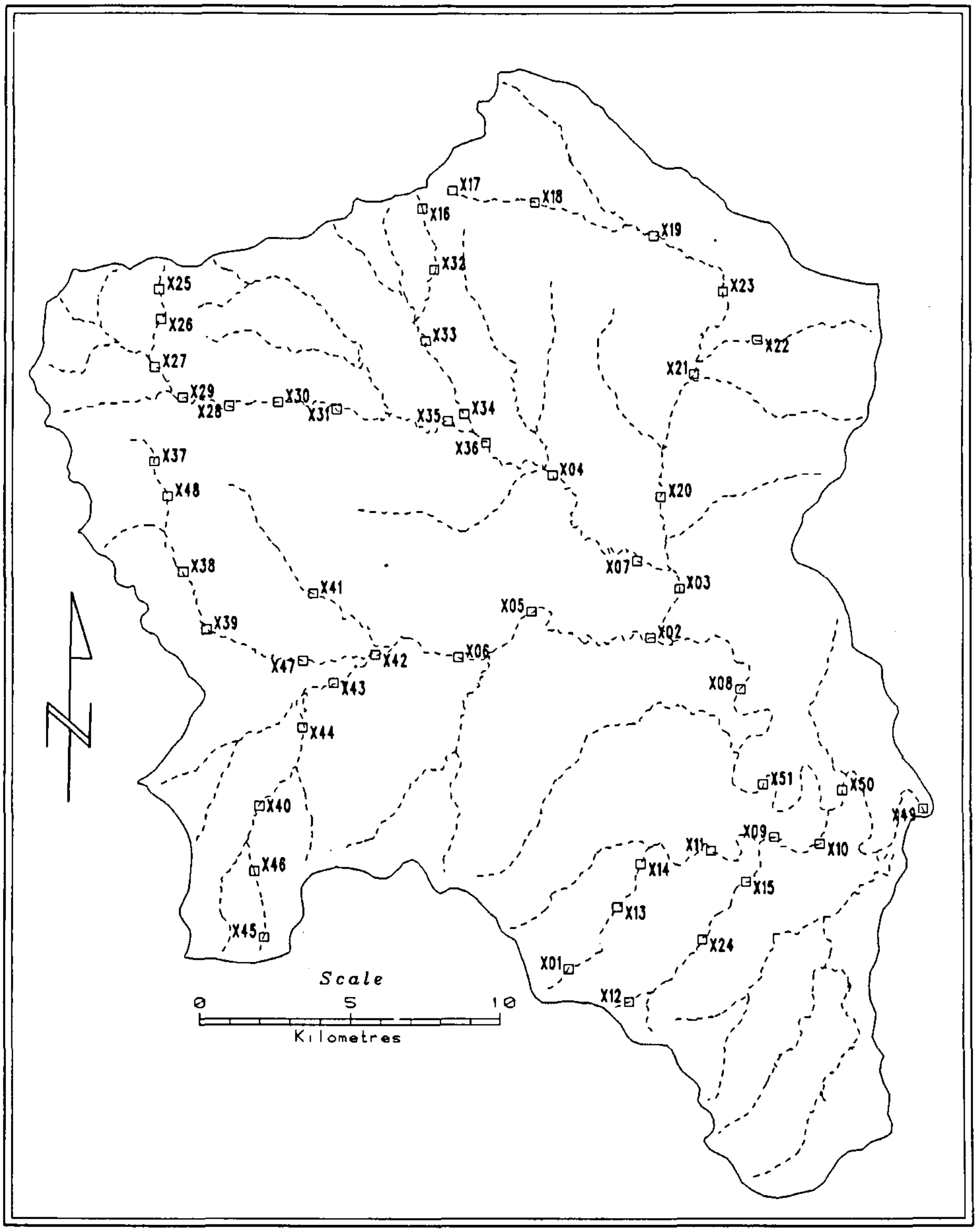


Figure 5.3 Location of the surveyed channel sections.

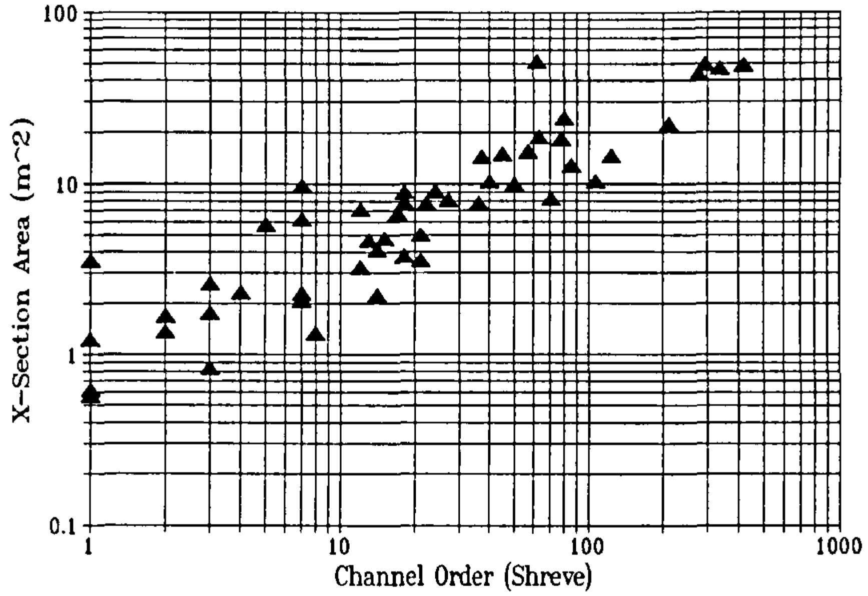


Figure 5.4 Relationship between Shreve channel order and channel cross-section area.

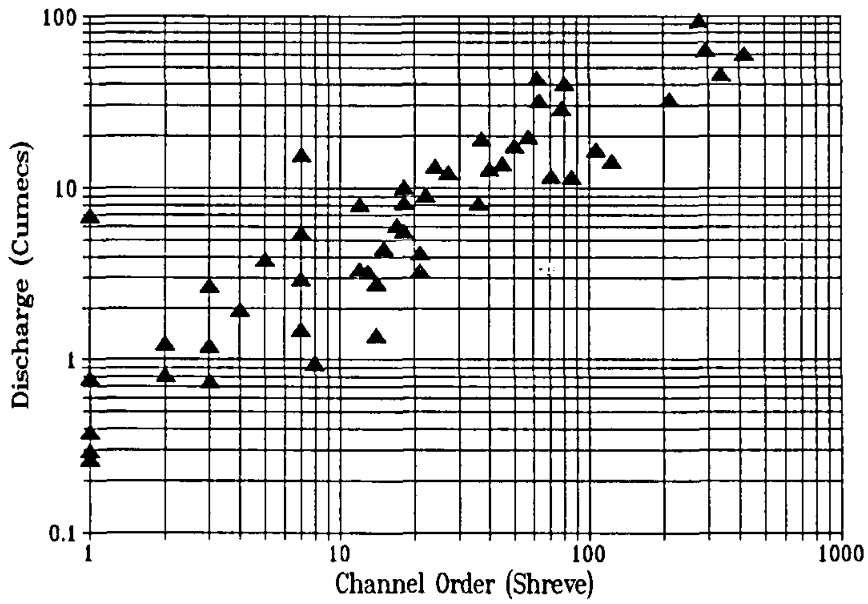


Figure 5.5 Relationship between Shreve channel order and estimated bankfull discharge.

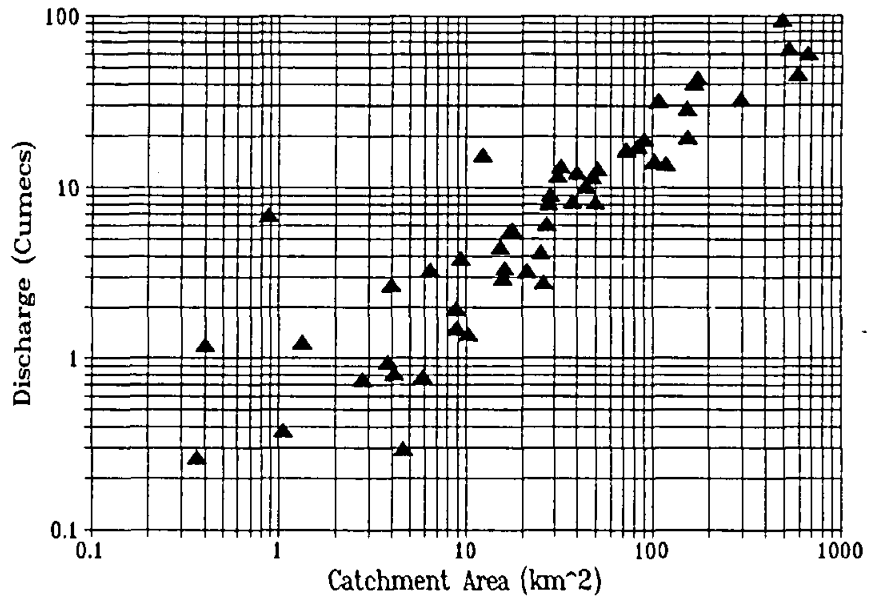


Figure 5.6 Relationship between catchment area and estimated bankfull discharge.

# 6. SOILS AND ALLUVIAL DEPOSITS.

## 6.1 Soil classification and distribution.

The limited available SIRI land type information (map and associated memoirs) groups the soils encountered in the catchment into 5 pedosystems. Within these pedosystems, 9 soil forms of the South African taxonomic soil classification system were identified by Hensley and Sami (1991) in a survey which covered the main soil-vegetation ecotopes and terrain units. These soil forms, as well as the principal subordinate soil families, are shown in Table 6.1. The percentage occurrence of each of these soil forms is shown in figure 6.1.

Table 6.1. Soil Forms and Series encountered in the catchment

| Soil Form | Principal Soil Families |
|---|---|
| Cartref (Cf) | Witzenberg |
| Dundee (Du) | Visrivier |
| Glenrosa (Gs) | Dumisa |
| Hutton (Hu) | Stella, Ventersdorp |
| Mispah (Ms) | Myhill, Carnarvon |
| Augrabies (Ag) | Hefnaar, Giyani, Shilowa |
| Sterkspruit (Ss) | Bethulie, Smithfield |
| Swartland (Sw) | Shangoni, Amandel, Riebeeck |
| Valsrivier (Va) | Goedemoed, Aliwal, Serona, Helvetia |

A more detailed grid based soil survey was carried out by project staff with the help of student assistants over the period November 1989 to January 1990. This survey was based on sampling one or more topographic transects (hilltop to valley bottom) in each of 59 2' by 2' grids covering the majority of the catchment. Data collected for each terrain unit of the transects included information on slope angle, dominant vegetation type, geology, soil depth and structure, and textural data. The three sets of data (SIRI, Hensley and Sami, and IWR) compliment each other in that the IWR survey did not attempt to identify soil form or series, but contains other more detailed information than is available from the generalised soil classification surveys.

The SIRI and IWR surveys both contain information about soil distribution according to the major terrain type units (the IWR survey followed the approach adopted by SIRI). The distribution of these units within the catchments is given in table 6.2 and the following two sections discuss the soil characteristics within these zones. The distribution of different soil forms within each of the terrain units is given in figure 6.2.

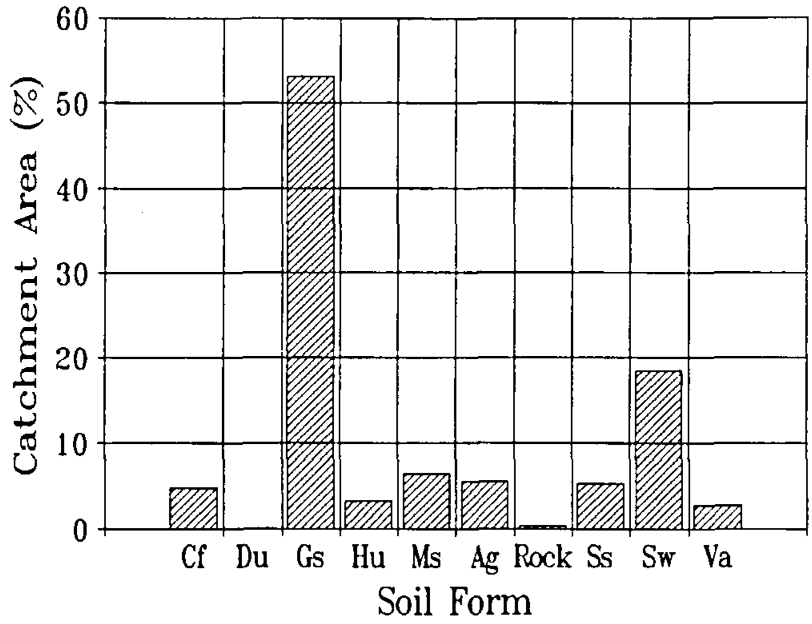


Figure 6.1 Percentage distribution of soil forms in the Bedford catchments (SIRI data).

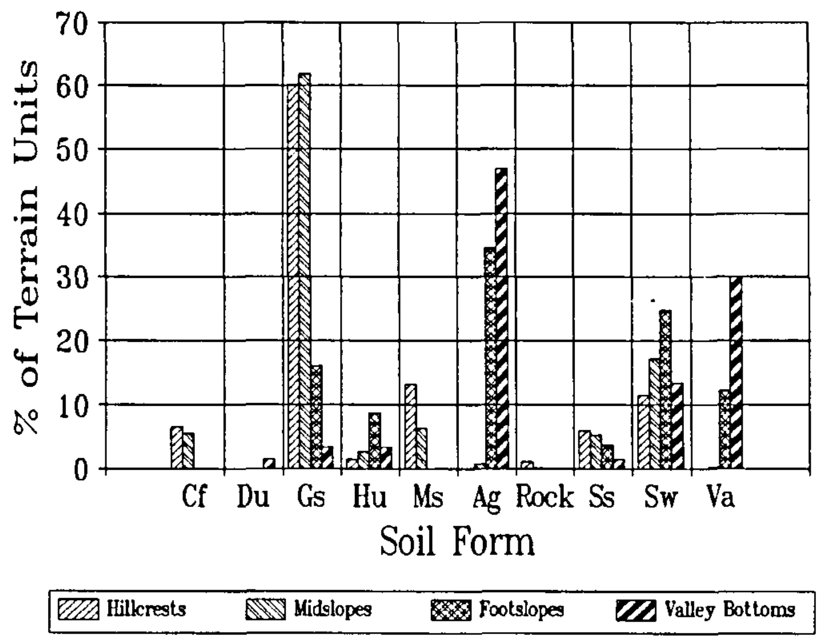


Figure 6.2 Distribution of soil forms within the four terrain units (SIRI data).

Table 6.2 Distribution of terrain type units

| Terrain Type | Catchment Area (%) |
|---|---|
| Hillcrests | 14.7 |
| Midslopes | 71.2 |
| Footslopes | 9.1 |
| Valley Bottoms | 4.9 |

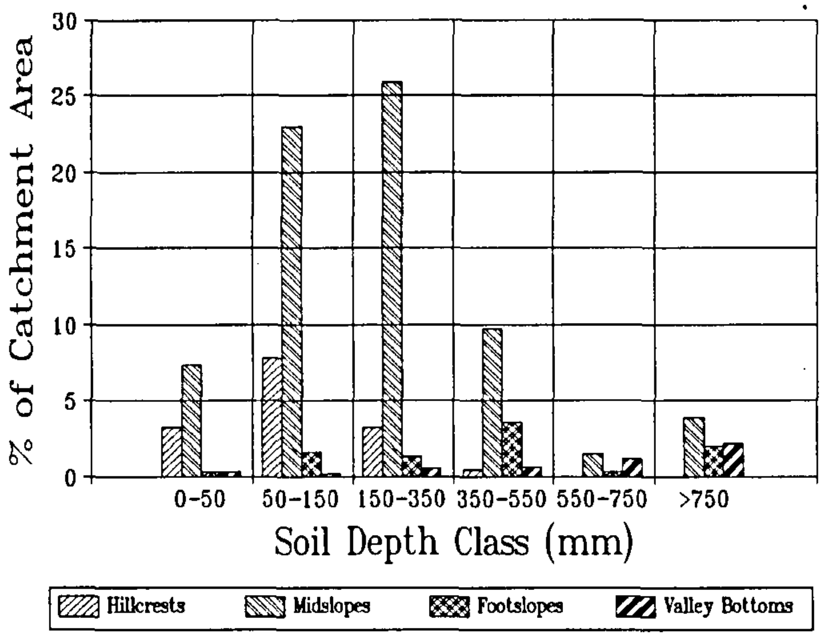


Figure 6.3 Distribution of soil depths (IWR survey) within the Bedford catchments.

### 6.1.1 Hillcrests and Midslopes.

These topographic zones cover between 85-90% of the catchment (table 6.2) and have soil depths which are highly variable but generally do not exceed 400 mm (figure 6.3). The predominant soils of these upland areas are of the Glenrosa form (figure 6.2) and have a sandy loam or sandy clay loam texture (figure 6.4). These weakly developed soils are found on hills capped by sandstone beds and have a laterally discontinuous B horizon which merges into saprolite and weathering bedrock in various degrees of breakdown. On some hillslopes where the B horizon is impermeable an overlying E horizon has developed, which suggests that lateral flow probably occurs. These soils are classified as Cartref Form. Where soils have developed on extremely resistant unfractured rock no B horizon or bedrock weathering can be observed. These soils are classifed as Mispah, are generally shallow and rarely exceed 200 mm in depth (figure 6.5). Hilltops covered by Mispah soils are more prevalent in the southern half of the catchment and can usually be identified by the large number of unweathered rock fragments and bedrock outcrops which cover the surface. In the northern half of the catchment, slightly higher rainfall and infiltration rates have resulted in greater illuviation and a more strongly developed soil structure. Where this process has occurred to the extent that a distinct B horizon enriched with clay can be observed, the soils are classified as Swartlands. This process is especially prevalent in the north-western part of the catchment, where hillcrests predominantly form flat-topped plateaus and 45% the soils are of the Swartland form. In this region, Glenrosas only occupy 10-15% of upland areas, compared to 70-80% throughout the rest of the catchment. In a further 25% of these upland soils, illuviation has progressed to the stage where the clay content of the B horizon is twice that of the A horizon. These soils are classified as Sterkspruits.

### 6.1.2 Footslopes and valley bottoms.

No one soil form dominates these terrain units, however, the most predominant soils are sandy clay loams and clay loams of the Augrabies form (figures 6.2 and 6.4). These are weakly structured soils developed on unconsolidated colluvial or alluvial deposits which exceed 600 mm in depth (figure 6.5). The B horizons of these soils are characterised by the accumulation of carbonates, which reflects insufficient leaching of mobile salts. In some localities, the accumulation of carbonates has occurred to such an extent that calcium nodules and even hardpan carbonate horizons are encountered. This is more prevalent in the south, and when it occurs the soils are classified as Brandvleis and Coegas. As these soils are similar to other soil forms except for the degree of carbonate accumulation, are of limited lateral extent and are interspersed with other soil forms, it is difficult to characterise their spatial extent. In unconsolidated valley bottoms, where relatively fine sediments have been deposited (clay loams, clays, silty clays), a moderate to strong structure has developed in the B horizon as a result of illuviation. Where this has occurred, Valsrivier soils are found. In a few localities where stratification can still be observed in the alluvial deposits, Dundee soils are present. Where neither colluvial or alluvial deposits are present, soils have developed over weathering bedrock. These soils range from relatively shallow Glenrosa and Swartlands depending on the structural development of the B horizon. In areas where either dolerite or sandy deposits are the parent material, weakly structured sand and loamy sand textured Hutton soils have developed.

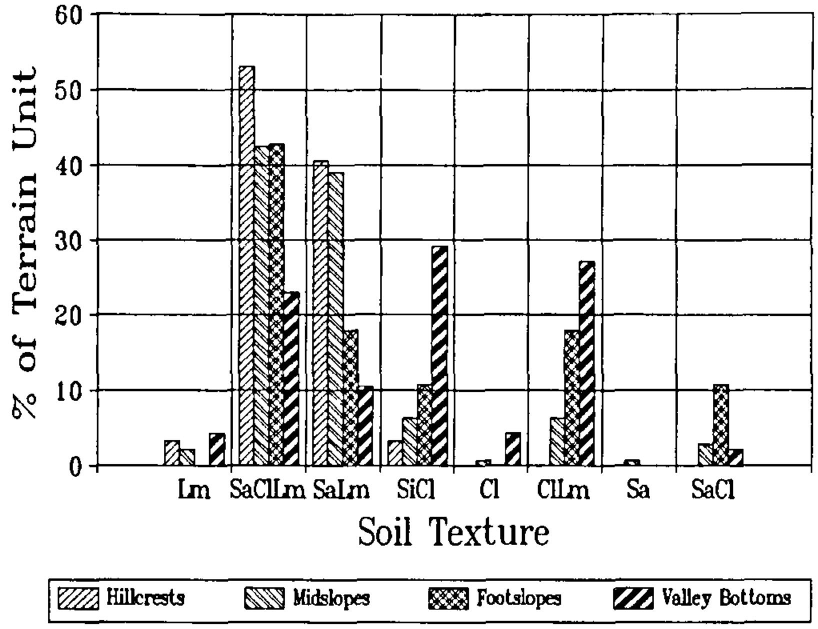


Figure 6.4 Distribution of textural classes by terrain unit (IWR data).

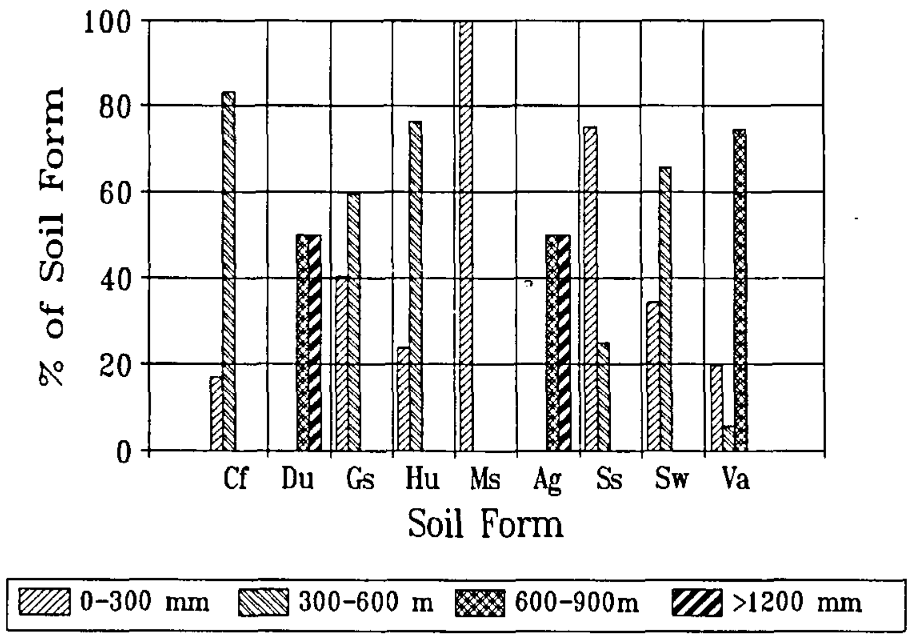


Figure 6.5 Distribution of soil depths within each soil form (SIRI and IWR data).

## 6.2 ALLUVIAL DEPOSITS.

This section of the report discusses the nature of the alluvial deposits found in the valley bottoms of some of the streams in the Bedford catchments. The field and laboratory work was carried out over the period November 1990 to February 1991 by a group of students of the Department of Geography at Rhodes, one of whom used the information for an undergraduate dissertation (Engelbrecht, 1991). Although these deposits are referred to within the report as alluvium, there exists some doubt about whether they are made up completely of alluvially deposited sediments. It is quite possible that they are a combination of alluvial and colluvial deposits washed in from the valley sides.

The field data collection programme began with the identification of the major alluvial areas from the 1:20 000 colour areal photographs and selection of representative sites. At each site the topography of the valley bottom profile was surveyed at a cross section, auger holes sunk to determine the depth to bedrock and samples of the material collected at several depths to determine textural properties. The aerial photos, field survey and material depth data were analysed to obtain estimates of the total volume of alluvial material in the area. The texture data were used to estimate indices of moisture holding characteristics and the two data sets combined to provide estimates of the total capacity of the alluvial deposits to absorb water.

Three major areas of alluvial deposits were identified as well as several minor ones (figure 6.6). The area covered is some 15.5 $km^2$, or 2.3% of the total catchment area. A total of 29 cross sections were surveyed and sampled within these areas. Each sample cross section has been considered representative of a defined alluvial surface area and a number of estimates made for each representative area in table 6.3. The material is generally of a sandy loam texture, with the coarse fraction generally below 1% and a mean bulk density of about 1.5 g $cm^{-3}$. In general terms, bulk densities appear to decrease with depth, partly due to a reduction in clay content (Hughes and Sami, 1991).

The 'Wilting Point' (WP), 'Field Capacity' (FC) and porosity values have been estimated from the textural properties of the sediment samples and are merely used to indicate lower and upper bounds to moisture states (table 6.3). The survey indicates that there is a total of about 25 mill. $m^3$ of alluvial material, representing a water storage potential of some 11 mill. $m^3$ (based on porosity). 50% of this potential volume is likely to be held at tensions below free gravitational drainage (-30 kPa), while 28% is held at tensions below 'Wilting Point' (1500 kPa).

Where the sampled alluvial areas correspond to monitored soil moisture sites the calculated values for WP agree reasonably well with minimum moisture contents measured after prolonged drying periods. Similarly, estimated 'Field Capacity' values are similar to the measured soil moisture values obtained soon after saturation conditions were known to have occurred.

Table 6.3 Alluvial areas - Characteristics of sample cross sections.

| Site ID | Mean depth (m) | Area ($10^6m^2$) | Volume ($10^6m^3$) | FC - WP (%) | Porosity (%) | Water content (Por-WP)*Vol $10^3m^3$ | Water content Por*Vol $10^3m^3$ |
|---|---|---|---|---|---|---|---|
| B01/01 | 1.02 | 0.12 | 0.12 | 10.6 | 38.2 | 32.4 | 46.7 |
| B01/02 | 0.51 | 0.29 | 0.15 | 8.5 | 41.9 | 47.4 | 61.8 |
| B01/03 | 1.52 | 1.01 | 1.53 | 9.7 | 41.9 | 471.2 | 643.2 |
| B01/04 | 2.54 | 1.39 | 3.53 | 11.1 | 47.4 | 1038.3 | 1676.5 |
| B02/01 | 1.86 | 0.38 | 0.70 | 10.2 | 37.3 | 182.5 | 263.0 |
| B02/02 | 0.95 | 0.95 | 0.91 | 9.5 | 41.9 | 285.7 | 379.9 |
| B02/03 | 0.79 | 0.24 | 0.19 | 11.1 | 42.4 | 49.9 | 80.5 |
| B02/04 | 1.03 | 0.39 | 0.40 | 8.4 | 42.0 | 125.4 | 169.4 |
| B02/05 | 0.62 | 0.97 | 0.60 | 8.2 | 44.0 | 198.8 | 264.7 |
| B02/06 | 1.46 | 0.62 | 0.90 | 9.3 | 40.4 | 273.2 | 365.2 |
| B02/07 | 0.96 | 0.28 | 0.27 | 8.4 | 43.6 | 93.3 | 117.3 |
| B02/08 | 0.51 | 0.26 | 0.13 | 7.8 | 50.6 | 47.2 | 67.4 |
| B02/09 | 0.42 | 0.62 | 0.26 | 8.4 | 50.2 | 99.3 | 131.4 |
| B02/10 | 0.45 | 0.21 | 0.09 | 8.4 | 50.2 | 36.2 | 47.9 |
| B03/01 | 2.49 | 1.23 | 3.05 | 9.0 | 43.2 | 969.0 | 1321.1 |
| B03/02 | 1.25 | 1.08 | 1.35 | 8.4 | 46.9 | 453.0 | 631.8 |
| B03/04 | 3.26 | 0.63 | 2.05 | 9.7 | 46.5 | 649.7 | 955.7 |
| B03/05 | 1.86 | 0.75 | 1.40 | 10.1 | 38.1 | 344.7 | 531.9 |
| B03/05 | 1.32 | 0.26 | 0.34 | 10.1 | 38.1 | 84.7 | 130.7 |
| B03/06 | 0.83 | 0.25 | 0.21 | 10.1 | 38.1 | 51.5 | 79.4 |
| B03/07 | 2.00 | 1.10 | 2.16 | 8.1 | 49.1 | 793.9 | 1061.6 |
| B03/08 | 2.98 | 0.25 | 0.74 | 9.3 | 38.5 | 203.8 | 286.7 |
| B03/09 | 3.32 | 0.15 | 0.50 | 9.3 | 38.5 | 136.3 | 191.8 |
| B03/10 | 3.36 | 0.27 | 0.91 | 9.3 | 38.5 | 248.2 | 349.2 |
| B03/11 | 2.19 | 0.85 | 1.86 | 10.1 | 38.1 | 486.4 | 709.0 |
| B04/01 | 0.58 | 0.58 | 0.34 | 6.5 | 47.3 | 135.4 | 160.4 |
| B04/02 | 0.61 | 0.25 | 0.15 | 9.6 | 47.4 | 52.3 | 72.7 |
| B04/03 | 1.03 | 0.04 | 0.04 | 10.7 | 41.3 | 12.0 | 17.1 |
| B04/04 | 0.76 | 0.06 | 0.05 | 7.6 | 55.3 | 20.0 | 25.3 |

As a later section will demonstrate, the effects of the presence of alluvial valley fills on runoff processes, particularly transmission losses, depends upon several factors. Clearly, the textural and related infiltration and water holding capacities will be important. But it is also evident that the configuration of the channel with respect to the deposits is also very important. Some of the channels passing through the alluvial areas are well defined and developed with bedrock beds. Others are less well defined and have gravel beds overlying alluvial deposits. It is the latter situation where transmission losses are likely to be highest. and there is assumed to be far less opportunity for losses to occur in the former situations. It is therefore not only the presence of alluvial material that is of sole importance.

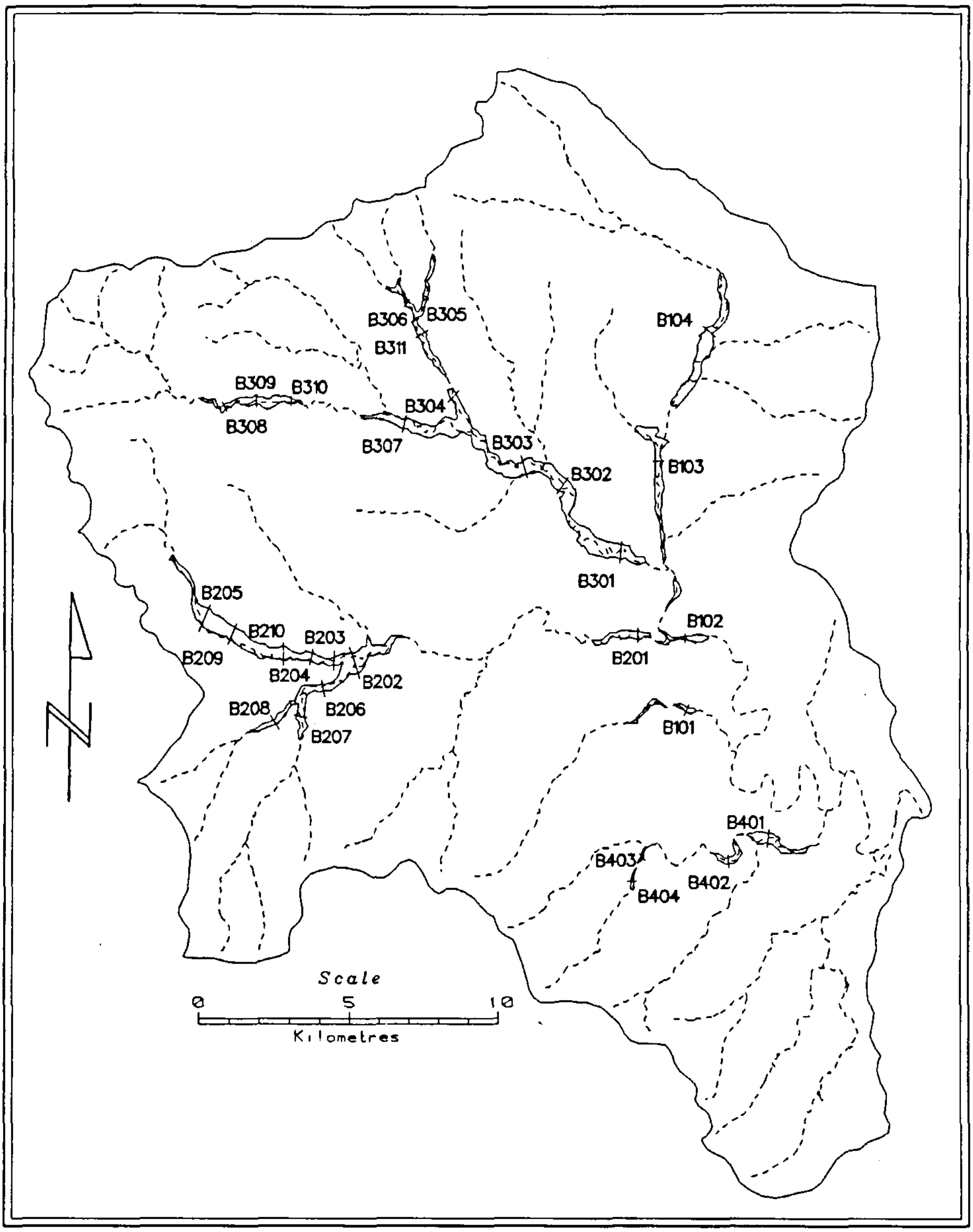


Figure 6.6 Distribution of alluvial areas and location of sample sites.

# 7. LAND USE AND VEGETATION.

The information used to characterise land use and vegetation has been drawn from two surveys. One was carried out at the same time and using the same sites as the soil survey and the dominant vegetation type and species was identified at each sample site. The second survey was based on the 1:20 000 colour aerial photography coupled with some ground truth. The scale of the photographs is not sufficient to differentiate between different grass, shrub, bush or tree species and therefore the second survey concentrated on identifying the areas occupied by different densities of tree and bush cover.

In general terms, the Bedford catchments fall into Acocks' 'Eastern Province Thornveld' classification, where a range of grasses (Rooigras, Spear Grass, Turpentine Grass and others -see appendix B), Karoo Forbes and *Acacia Karoo* thorn trees would be expected to occur. The major land use of the area is grazing by sheep and cattle and in the past has clearly been subjected to variable degrees of overgrazing. The degree of overgrazing and subsequent invasion of the grasslands by either *Acacia Karoo* or Karoo Forbe species, or both, appears to account, to a large extent, for the present day spatial vegetation patterns. The evidence for this can be clearly seen in the field, where a camp of good grassland (with a wide species diversity) lies immediately adjacent to a camp dominated by *Acacia Karoo* thorn bushes with poor grass cover.

Two main types of invasion seem to be, or have been, active in this area. *Acacia Karoo* invasion takes place through the selective grazing out of the *Themeda* (Rooigras) grasses to produce a stage where *Digitaria* and *Sporobolus* species dominate. Acacia seeds are distributed by grazing animals, where they can lay dormant for long periods of time until suitable germination conditions exist. When they germinate large areas can become covered with young *Acacia* trees in a very short period of time. Sweet palatable grasses (e.g. Stap's Buffalo Grass) develop under the bush clumps, which then promote concentrated grazing and the development of bare patches during much of the year and particularly during dry periods. The use of these areas for shade also results in trampling and soil surface compaction.

The second form of invasion is by Karoo Forbe species and occurs at most levels of overgrazing, whether *Acacia Karoo* species are present or not. Both forms of invasion result in poorer ground surface cover with resulting increases in the potential for surface crusting, lower infiltration rates and potentially higher rates of erosion..

Figure 7.1 illustrates the percentage of the total catchment area covered by seven classes of vegetation and land use as identified from the 1:20 000 aerial photos. No distinction is made in either this diagram or figure 7.2 (which shows the spatial distribution of the different vegetation covers) between true grassland and Karroid (basal cover dominated by Karoo Forbe species). The dominant classes (74% of the area) are grassland or Karroid with no *Acacia* and with up to 25% cover by *Acacia* or other bushes and trees. The grid based survey of dominant vegetation type carried out during the soil survey classified 64% of samples as grassland or Karoo Forbes and 36% as thornveld. Given the different approaches used, there is reasonable agreement between the two surveys and it is assumed that some of the 0-25% bush/tree cover group has not been classified as thornveld during the grid survey. 30% of the grid samples were identified as grassland and 34% as Karroid, but there are distinct differences between the northern and southern halves of the catchment as illustrated in table 7.1. The greater proportion of Karroid Forbes species in the southern half is clearly demonstrated and can be easily verified in the field.

Table 7.1 Differences between dominant vegetation groups in the north and south.

| Area | Grassland (% samples) | Karroid (% samples) | Thornveld (% samples) | No. of samples |
|---|---|---|---|---|
| North | 37 | 23 | 40 | 197 |
| South | 21 | 48 | 31 | 147 |
| Overall | 29 | 36 | 35 | 344 |

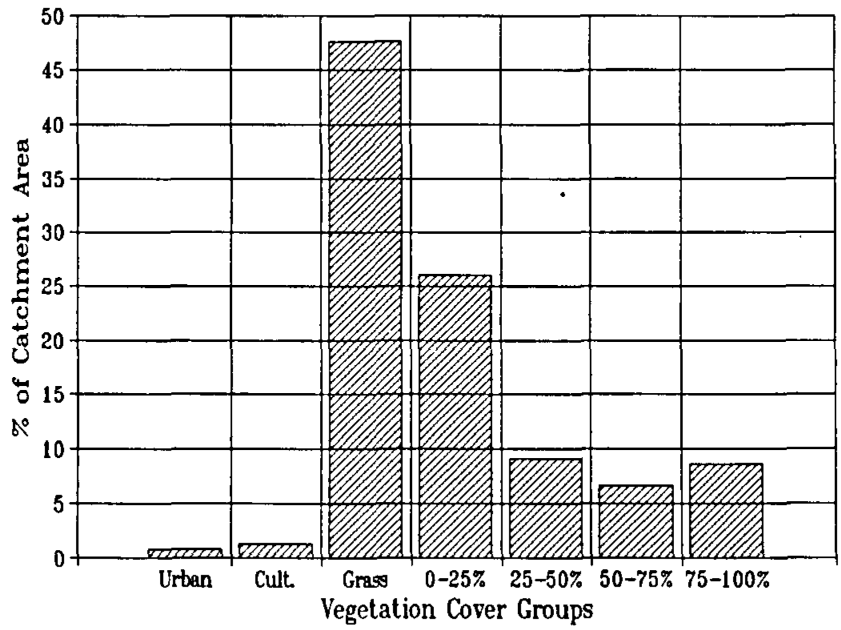


Figure 7.1 Proportion of catchment area occupied by different vegetation covers (Grass refers to those areas of grassland and Karoo Forbes with no bush cover and the percentages refer to the extent of bush cover in the other categories).

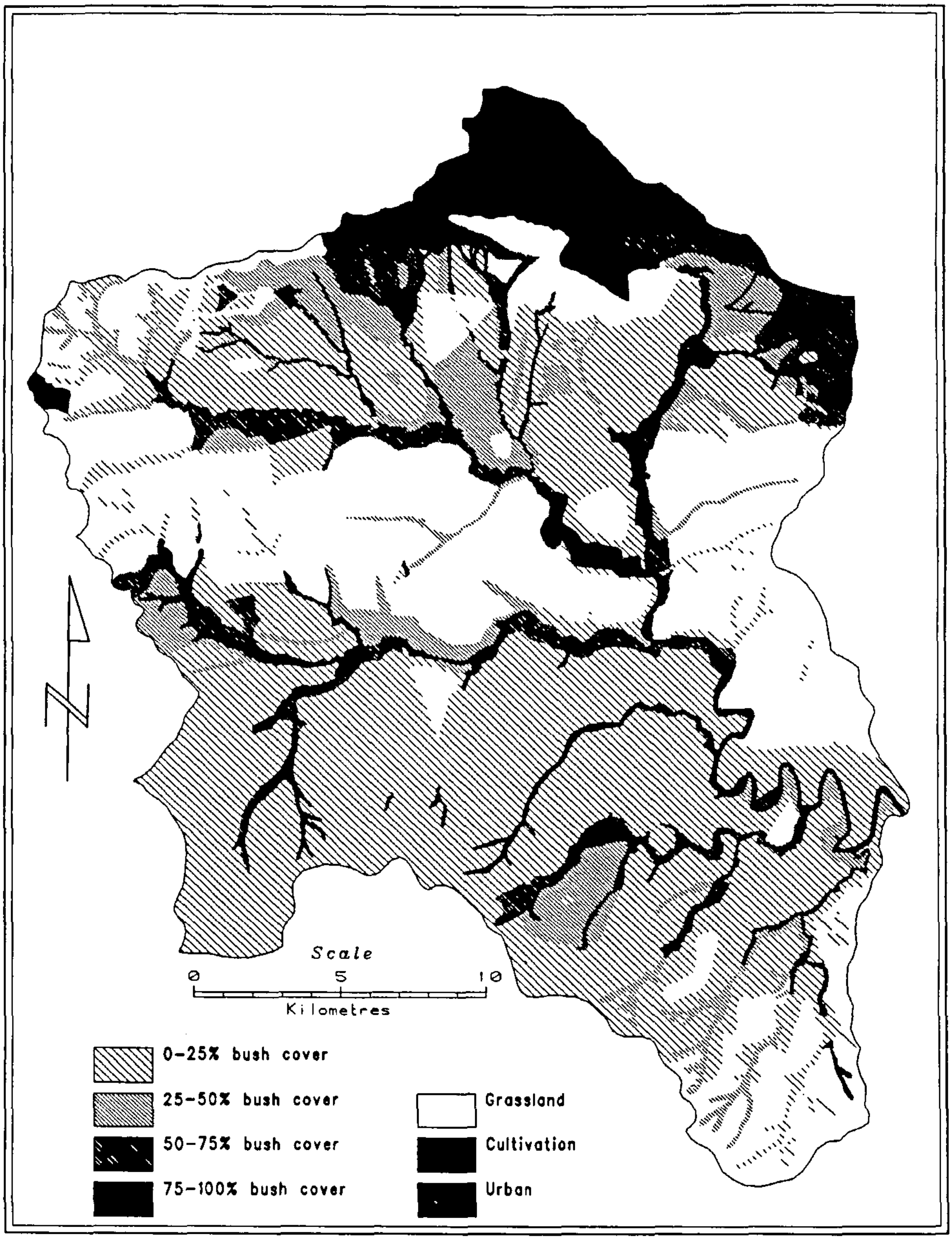


Figure 7.2 Distribution of different vegetation covers based on % cover of bush.

# 8. SOIL MOISTURE.

## 8.1 Infiltration characteristics.

Infiltration characteristics under various vegetation and soil surface conditions were derived from a field survey conducted by project staff. The results were obtained using a Department of Agriculture sprinkling infiltrometer (Reinders and Louw, 1984). Infiltration curves are determined from the cumulative infiltration curve and are defined by two empirical constants, k and c, so that:

$$I = k * c * t^{k-1}$$

where I is the infiltration rate in mm $h^{-1}$ and t is the elapsed time in hours since infiltration began. The type of vegetation and soil conditions tested, resultant mean k and c values and final infiltration rates are listed in Table 8.1. Final infiltration rates have been defined arbitrarily as the rate after 60 minutes. The observed infiltration curves are shown in figures 8.1 - 8.6.

Table 8.1 Infiltration characteristics for various vegetation types and soils.

| Dominant Vegetation Type | Dominant Soil Forms and Condition | N | Mean k | Mean c | Final Infiltration rate (mm/h) |
|---|---|---|---|---|---|
| Karroid | Mispah Non-crusted | 4 | 0.26 | 2.31 | 1.80 |
| Karroid | Mispah Crusted | 3 | 0.25 | 1.91 | 1.73 |
| Karroid/grass | Swartland, Glenrosa Non-crusted | 2 | 0.39 | 1.55 | 3.08 |
| Karroid/grass | Swartland, Glenrosa Crusted | 2 | 0.17 | 2.38 | 0.83 |
| Grass/thornveld | Swartland, Glenrosa Non-crusted | 2 | 0.54 | 2.46 | 12.49 |
| Grass | Swartland, Glenrosa Shallow | 7 | 0.32 | 2.02 | 2.42 |
| Gras | Swartland, Glenrosa Colluvium | 2 | 0.47 | 4.61 | 14.32 |
| Grass | Swartland, Glenrosa Overgrazed | 2 | 0.26 | 2.76 | 2.07 |
| Grass/riverine | Valsrivier, Augrabies Alluvium | 6 | 0.40 | 2.19 | 5.01 |

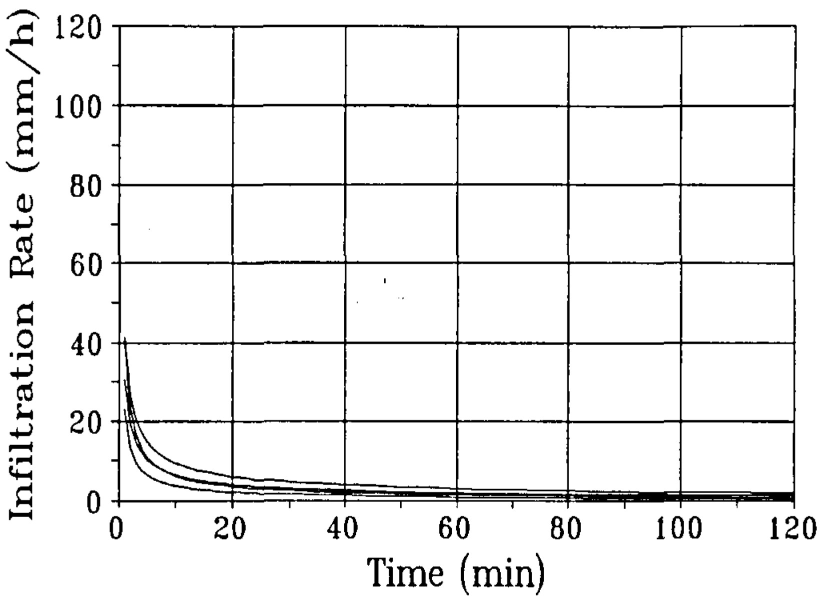


Figure 8.1. Infiltration curves for non-crusted soils under Karroid vegetation.

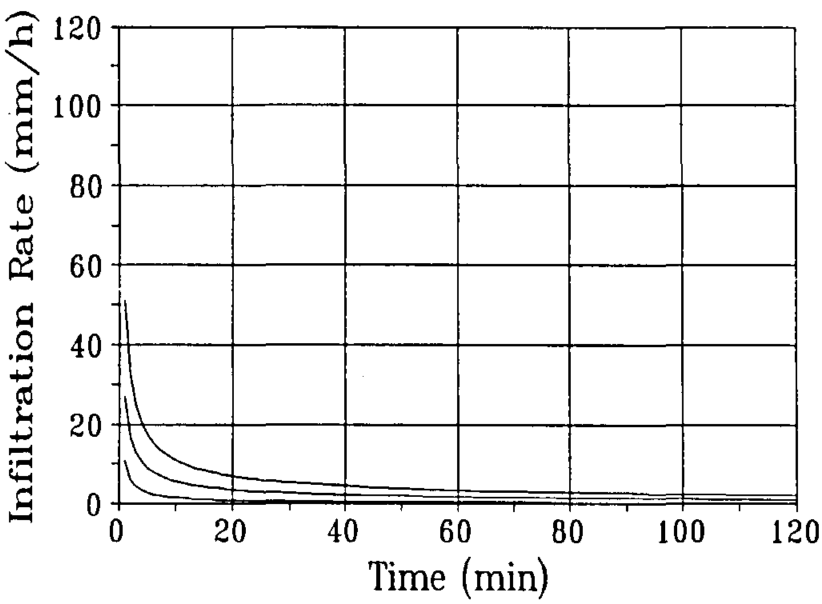


Figure 8.2. Infiltration curves for crusted soils under Karroid vegetation.

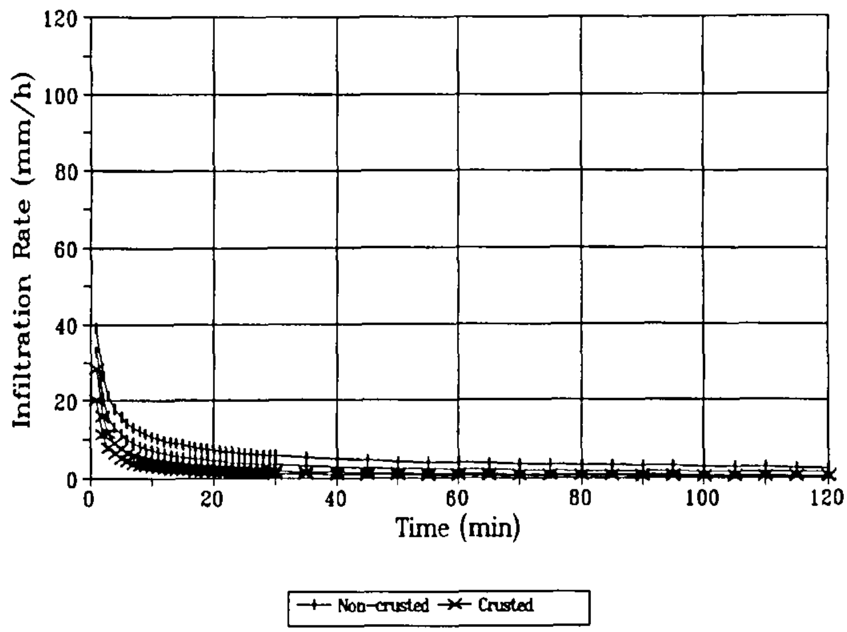


Figure 8.3. Infiltration curves for soils under mixed Karroid and grassland vegetation.

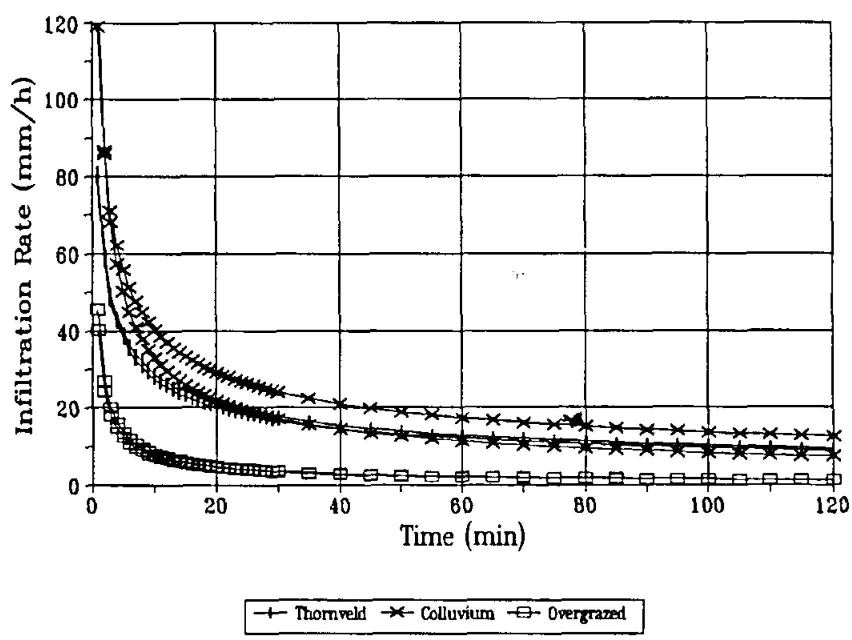


Figure 8.4. Infiltration curves for soils under grassland vegetation.

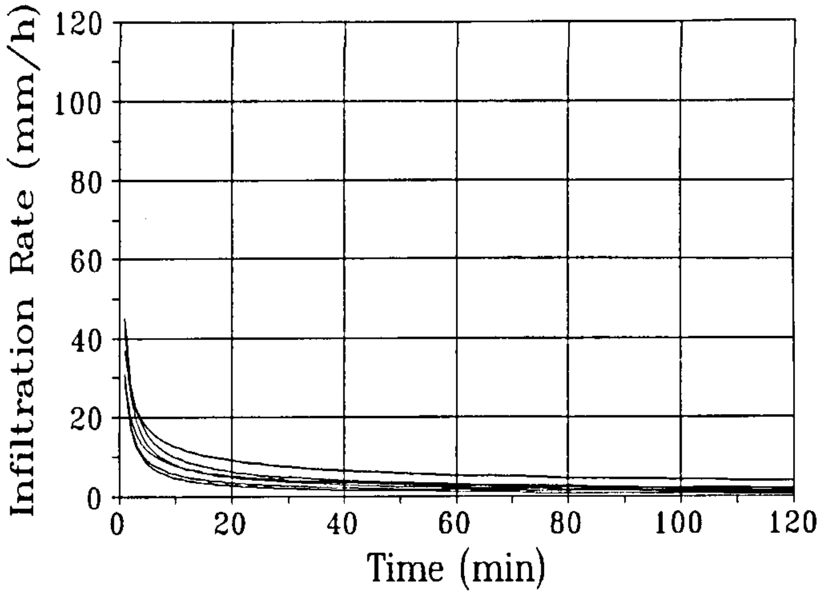


Figure 8.5. Infiltration curves for shallow soils under grassland vegetation.

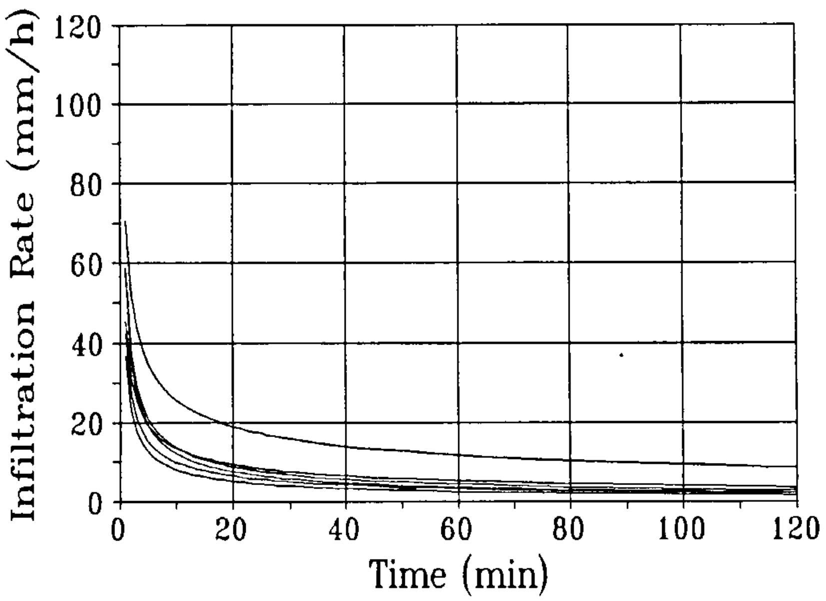


Figure 8.6. Infiltration curves for soils developed on alluvium.

The infiltration curves show that there is very little spatial variation in final infiltration rates when vegetation and soil surface conditions are similar. There is, however, a great discrepancy in initial infiltration rates (figures 8.1-8.6) and a smaller one in final infiltration rates (table 8.1) between the different coverages. Initial infiltration rates vary from about 10 mm $h^{-1}$ to 150 mm $h^{-1}$, while final infiltration rates range from less than 1 to 15 mm $h^{-1}$. The lowest infiltration rates are found in crusted soils covered by Karroid vegetation. Under these conditions, initial infiltration rates are generally less than 30 mm $h^{-1}$. As these regions also have low k values (table 8.1), infiltration rates decline rapidly to less than 10 mm $h^{-1}$ in under 10 minutes (figure 8.2 and 8.3). The highest infiltration rates are found on colluvial footslopes where denser vegetation and deeper soils are found. Similarly, hillslopes covered by thornbush and grass, usually well vegetated with relatively deep soils, also have high infiltration rates. These regions have initial infiltration rates which exceed 80 mm $h^{-1}$ (figure 8.4). In addition they also have the highest k values, which implies that their infiltration rates decline at a slower rate than other soils. Hillslopes which have been overgrazed, or where the soil cover is shallow, have infiltration capacities approximately six to seven times lower than well vegetated areas (table 8.1). They also experience a more marked decline in infiltration rates over time, since they also have lower k values.

As a result of the large variations in initial infiltration rates, it would be expected that short duration storm events would generate overland flow from partial areas of the catchment where the infiltration rate is exceeded by rainfall intensity. These would most likely be on hillslopes, where soils are shallower, or where overgrazing and surface crusting has occurred. The higher infiltration rates encountered on the footslopes and alluvial valley bottoms would result in the re-infiltration of overland flow coming from the hillslopes. Longer duration events would likely cause more widespread overland flow due to the smaller variance in infiltration rates as time increases.

## 8.2 Soil moisture dynamics.

The data from the neutron access tube sites (section 2.5) are the only base upon which changes in soil moisture content can be assessed. Fortunately, the instrumentation was established fairly coincident in time with two major rainfall events which generated widespread runoff in the catchments. The first of these events occurred in October 1989 and the second in November of the same year. The first access tube site (NYN01 to NYN03) was established between the two events, while the others were established between December 1989 and March 1990.

Figures 8.7 to 8.12 illustrate some of the dynamics of moisture status variation at the three sites using three dimensional surface plots. It is difficult to portray the time series of moisture variation accurately and the data have been smoothed (in time and depth) to improve the visual appearance.

The first site provides an ideal opportunity to assess the changes in soil and alluvial material moisture content immediately before and after a major runoff event, as well as the way in which the material dries out during the following months. The effects of the event and some implications with respect to channel transmission losses have been written up in a published scientific paper (Hughes and Sami, 1991) and are also incorporated into section 2.4 of the main report. The major conclusions are that during some flow events, even up to a return period of 5 years, all runoff from 66% of the catchment can be absorbed, giving transmission losses as high as 75%. Larger events, which can transmit water across the alluvium, are likely to have lower percentage losses, but the volume of loss is still substantial. The effects on soil and alluvium moisture dynamics is that the increment during the storm is far greater than can be accounted for by rainfall on the valley bottom area itself.

Several points are illustrated by the moisture data for the 14 access tubes at site 1 :

i Two of the tubes, situated away from any major inundation, showed very little immediate response to the storm rainfall suggesting a very effective crusting mechanism (figure 8.7 for example).

ii One of the above tubes shows a delayed response (after 21 days) in the deeper layers, indicating some lateral subsurface re-distribution at depth (figure 8.7).

iii Other sites also demonstrate a delayed response at depth which could be accounted for by lateral or vertical re-distribution (figure 8.9).

iv Some tubes demonstrated an immediate response throughout their depth and as deep as 5.0m, but these were sites close to the end of the well defined gravel channel bed. The implication is much more rapid infiltration and permeability at these points than in other parts of the valley bottom, where well defined continuous channels with gravel beds are absent.

Approximately a month after this event, the trend in the moisture content at most levels in most holes is an exponential drying out, with no additional increments to moisture right up to the present day (August 1991). The rate of drying out and the minimum moisture content reached some 18 months after the November 1989 event are highly variable between the tubes and at different depths for each tube. This variability is not explicable only in terms of the differences in texture. Other effects such as differences in vegetation rooting depth and variations in vertical and lateral unsaturated moisture re-distribution are clearly important.

Fluctuations from the general drying trend have occurred at most 0.15 and 0.3m levels. Only on two occasions, and not in response to noticeably (from collected rainfall data) large events, have the deeper layers shown any fluctuations. This has only occurred at tubes which are situated close to hollows and channel features close to the valley side and in most cases the response is greater than can be accounted for rainfall (figure 8.8). This implies some localised input of surface runoff onto the valley floor from the slopes or a tributary channel with subsequent ponding and infiltration.

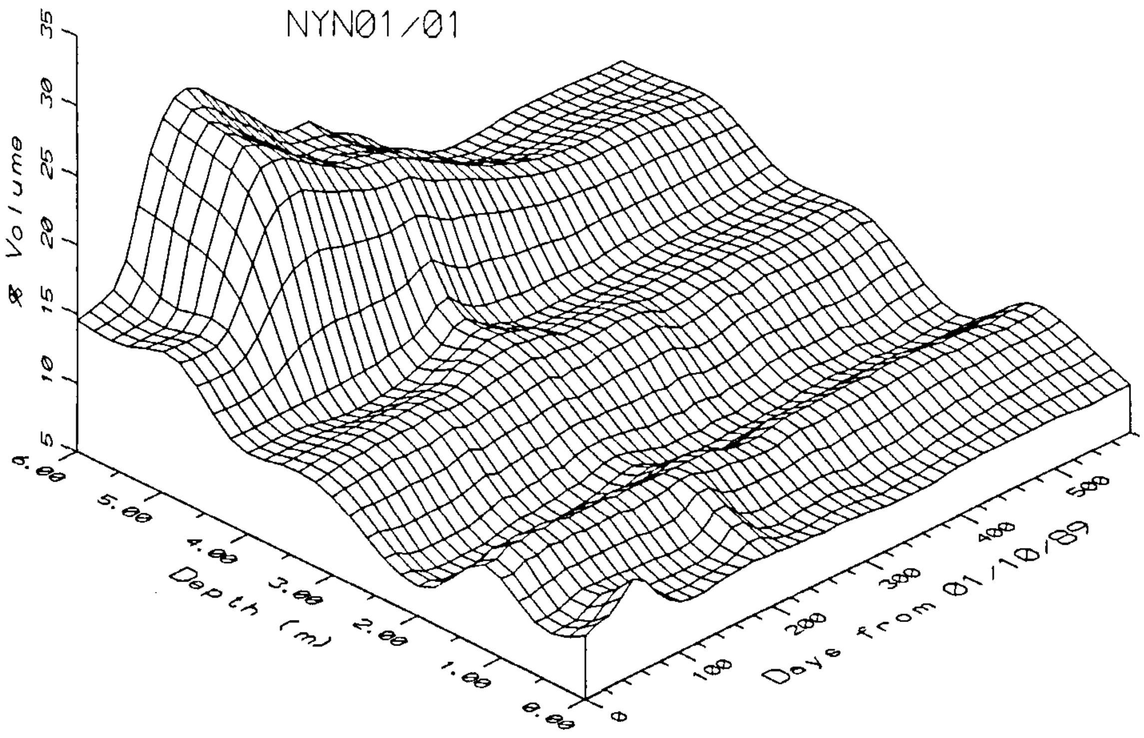


Figure 8.7 Time series of soil moisture variation at NYN01/01. A delayed response in the deeper layers (> 5.0m) can be seen.

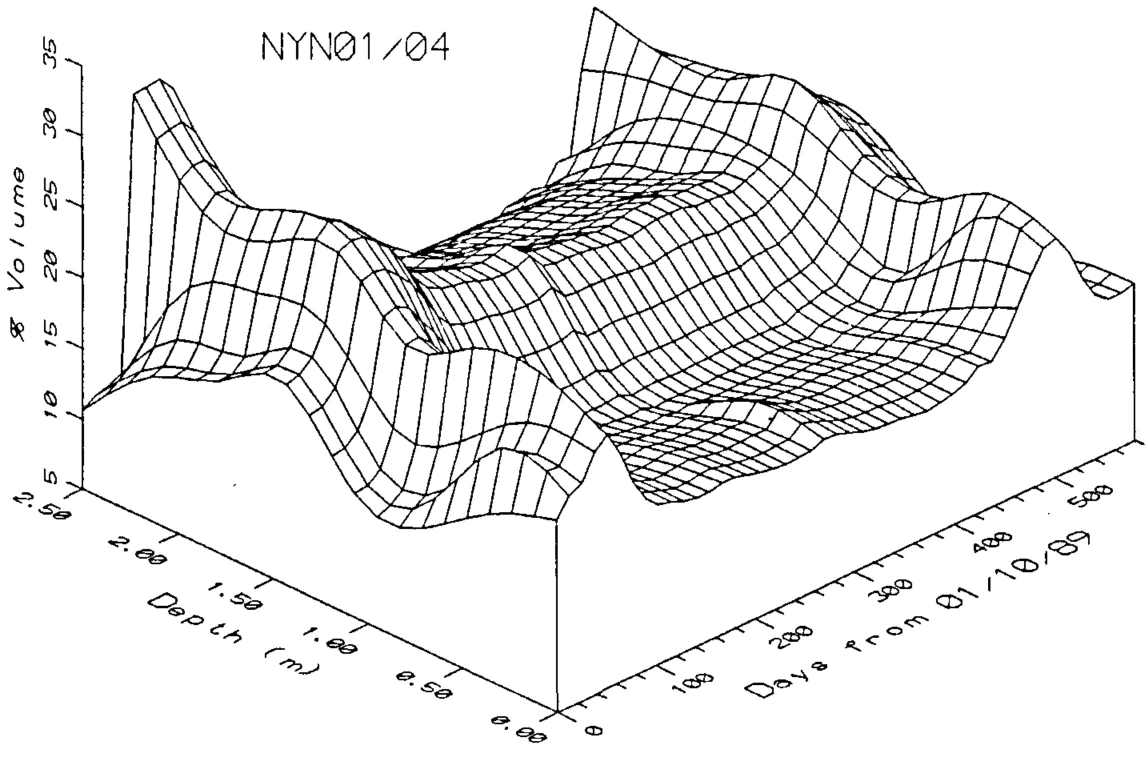


Figure 8.8 Time series of soil moisture variation at NYN01/04. All layers respond to the November 1989 event as well as to an event in January 1991.

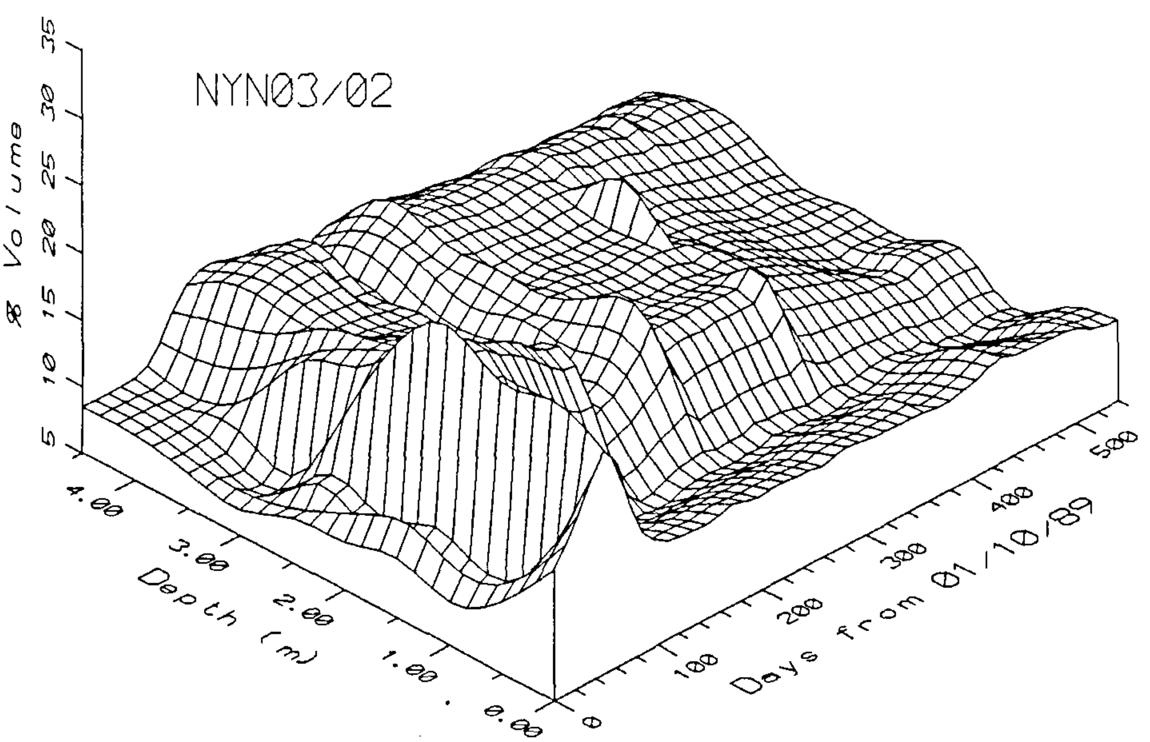


Figure 8.9 Time series of soil moisture variation at NYN03/02. While the surface layers and depths to about 2.0m demonstrate an immediate response to the November 1989 event, the deeper layers response is delayed.

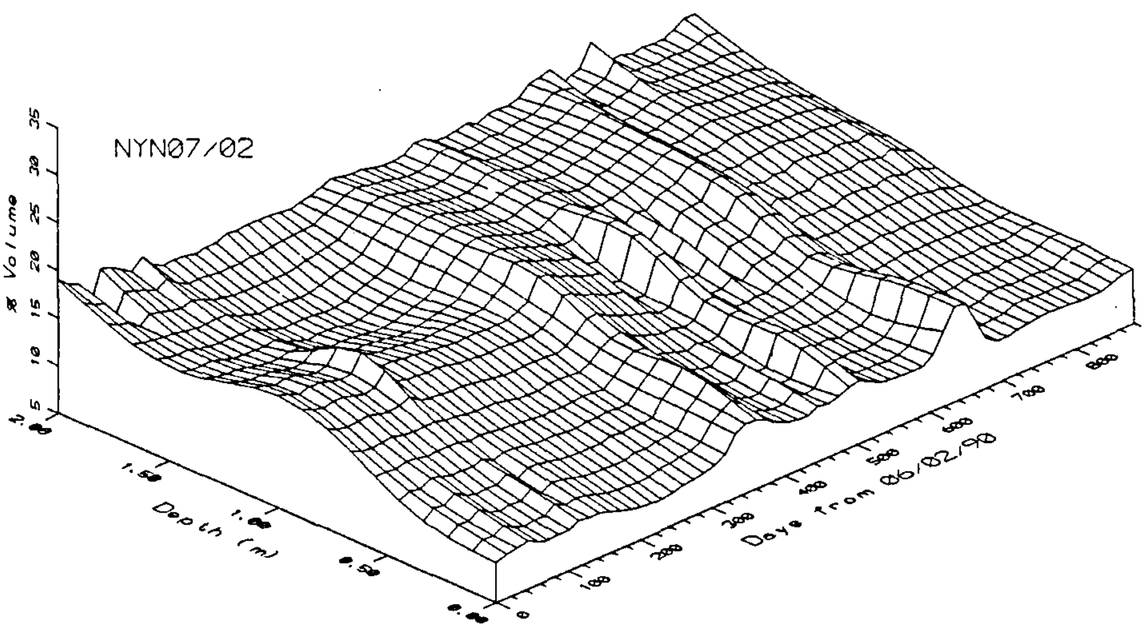


Figure 8.10 Time series of soil moisture variation at NYN07/02. This hole was installed after the November 1989 event and lies close to a hollow on the valley floor.

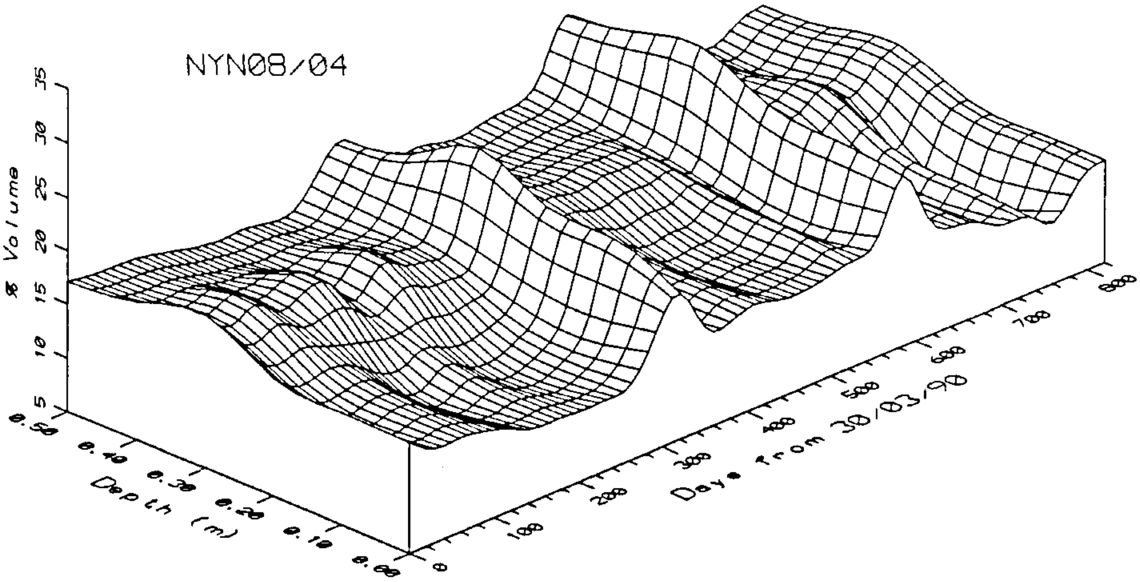


Figure 8.11 Time series of soil moisture variation at NYN08/04. This is a shallow hole on the valley side of the first order catchment and shows fluctuations associated with minor and major rainfall events.

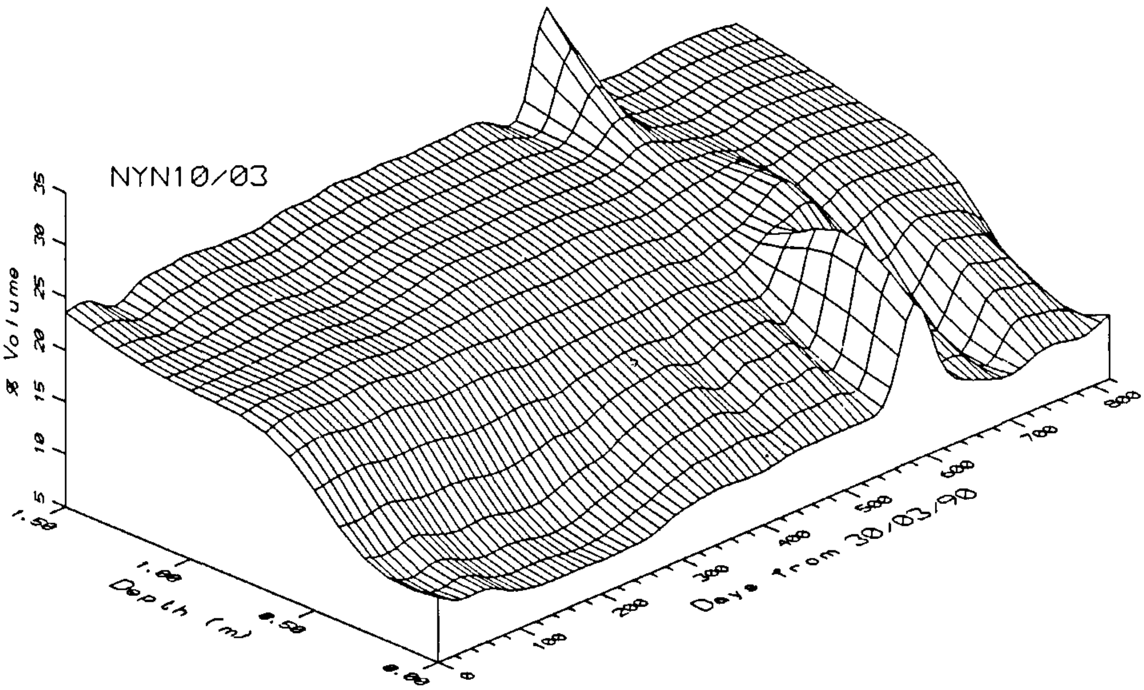


Figure 8.12 Time series of soil moisture variation at NYN10/03. This is a valley bottom hole in the first order catchment and shows the sustained higher moisture levels in the deeper layers.

The second group of access tubes were established after the November 1989 event but still within the period when the moisture content was relatively high in many of the first sites holes. Very few of the 16 holes at this site show any evidence of the event (figure 8.10), nor any response to events since then. There is a much better defined channel at this site and the bed is predominantly bedrock. There therefore seems to be much less evidence of transmission losses and resulting increment to soil and alluvium moisture content. Where a recession curve is found at the beginning of the observation period, the tubes are located close to hollows in the valley floor and where the normal channel becomes constricted and less well defined. These tubes also show at least some response to one or two later events (figure 8.10). The conclusion reached is that transmission losses through the banks of well defined channels is not an important process. For losses to be significant, either seepage through a gravel bed into the underlying alluvial material, or infiltration of overbank flows into the surface of the valley floor, must take place. Some of the relatively minor (in some cases non-existent) fluctuations in the shallow levels of some tubes suggests that surface crusting of the valley bottom soils plays a significant role.

Many of the holes at the third site are only deep enough to allow a reading to be taken down to 0.3m (figure 8.11) and some only at 0.15m. All the tubes show fluctuations at these depths which can be approximately related to rainfall events that occurred up to several days prior to the moisture readings. However, the frequency of moisture readings is not sufficient to develop any relationships between rainfall characteristics and moisture increments. Where deeper soils do exist (up to 2.0m), the deep horizons appear to have remained relatively wet (close to 20% moisture by volume, figure 8.12) throughout the period of record. This may be partly due to relatively frequent additions of moisture during the summer months caused by re-infiltration of small amounts of runoff generated on the slopes during intense convective storms. Saturated surface conditions and runoff on the slopes, but not in the valley bottom, have been observed on several occassions. The relatively shallow rooting depth of the grass vegetation and the higher moisture retention properties of the deeper horizons may also contribute to sustaining the moisture contents of the valley bottom lower soil layers. Further investigations, of the runoff generation mechanisms and associated soil moisture dynamics of typical first order catchments should provide more information.

# 9. SURFACE HYDROLOGY.

## 9.1 Patterns of runoff generation.

There have been too few runoff events over the period of this study to define the patterns of runoff generation in truly quantitative terms. However, the information contained within the previous sections and a number of qualitative observations of the processes active in the catchments during a number of rainstorm events with different characteristics do allow a number of factors to be identified which together allow a conceptual model of the major runoff producing mechanisms to be proposed.

i Soil depth is variable throughout the area, lying between virtually zero and over 1m. While, the shallower soils are often found on the valley sides and the deeper ones in the valley bottoms, this is not always the case. In the valley bottoms, where alluvial or colluvial material has accumulated, there may be several metres of additional unconsolidated material lying below the soils proper.

ii Similarly, ground vegetation cover is also spatially variable as well as being temporally variable depending upon season as well as recent rainfall history. Again, the valley bottoms often have the better developed ground cover.

iii In response to the above two variations it is not surprising that the surface infiltration characteristics are also variable. The data gathered from the infiltration studies confirm the existence of crusting in areas where the surface cover is very sparse and the fact that infiltration rates are much higher in the bottom slope areas where the grass cover is more dense.

iv Comparison of rainfall intensities with infiltration rates suggests that there will be a substantial variability in the areas which generate infiltration excess surface runoff. The variations in rainfall intensity that occur over the area during one event, as well as between rainfalls of different types, suggests that the actual occurrence of this type of runoff generation mechanism will be highly variable in space and time.

v The fact that infiltration rates can be variable down a slope, with the higher rates often occurring in the valley bottoms, suggests that runoff generation on parts of the slope and re-infiltration further down the slope is a highly probable process, particularly during short duration, high intensity convective storms.

vi Several factors lead to the conclusion that during summer convective events, the development of saturated areas is highly unlikely. These include the frequency of storm events, their total depth of rainfall, the high rates of evaporation between events and the total soil profile available storage even for some of the relatively shallow (0.2m) soils. During relatively large convective storms, where infiltration excess runoff occurs on the slopes which re-infiltrates into the valley bottom soils, there may be some potential for small saturated areas to develop.

vii During large area, long duration events (notably cut-off low events such as November 1989), there is a great deal more potential for saturated areas to develop and it is quite likely that the runoff generation mechanisms during these storms are quite different to those prevailing during convective storms.

viii On the relatively gentle slopes, which cover a large part of the catchment, and where the roughness of the micro-topography is high, the potential for depression storage is relatively high. It is very difficult to quantify this effect, but field observations during rainfall storm events provide qualitative evidence.

ix There is ample evidence, even from the few events that have been observed, to suggest that transmission losses through channel beds as well through 'floodplain' surfaces play a role in determining patterns and volumes of channel flow (see section 6 and Hughes and Sami, 1991).

A convective storm event occurred in February 1991 and resulted in a small amount of flow being recorded through the H-flume (NYQ07) at the outlet of the first order catchment, B6. The amount of flow, the rainfall intensity and the information that is available on infiltration curve characteristics were used to try and understand the runoff processes involved during this event. However, it is clear that much more data are required over a wider range of event sizes before such an analysis can be realistically attempted. Using the infiltration curves, not accounting for depression storage, but making some attempt to allow for re-infiltration in the lower slope and valley bottom areas, results in an estimated runoff depth for the storm of some 0.4mm (total rain depth is 12.6mm over 2.5hr). The actual recorded runoff depth was a mere 0.0065mm. This example is included only to illustrate that the small size of the events, their infrequency and the number of variables involved in the runoff generation process that cannot be effectively quantified, means that it is very difficult to confirm conceptual ideas with actual quantitative data.

## 9.2 Streamflow variations.

Table 9.1 lists most of the runoff events that have been observed at the flow gauging sites NYQ01 to NYQ06 during the period 1989 to early 1991. It is clear that not many have occurred over approximately a 2.5 year period of measurement and apart from the event in November 1989, the others have contributed only small amounts of flow.

Although no events are listed for NYQ03, the baseflow from the November event carried on well into March of 1990 and several very small events (highest peak of 0.04 $m^3 s^{-1}$) were superimposed upon this. This is the only station to demonstrate this kind of sustained baseflow apart from the main weir at NYQ01. This feature may of course be related to the rather large dam just upstream of the gauging station.

The event of February 1991 appears to have been the result of an intense storm which was limited to the southern central part of the catchment and did not even extend very far into the catchment of NYQ06. The lack of response in NYQ05, relative to NYQ06, when the former appears to have received the higher rainfall, points to some differences in their response characteristics. This may also be seen by comparing the peak flows and durations of the October and November 1989 events. The smaller catchment (NYQ06) has the longer durations and the higher flows.

Table 9.1 List of major runoff events in the five gauged catchments.

| Station | 02/10/89 | 14/11/89 | 17/11/89 | 12/12/89 | 01/02/91 | 04/02/91 |
|---|---|---|---|---|---|---|
| NYQ01/02 | 6 days<br>0.82 | 27.5 days<br>>70 | | 15.5 days<br>1.32 | 9.5 days<br>0.11 | |
| NYQ03 | Missing | Missing | | | | |
| NYQ04 | 2 days<br>0.25 | 2.5 days<br>16.6 | 3 days<br>0.78 | | | |
| NYQ05 | 1.5 days<br>0.02 | 6.5 days<br>3.0 | | | | |
| NYQ06 | 5.5 days<br>0.83 | 8.5 days<br>4.03 | | | 1 day<br>0.60 | 3 days<br><0.01 |

The number of days refers to the approximate duration of flow for that event.
The other figure is the peak discharge in $m^3 s^{-1}$.

There is very little that can be concluded form the available figures at present, owing to the small number of events. Only when more data are available will comparisons between the different catchments be able to be made. Any attempt at analysis at this stage would be pure speculation.

## 9.3 Impoundments.

A total of 364 farm dams have been identified within the Bedford catchments using a combination of 1:50 000 topographic maps and the specially flown 1:20 000 colour aerial photography. Of these a sample of 31 have been surveyed in the field to determine their depth/area/volume relationships. The full supply area for the remaining dams has been determined by digitising direct from the aerial photographs. The technique involved using at least four control points, identifiable on both the 1:50 000 topographic sheets and the photos and surrounding a group of dams to scale the specific area on the photos. Figure 9.1 illustrates the percentage errors between field surveyed areas and the areas determined from digitising the aerial photo image of the 31 dams. The figure indicates that some 60% of the areas were digitised to within 10% of the surveyed area. Earlier attempts to size the dams from both the 1:50 000 maps and 1:50 000 black and white aerial photography were not successful.

The field survey data has been used to develop approximate relationships between full supply area and volume. It was not possible to derive a single relationship for all dams and consequently one equation for dams up to 6000 $m^2$, and one for those greater than this size is used. The equations are as follows :

$$\text{Volume (m}^3\text{)} = [\text{Area(m}^2\text{)} / 50.0]^{1.817} \qquad \text{for areas} < 6000 \text{ m}^2$$

$$\text{Volume (m}^3\text{)} = 1000 * [\text{Area(m}^2\text{)} * 0.0017 - 4.0] \qquad \text{for areas} > 6000 \text{ m}^2$$

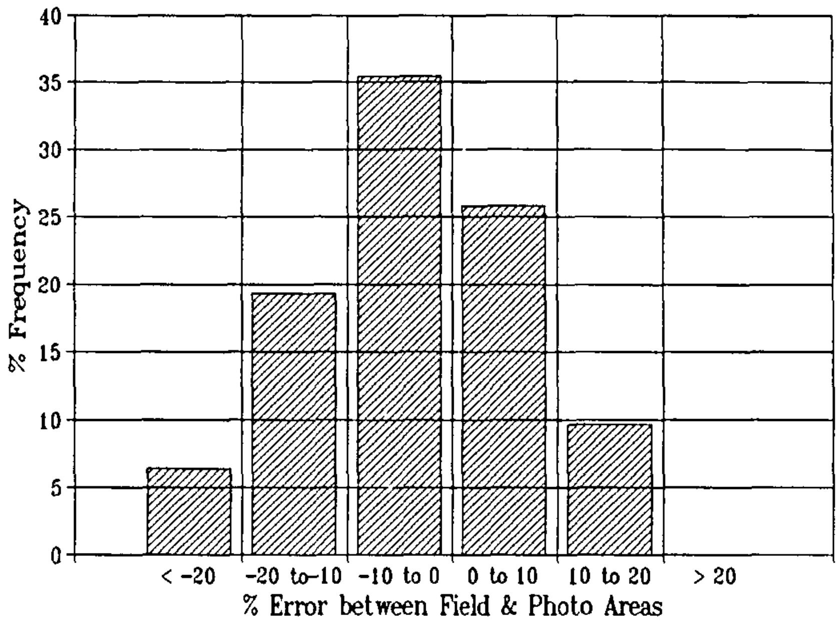


Figure 9.1 Percentage error in aerial photo estimated full supply area.

These relationships have been used to estimate the volumes of the remaining dams. The catchment areas of all the dams and the downstream sequence relationship between dams have also been determined. Figures 9.2 and 9.3 illustrate the frequency of dams falling into several volume and catchment area categories. Clearly, most of the dams are small (less than 2 000 m$^3$) and drain relatively small areas (less than 2 km$^2$). The runoff capacity of all the dams has been calculated from the catchment areas and the full supply volumes and taking into account the amount of runoff absorbed by upstream dams. Figure 9.4 illustrates that most dams only require up to 2mm of runoff to fill them, but there is a significant number that require 10mm or more. Figure 9.5 relates the runoff capacity to the upstream catchment area of the dams and it is evident that most of the high capacity dams have relatively small catchment areas. The plotted catchment areas have not taken into account any of the artificial runoff harvesting that takes place in the catchment. This is achieved using contour furrows to intercept slope runoff and effectively increase the catchment area of some dams. These features often account for the rather excessive dam sizes (relative to catchment area) that are sometimes found. The one that stands out is the large dam between Malangskraal and Elizabeth Farms in the north east part of the catchment. This dam has a runoff capacity of more than 10mm and effectively absorbs all runoff from the catchment area draining the mountain north of Bedford in all but the largest events.

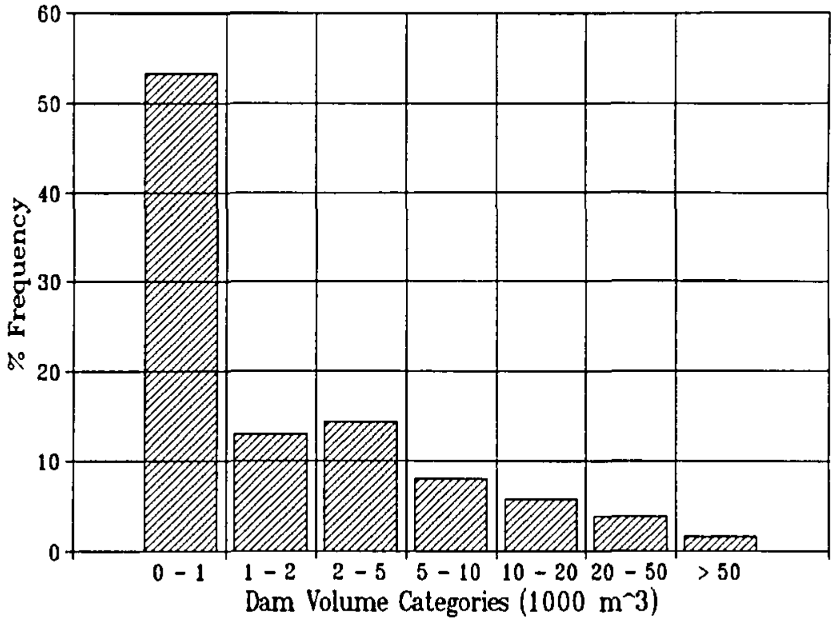


Figure 9.2 Frequency histograms of dam volumes.

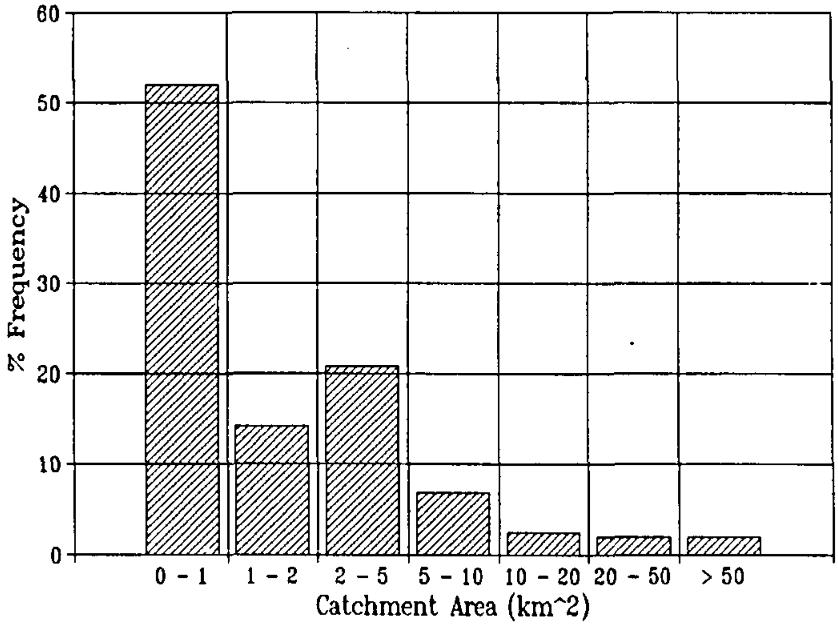


Figure 9.3 Frequency histograms of dam catchment areas.

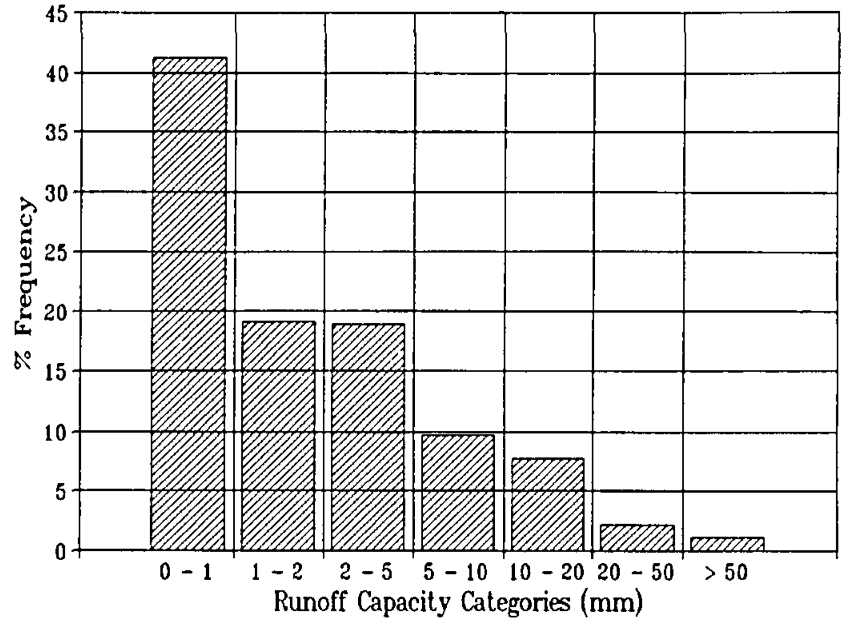


Figure 9.4 Frequency histograms of runoff capacity.

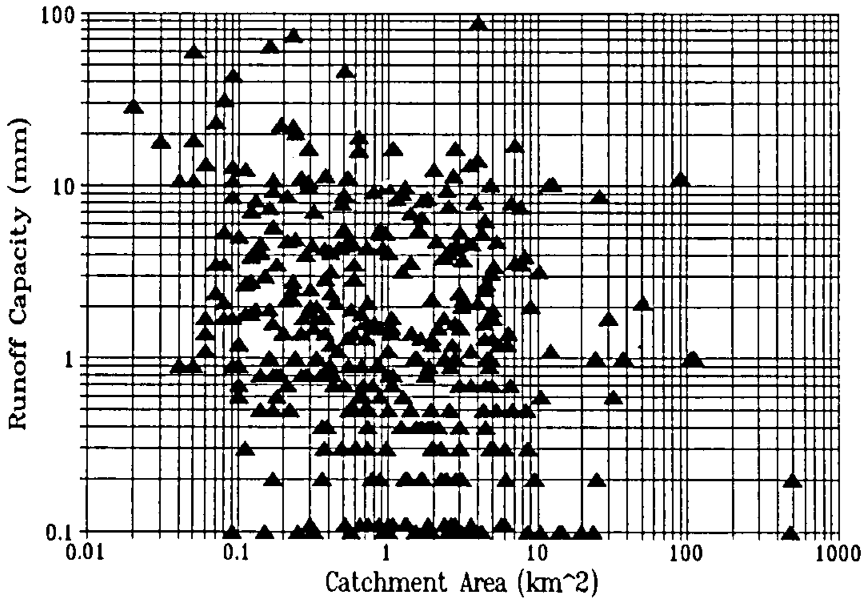


Figure 9.5 Relationship between dam catchment areas and runoff capacity.

# 10. GROUNDWATER HYDROLOGY.

## 10.1 Hydrogeology.

Most of the sedimentary rocks of the Beaufort Group, as well as the dolerite dykes, have extremely low permeabilities and porosities in their consolidated state. However, the jointing and fracturing which have resulted from the intrusion of dolerite and from the directed stress of the Cape orogeny have imparted highly variable secondary permeabilities to these rocks. Since the sandstones have undergone a high degree of lithifaction, it can be assumed that they deform in a brittle fashion and fracture in reponse to stress. The mudstones behave in a more ductile fashion due to their high clay content, resulting in a more plastic response to directed stress. As a result, sandstone beds located in the vicinity of dolerite intrusions and changes in bedding dip (Appendix A) are the predominant water bearing formations in the catchment.

## 10.2 Yields.

The quantity of water capable of being abstracted from these fracture zones and its sustainability is dependent on the regional inter-connectedness of fractures but is usually very limited. According to a survey of local farmers, borehole yields range from 0 to 100 000 l $h^{-1}$ (figure 10.1). This yield distribution, however, is not regionally representative of aquifer transmissivites since the results are based on the existing borehole network, which has been established with a subjective bias; almost all boreholes being located in valley bottoms. A study by Sami (Appendix A) discusses the geologic factors which affect borehole yields and the probabilities of achieving expected yields in different geologic environments. This study shows that boreholes located adjacent to dolerite intrusions, or in the vicinity of changes of bedding dip have significantly higher yields than boreholes located near faults, fold axes or where no structural deformation can be observed. Furthermore, these boreholes always struck water and 60% have yields greater than 3600 l $h^{-1}$, whereas up to 20% of boreholes in undeformed beds are dry and only about 30% have yields exceeding 3600 l $h^{-1}$. The study also showed that borehole depths and the mean saturated depth of the aquifer penetrated did not significantly affect yields, implying that productivity is not dependent on the area of the saturated seepage face. Therefore, massive blocks of the aquifer do not transmit water and yield is dependent on the permeability of discrete fracture traces intercepted by the borehole. A parameter which affects borehole yield is the catchment order in which the borehole was located, with boreholes in higher order catchments prdoducing significantly higher yields. These higher yields may reflect the larger potential catchment areas of boreholes in higher order catchments. Alternatively, stream order may be an index of the erodability and potential fracturing of the underlying rock, and hence of permeability, since streams tend to develop along the axes of structural weaknesses.

## 10.3 Water levels.

The existence of artesian conditions and large water level variations in adjacent boreholes indicates that semi-confining conditions may exist. Rest water levels therefore represent a piezometric surface rather than a contiguous water table. Figure 10.2 shows that the regional hydraulic gradient is from west to east, reflecting the geologic barrier to north-south flow caused by the dolerite dykes. Local flow convergences exist in the two valleys occupied by east-west flowing streams.

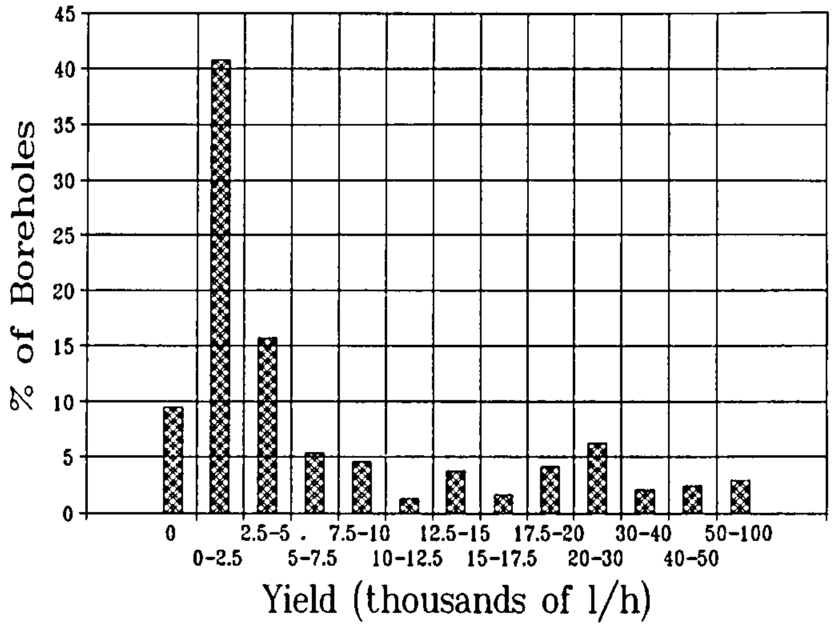


Figure 10.1 Frequency distribution of borehole yields.

Water levels in the monitored boreholes indicate that there has been only one major recharge event since April 1989 (figures 10.3 and 10.4). This occurred following the rains of October and November 1989 (section 3.3). Water levels in the various boreholes responded differently to this event. North of the central dolerite dyke, water levels in borehole BCG03, the most westerly site, began to rise immediately following the recharge event of November 14, rising 2 m by December 13, 1989, 30 days after the storm event (figure 10.5). This response implies that recharge of a local origin is occurring. Local recharge, approximately 70% of the total received by the borehole (figure 10.6), apparently halts at this time, since no further increase is observed by January 11, 1990. Water levels in BCG03 subsequently rose gradually until approximately 140 days, when the maximum water level was reached in April 1990 (figure 10.7). This subsequent delayed 1 m rise may reflect slower diffuse vertical recharge or lateral inflow from upgradient recharge zones.

Eastward along the topographic convergence, borehole BAG03 kept rising until August 1990, 275 days after the event, whereas BAG10 kept rising for 530 days, reaching its maximum level in April 1991 (figure 10.7). This time lag suggests that eastward groundwater flow is an important source of recharge for boreholes in the central part of the catchment. Unfortunately, since these boreholes were not monitored at the time of the recharge event, the existence and magnitude of any local recharge cannot be ascertained. BBG20, located at the western edge of the catchment near the northern edge of the central dyke, exhibits a 0.2m rise (35% of total recharge), within 10 days of the recharge event (figures 10.5 and 10.6). Lateral redistribution subsequently results in a further 0.4m rise over 420 days (figure 10.7).

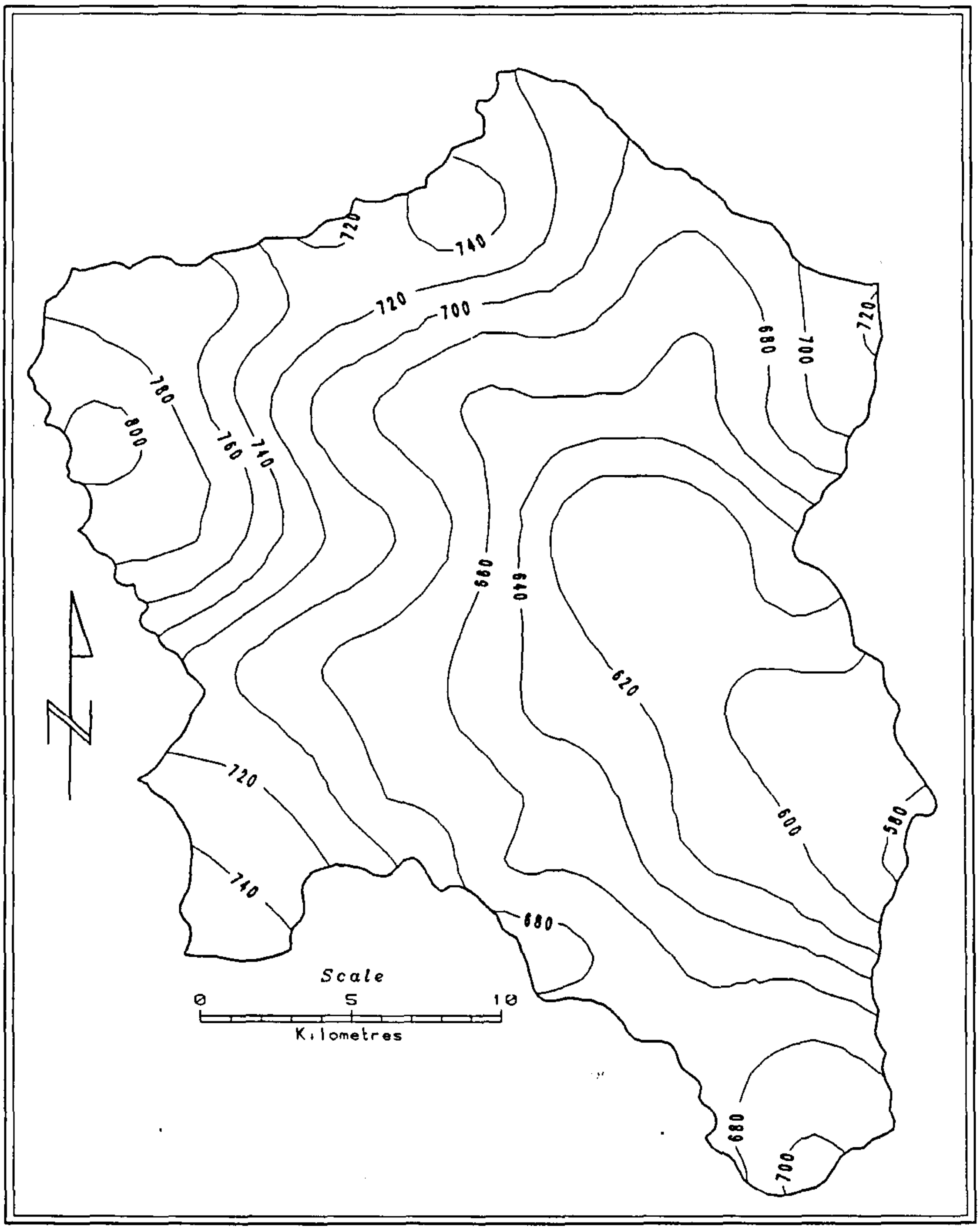


Figure 10.2 Approximate piezometric surface based on borehole rest water levels.

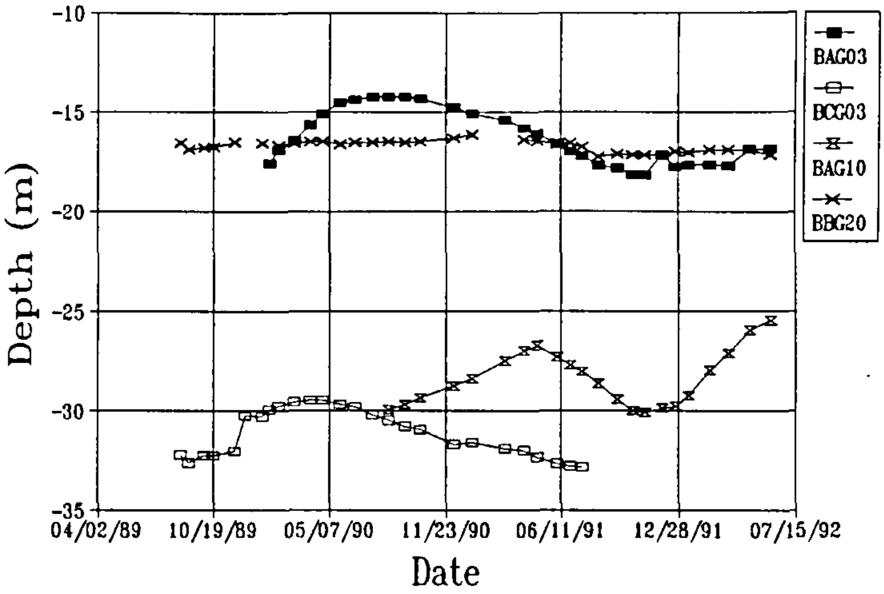


Figure 10.3 Time series of water level depths in boreholes north of the central dolerite dyke.

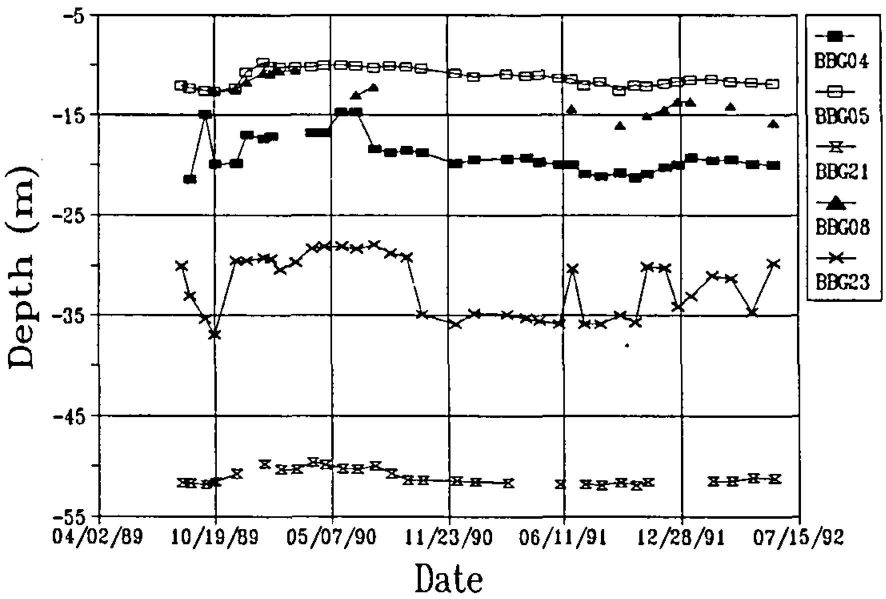


Figure 10.4 Time series of water level depths in boreholes south of the central dolerite dyke.

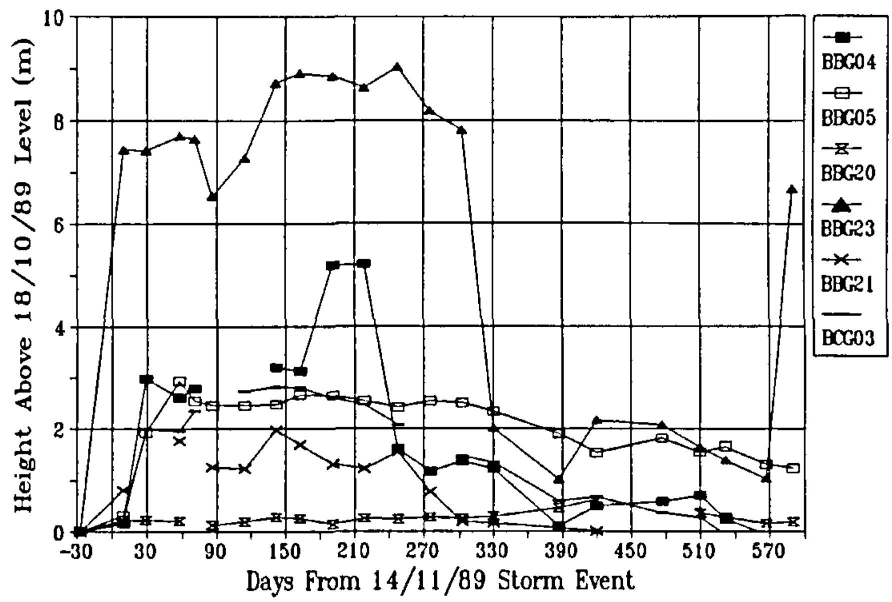


Figure 10.5 Height of water levels above 18/10/89 baseline.

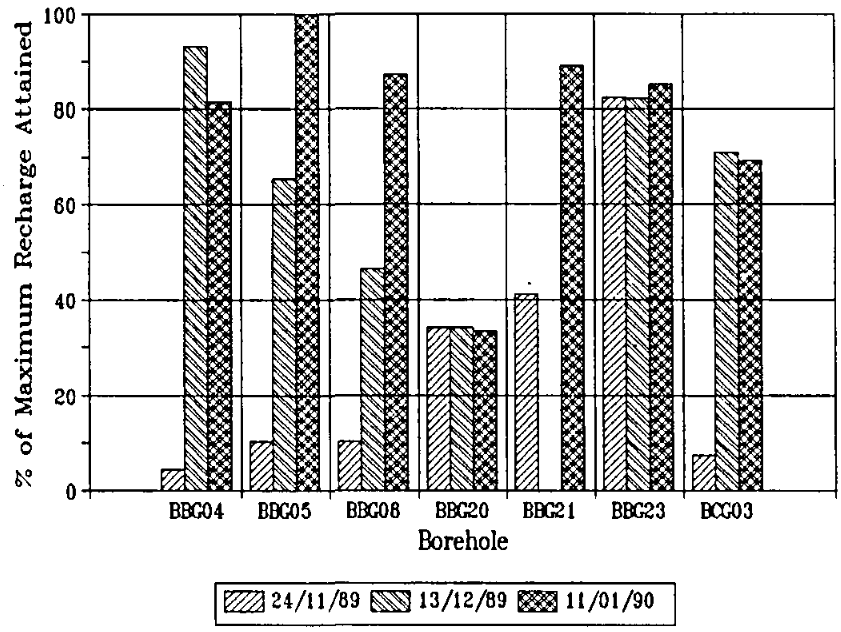


Figure 10.6 Percentage of total borehole recharge occurring after 10, 29 and 58 days following the November 14, 1989 storm event.

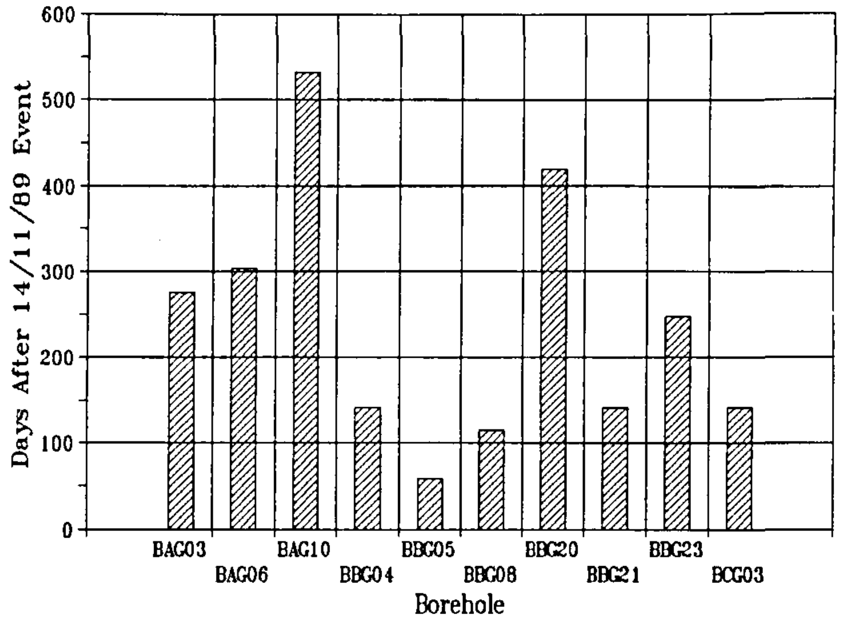


Figure 10.7 Approximate number of days after November 14, 1989 storm event at which boreholes reached their maximum water level.

South of the dolerite dyke boreholes BBG04, BBG05, BBG08, BBG23 and BBG21 all show an immediate response to the November event (figure 10.4). The large rise in BBG23 may be an error as the windmill failed subsequent to the baseline reading in October 1989. As a result, a significant portion of the water level rise recorded in November 1989 may be due to recovery instead of recharge. Upon repair of the windmill and a return to a normal abstraction regime in October 1990, water levels immediately dropped nearly 6 m. In addition, the near 6 m increase recorded in June 1991 also reflects a period where abstraction was halted. It is therefore likely that the actual water level rise resulting from natural recharge is in the vicinity of 3 m instead of the recorded 9 m (figure 10.5). The delayed peak of May and June 1990 in BBG04 may also be an error, since an obstruction developed in the borehole at this time. Consequently, this peak is ignored in figure 10.7. BBG05, the furthest south, reached its maximum water level in about 60 days following the recharge event. BBG04, BBG08 and BBG21, within the fracture zone and flow convergence immediately south of the dyke, were recharged for 140, 120 and 140 days respectively (figure 10.7). Therefore, with the exception of BBG23, most of the water level rise in these boreholes occurs immediately following the recharge event and a delayed rise from lateral redistribution is not as significant as to the north.

## 10.4 Groundwater Recharge.

As all the boreholes have been selectively sited in low lying areas adjacent to stream channels, they are located near potential recharge zones. The time lag data, however, shows that none of the boreholes reached their maximum water levels within a month of the event.

This suggests that recharge rates are slow. The rapid responses observed by November 24 cannot be attributed to a rapid response to the November 14 event, since they may reflect recharge from the October 2-3 event. The long time lags exhibited by the centrally located boreholes also suggests that the spread of groundwater from recharge zones to adjoining parts of the aquifer is also slow. The significant delay exhibited by BAG10 implies that dewatering of the aquifer by subsurface drainage is a relatively slow process, despite a regional hydraulic gradient of approximately 0.012 (figure 10.2). Regional transmissivities must therefore be low and groundwater conditions relatively stagnant.

Due to the signifance of fractures on the hydrogeology and the highly variable permeabilities they create in relation to the limited number of observation boreholes, and as several of the boreholes reflect lateral groundwater redistribution, it is not possible to use conventional saturated volume fluctation methods to calculate natural recharge. Further theoretical constraints which limit the applicability of such methods are discussed in Sami (1991).

An alternative geochemical recharge estimation model presented in Sami (1991) and has been tested in this catchment. Preliminary results indicate that mean annual recharge varies spatially from 0 to 12 mm $y^{-1}$ with a mean of about 4.5 mm $y^{-1}$ (equivalent to approximately 1% of the MAP). The highest recharge rates occur in areas where surface ponding develops over shallow soils and where transmission losses occur in gravel bed and fractured rock channels. The lowest rates are in the northeastern quadrant where relatively deeper soils exist.

The November 1989 event generated approximately 12-15 mm of recharge, equivalent to 10% of rainfall. This large influx may be attributed to the long duration and high total rainfall input of this event. This suggests that recharge may be infrequent event and dominated by large events which generate larger than average recharge fractions.

### 10.5 Aquifer Hydraulic Parameters.

Pump tests have been carried out on 2 boreholes located on the farm Request in order to obtain aquifer transmissivity and storativity values. The physical parameters of these test holes and any observation holes are given in tables 10.1 and 10.2. Suitable locations for further pump tests are few as boreholes tend to be dispersed and the availability of observation holes is limited.

Table 10.1 Physical parameters of borehole BRG05.

| Site | Distance (m) | Elevation (m) | Water level (m) | Depth (m) | Diameter (mm) | Casing (m) |
|---|---|---|---|---|---|---|
| BRG05 | | 752 | -29.63 | 70 | 165 | 10 |

Table 10.2 Physical parameters of borehole BRG07 and associated observation holes.

| Site | Distance (m) | Elevation (m) | Water level (m) | Depth (m) | Diameter (mm) | Casing (m) |
|---|---|---|---|---|---|---|
| BRG07 | | 843 | -41.36 | 90 | 165 | 10 |
| OB1 | 38.35 | 845 | -44.38 | | 165 | 10 |
| OB2 | 44.25 | 842 | -39.97 | | 165 | 10 |

An evaluation of the data from constant rate pump tests provides some information on the aquifer's hydraulic parameters. The results of the tests are given in Table 10.3. Two borehole recovery methods of analyses were used, Recovery I is based on calculated recovery while Recovery II is based on residual drawdown as a function of cumulative time/recovery time (Driscoll, 1986).

Table 10.3 Estimates of aquifer hydraulic parameters from pump tests.

| Borehole | Method | Transmissivity ($m^2 d^{-1}$) | Storativity |
|---|---|---|---|
| BRG05 | Cooper Jacob | 137 | |
| BRG05 | Recovery I | 98 | |
| BRG05 | Recovery II | 112 | |
| BRG07 | Cooper Jacob | 58 | |
| BRG07-OB1 | Cooper Jacob | 56 | 0.011 |
| BRG07-OB1 | Recovery I | 78 | 0.013 |
| BRG07-OB1 | Recovery II | 89 | |
| BRG07-OB2 | Cooper Jacob | 63 | 0.008 |
| BRG07-OB2 | Recovery I | 90 | 0.009 |
| BRG07-OB2 | Recovery II | 106 | |

The high yield borehole (18 000 l $h^{-1}$) BRG05 is located in a third order catchment and was pumped for 24 hours at a rate of 72 $m^3$ $day^{-1}$. Water levels were monitored in the hole, and in the 2 nearest observation holes (about 1 km away) which did not respond to abstraction. As a result, coefficients of storage could not be determined. The graphs for this pump test and the subsequent recovery are shown in figures 10.8 and 10.9. Figure 10.8 shows that drawdown is not quite linear. The increasing slope of the time-drawdown curve within 10 minutes of the start of the test suggests that impervious boundaries are located fairly close to the borehole. This observation, along with the high measured transmissivities, imply that

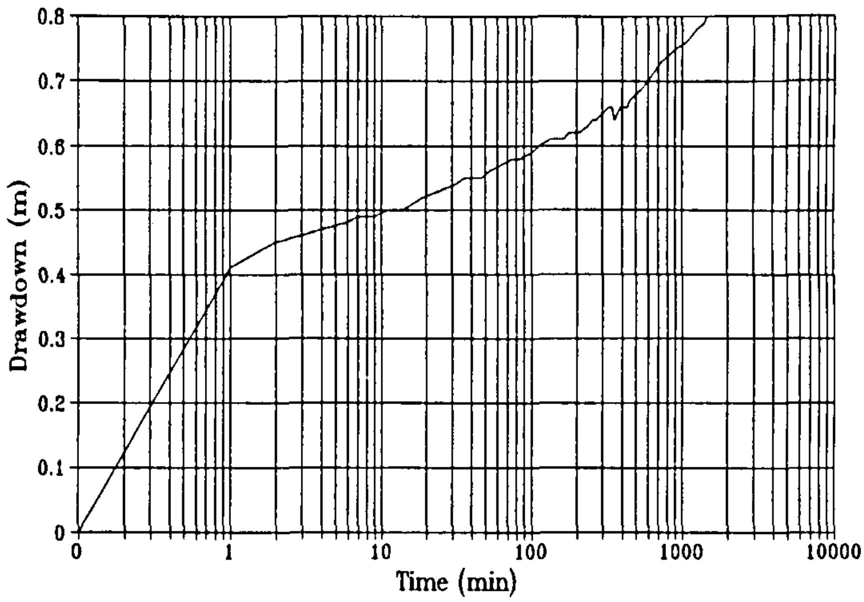


Figure 10.8 Pump test drawdown for borehole BRG05.

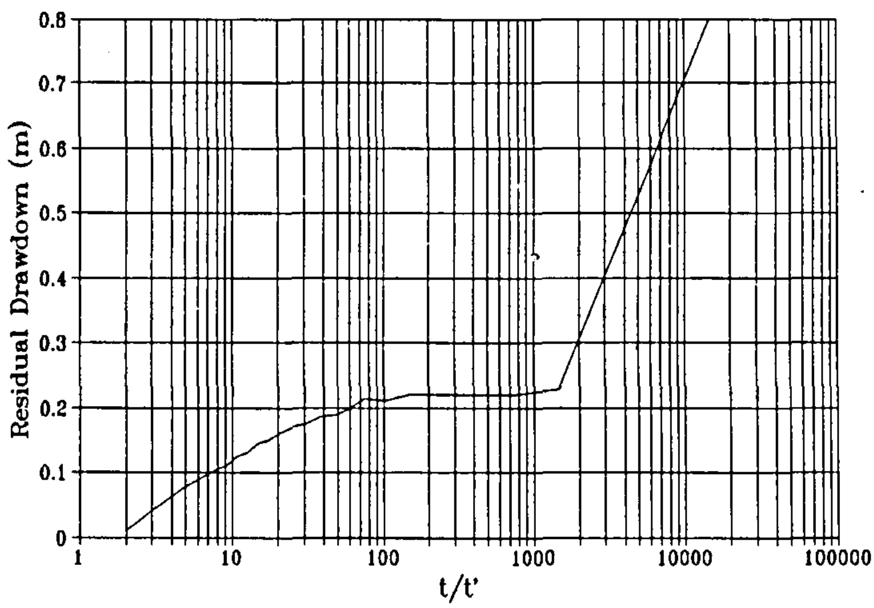


Figure 10.9 Pump test recovery for borehole BRG05.

the borehole taps highly permeable discrete fractures or joints. As the residual drawdown curve (figure 10.9) appears to intersect the y-axis close to 0m, the borehole completely recovers and must therefore be relatively well connected to the regional groundwater.

Borehole BRG07 is located in a first order catchment, has a yield of 1350 l $h^{-1}$ and was pumped for 24 hours at a rate of 62 $m^3$ $day^{-1}$. In addition to a Cooper Jacob analysis (figures 10.10 and 10.11), results from OB1 were also evaluated using the method suggested by Sen (1990) in order to verify whether linear flow conditions, assumed in a Cooper Jacob interpretation, exist. Drawdown measured in OB 1 was shown to be more similar to the theoretical linear flow type line rather than to turbulent flow type lines (figure 10.12), thus calculated transmissivities obtained by the traditional Cooper Jacob interpretation are valid. The recovery data from this pump test shows that the boreholes do not completely recover, which suggests that the aquifer recharging these boreholes is of limited extent. This may be due to the borehole's lying in a first order catchment or due to the existence of a poorly connected discrete fracture zone.

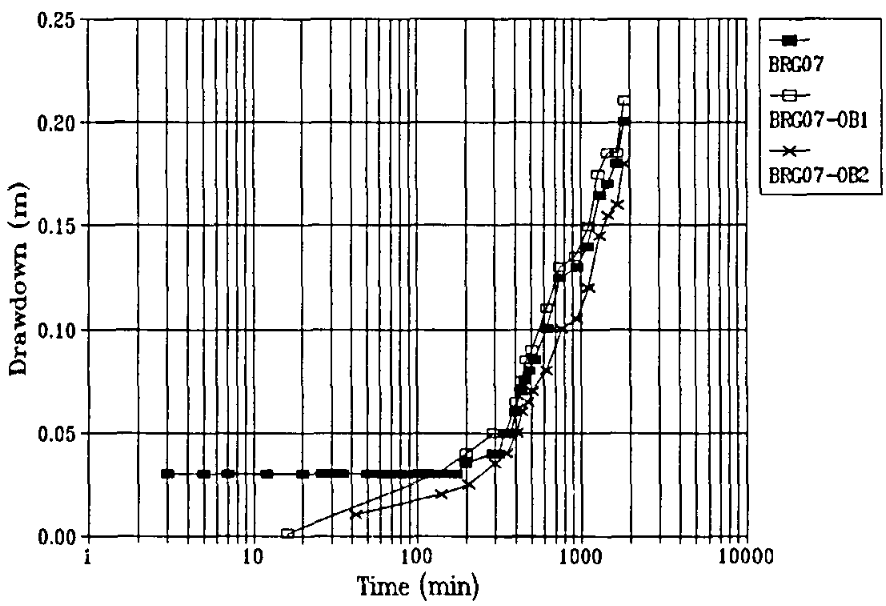


Figure 10.10 Pump test drawdown for borehole BRG07, BRG07-OB1 and BRG07-OB2.

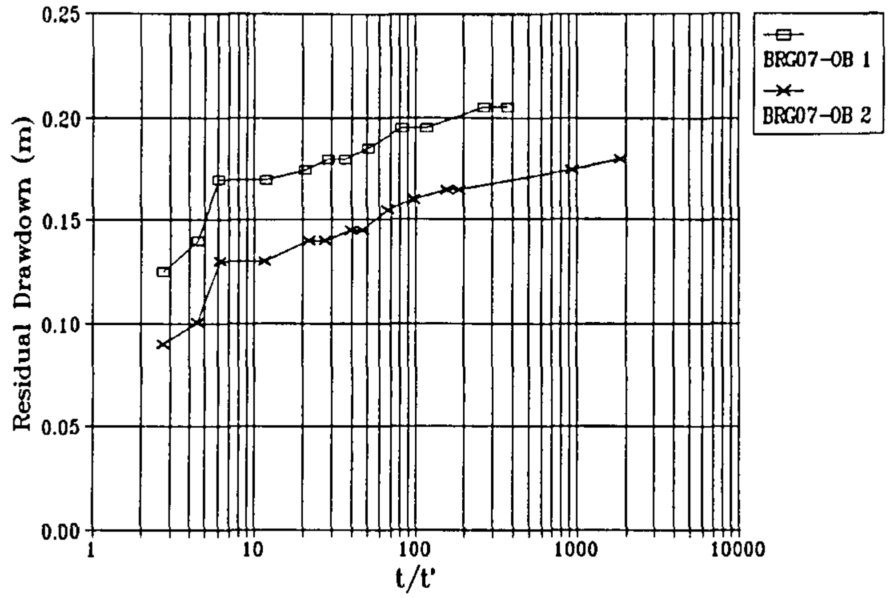


Figure 10.11 Pump test recovery for borehole BRG07-OB1 and BRG-OB2.

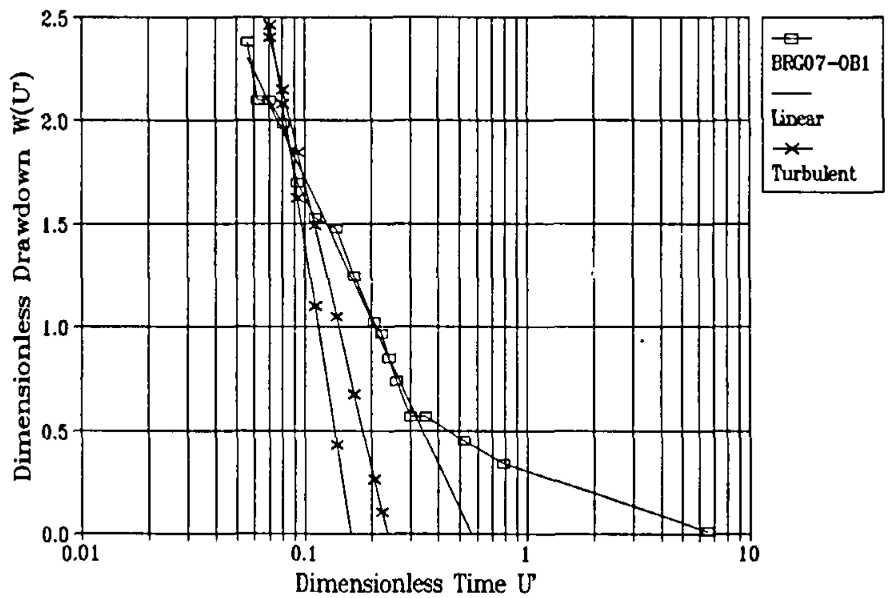


Figure 10.12 Pump test dimensionless time and drawdown for BRG07-OB1.

**10.6 Groundwater chemistry and geochemical processes.**

Groundwater chemical and environmental isotope data, the origin of dissolved salts and the geochemical evolution of groundwater are discussed in detail in a paper by Sami (1992) and in section 2.5 of the main report and are therefore only summarized here. Groundwater is predominantly of the Na-Cl type, with Na and Cl concentrations ranging from 4-19 and 3-22 millimoles $l^{-1}$ respectively. Na/Cl ratios vary between 0.58 and 1.49, generally decreasing with increasing salinity. Ca and Mg concentrations are below 5 millimoles $l^{-1}$. The groundwater $^{18}O$-$^{2}H$ relationship has a slope of 5.43, which implies that the water has been subject to evaporative enrichment prior to deep percolation. Variations in isotopic and chemical composition over relatively small distances imply that groundwater is not well mixed, confirming the existence of discrete fracture zones. Chemical and isotopic relationships suggest that dissolved Cl is primarily of meteoric origin and that brackish conditions cannot be attributed to mixing with connate water of marine origin, as has been previously suggested (Tordiffe, 1978). The uniquely metoric origin of Cl permits this ion to be used as a tracer whose concentration reflects mean annual recharge. Subsequent geochemical evolution is predominantly characterised by cation exchange, with Na in solution being exchanged for bound Ca and Mg from the clays in the aquifer matrix. The dissolution of the aquifer matrix by chemical weathering is also a prominent source of Ca and Mg, contributing between 2.5-4.5 millimoles $l^{-1}$. Chemical weathering of feldspars only contributes about 0.4 millimoles $l^{-1}$ of Na into solution.

## 11. REFERENCES


Driscoll, F.G. (1986) **Groundwater and Wells**, Second edition. Johnson Division, St. Paul, Minnesota.

Engelbrecht, G. (1991) **Characteristics of the alluvial sediments in the Bedford catchments.** Unpubl. Undergrad. thesis, Department of Geography, Rhodes University, Grahamstown.

Hensley, M. and Sami, K. (1992) **A description of the soils at selected sites in the Bedford catchments.** Unpublished report.

Hughes, D.A. and Sami, K. (1992) Transmission losses to alluvium and associated moisture dynamics in a semi-arid ephemeral channel system in southern Africa. **Hydrological Processes**, 6, 45-53.

Johnson, M.R. (1976) **Stratigraphy and Sedimentology of the Cape and Karoo Sequences in the Eastern Cape Province.** Unpubl. PhD thesis, Geology Department, Rhodes University, Grahamstown.

Kent, C.D. (1990) **A preliminary investigation into the space-time variations of rainfall events in the Bedford River catchments.** Unpubl. Hons. thesis, Department of Geography, Rhodes University, Grahamstown.

Kingsley, C.S. (1981) A composite submarine fan-delta fluvial model for the Ecca and Lower Beaufort Groups of Permian age. **Trans. Geol. Soc. S. Africa**, 84, 27-40.

Maclear, L.G.A. (1987) **A Hydrogeological Investigation of the Nyara River Catchment Near Bedford.** Unpubl. Hons. thesis, Department of Geography, Rhodes University, Grahamstown.

Patrick, N.A. (1989) **The effect of storm patterns on runoff.** Unpubl. MSc thesis, Faculty of Engineering, University of the Witwatersrand, Johannesburg.

Reinders, F.B., Louw, A.A. (1984) **Infiltration: Meassurement and Use.** Division of Agricultural Engineering, Department Agricultural Technical Services, Silverton, Republic of South Africa.

Sami, K. (1991) Modelling groundwater recharge in semi-arid environments. **Proceedings of the Fifth South African National Hydrological Symposium, Stellenbosch.**

Sami, K. (1992) Recharge mechanisms and geochemical processes in a semi-arid sedimentary basin, eastern Cape, South Africa. **Journ. Hydrol.** (In press).

Sami, K. (1992) Locating high-yielding boreholes in fractured Karoo aquifers. (Submitted for publication to **Water SA**).

Sen, Z. (1990) Dimensionless straight-type lines for aquifer tests. **J. Hydr. Engrg.**, 116 (9), 1145-1156.

Tankard, A.J., Jackson, M.P.A., Erikson, K.A., Hobday, D.K., Hunter, D.R., Mister, W.E.L. (1982) **Crustal Evolution of Sothern Africa.** Springer-Verlag, New York.

Tordiffe, E.A. W. (1978) **Aspects of the Hydrogeochemistry of the Karoo Sequence in the Great Fish River Basin, Eastern Cape Province, with Special Reference to the Groundwater Quality.** Unpubl. PhD thesis, University of the Orange Free State,Bloemfontein.

Truswell, J.F. (1977) **The Geological Evolution of South Africa.** Purnell, Cape Town.

# LOCATING HIGH-YIELDING BOREHOLES IN FRACTURED KAROO AQUIFERS

K. Sami
Institute for Water Research
Rhodes University
P.O. Box 94
Grahamstown 6140, South Africa

## ABSTRACT

Boreholes in a sandstone and mudstone aquifer were classified according to their position relative to structural features identified on a photogeologic map. The yield distributions of boreholes adjacent to dolerite or in the vicinity of changes in bedding dip along the dip or along the strike where significantly higher than the yield distribution of boreholes located where no structural deformation could be observed. No statistical difference was found between the yield distributions of boreholes located adjacent to faults or along fold axes and that where there is no observed deformation. No correlation was observed between yield and the saturated depth of the aquifer penetrated by boreholes, suggesting that well productivity is primarily dependent on the permeability of intercepted fractures not on the area of the saturated seepage face. Yields from boreholes located in higher order catchments were also considerably greater than yields in first and second order catchments. Yield probability curves have been derived for the different structural features. These show that locating boreholes adjacent to dolerite intrusions or changes in bedding dip increases the chances of drilling a successful borehole. The identification of these features from airphotos, therefore provides an economical means of locating boreholes without expensive geological surveys.

**Introduction**

More than 80% of South Africa's area is underlain by rocks with extremely low porosities and primary permeabilities, thereby restricting the occurrence of groundwater. Abstraction from these aquifers is limited to zones within 50 m of the surface where weathering and deformation processes have imparted a secondary permeability. The quantity of water capable of being abstracted from these fracture zones is dependent on the regional inter-connectedness of fractures and is usually very limited. Secondary permeabilities are highly variable and few boreholes are capable of yields greater than a few litres per second for any length of time. In spite of the limited exploitation potential of these aquifers, the scarcity of surface water supplies has caused 90% of South Africa's geographical area to be predominantly dependent on groundwater. Borehole water is used primarily for domestic water supply and stock-watering, however, many towns and small irrigation plots are also dependent on groundwater. It has been estimated that irrigation from boreholes is growing at 4.9% per annum and that 105 towns are exclusively dependent on groundwater (Dept. of Water Affairs, 1986). With the increasing pressure on surface water supplies, the growth in the utilization of groundwater is expected to continue.

Except for a few regions that have experienced over-pumping, it is generally acknowledged that groundwater resources have not yet been fully exploited and that possibilities exist for substantial increases in the current rates of abstraction (DWA, 1986). Increased exploitation will depend on identifying well connected and sufficiently permeable fracture zones where groundwater can be economically abstracted. Further development, however, is hampered by several factors:

- Water legislation which classifies groundwater as being privately owned, with the right of use restricted to the landowner.
- The limited knowledge of storage capacities and of the spatial and temporal distribution of recharge in most of the country's aquifers.
- A lack of hydrogeologic data, which results in the largely intuitive or haphazard siting of boreholes. Consequently, a larger than necessary percentage of boreholes are dry or of low yield and aquifers ares not exploited to their full potential.

Although current research is attempting to quantify recharge and the exploitation potential of aquifers, given the legal status of groundwater, the onus for its development will remain on individuals or local councils for the near future. Expensive hydrogeologic surveys are therefore not an economically feasible means of locating potential abstraction zones and siting boreholes. Inexpensive methods, such as photogeologic surveys, which are not dependent on frequently unavailable data provide a more cost effective alternative to locating boreholes for farmers and town councils.

The objectives of this paper are to determine which structural features whose surface manifestations are identifiable from aerial photographs are associated with significantly higher borehole yields in a fractured sedimentary aquifer. The paper will also investigate the increases in yield probabilities which result from drilling in the vicinity of these features.

**Study Area**

A 665 km$^2$ semi-arid research catchment, located 150 km from the coast in the Great Fish River Basin of the Eastern Cape Province, is being monitored by the Institute for Water Research at Rhodes University (Fig. 1). The catchment surrounds the town of Bedford at the foot of the Great Escarpment. The topography is one of rolling hills and ridges with gentle slopes (less than 8%) over more than 80% of the area. Local relief varies between 90 m and 150 m. Surface drainage consists a dendritic system of ephemeral channels developed on bedrock with occasional alluvial or colluvial patches.

The soils are predominantly sandy clay loams, clay loams and sandy loams and are of an alkaline nature. The depth of weathered material varies from less than 50 mm to 400 mm on the hillslopes, and up to 6 m in some valley bottoms. Infiltration capacities tend to be fairly low (less than 10 mm/hour), due to surface crusting. As a result, Hortonian overland flow is frequently observed, even during low intensity rainfall. Caliche nodules are often encountered in soils where significant infiltration occurs. The vegetation is classified as Grasslands with False Thornveld in the valley bottoms. Significant tracts have also been converted to Karoo or Acacia karoo thicket due to overgrazing. The mean annual rainfall is approximately 460 mm. Annual potential evaporation (based on regionalised Symons pan figures) is of the order of 1400 mm. The type of rainfall varies between short duration, high intensity convective storms mainly occurring during summer, to longer duration events of variable intensity and total depth which can occur at any time of the year. The latter, when associated with a low pressure cell over the interior and high pressure cells over the oceans to the south, are the major cause of high rainfalls and consequent widespread channel flow. During other rainfall events channel flow is observed to be highly localised, if indeed it occurs at all (Hughes and Sami, 1991). Numerous farm dams have been constructed to retain stormwater. The regional long term runoff coefficient is 3.19% (Tordiffe 1978). Surface drainage is thus an insignificant component of the long term water budget.

Land use is restricted to grazing by cattle, sheep, goats and small to medium sized game. Limited irrigation using groundwater is also practised in some valley bottoms.

**Geology**

The catchment is underlain by upper Permian age sandstones and mudstones of the Middleton Formation, as well as by subsequent intrusions of Jurassic dolerites. Its southern edge lies near the approximate northern boundary of the underlying Koonap Formation, while the northern boundary is located in the transition to the Balfour Formation. Together these 3 Formations make up the Adelaide Sub-Group of the Beaufort Group of sediments in the Karoo Sequence, a sequence which occupies more than 50% of South Africa. Roughly 60% of the catchment has not yet been mapped by the Geological Survey of South Africa and rock exposures and outcrops are generally sporadic and fragmentary, making geological observation difficult. As a result, available geological information is of a generalized nature, or based on interpretation from the 1:20 000 air photos.

The Middleton Formation consists of alternating cycles of fine-grained, massively bedded, lithofeldspathic sandstone of variable lateral extent fining upward into mudstone. Sandstone lithosomes vary from less than 1 m to 7 m in thickness with thinner beds being more abundant and represent 30-40% of the Formation (Johnson, 1976).

The Cape Orogeny which began in the early Triassic subjected the Middleton Formation to a directed stress from the south. The stress was insufficient to cause significant deformation and only minor folding and faulting are evident in the catchment. This tectonic uplift gave the strata a gentle dip to the North of less than 3° in the northern half of the catchment and between 4-20° in the southern half.

During the Jurassic period, the sediments were intruded by East-West trending basaltic dolerite dykes which exploited zones of weakness in the sedimentary structure (Truswell, 1977). The two major dolerite dykes in the catchment have a poor surface expression in the catchment. In places, however, they create small escarpments or ridges where the adjacent mudstones have been weathered away. Where the adjacent country rock consists of sandstone, the influence of dolerite is not as distinct. Because of the brittle deformation which often results from such intrusions, it is likely that fracture zones exist in the vicinity of these dykes.

Although rock outcrops are rare, bedding planes are readily observed on the aerial photos. Due to its more resistant nature, sandstone often dominates the topography. The aerial photos show that where the sandstone lenses pinch out, the underlying mudstone has been eroded away. As the result, the topography is dominated by gently sloping hills and ridges capped by sandstone lens, with underlying sandstone beds creating breaks in the slope.

As these rocks are dense and have undergone severe compaction, groundwater is restricted to joints and fracture zones. The confining conditions caused by massive blocks of unfractured rock suggest that water levels represent a piezometric surface rather than a water table. Rest water levels vary between 5 m and 35 m below the surface, with a hydraulic gradient to the south-east.

Little is known about the geohydrology of the area, however, transmissivities measured in fractured Karoo rocks generally range from 5 to 150 $m^2$/day (Reynders et al. 1985, Kirchner and Van Tonder 1990, Hughes and Sami 1991). Storage coefficients range from 0 to $10^{-4}$. Total dissolved solids in groundwater vary between 1000 and 2500 mg $l^{-1}$. Dissolved salts are of primarily meteoric origin and their spatial variations, reflect variations in recharge (Sami, 1992).

**Research Framework and Methodology**

Photogeologic mapping of the catchment (Geomap SA, 1966) has identified 2 east-west trending dolerite dykes and 1 dolerite sill in the north (Fig. 2). These intrusions are common in Karoo aquifers and experience has proven that their location is associated with high-yielding boreholes due to the fracturing they have caused in the adjacent country rock.

It was hypothesized that increased yields could also be associated with fracturing other deformation features, such as fold axes and faults. Since the strata in the vicinity of dip changes may also be geologically stressed, bedding dips were classified into 3 categories (Fig. 2) and the boundaries between these dip categories where also postulated as being potential fracture zones.

The research was designed to test whether statistically significant higher yields are associated with boreholes located in the vicinity of these observed structural deformations. Data on borehole yields and depth were collected by a survey of local landowners. Such records are the only available data for most aquifers in region.

When using such data, several limitations must be kept in mind. First, the data do not represent a random survey of the aquifer's flow parameters since boreholes tend to be preferentially sited in valley bottoms and along stream channels, where experience has shown that higher yields are expected (e.g. LeGrand, 1967). Secondly, the data may underestimate the frequency of dry or very low-yielding holes, since landowners may neglect to record the presence of these holes, or may not be aware of those which were drilled prior to their ownership. The data set, therefore, only provides an estimate of the yield distribution achieved by the drillers' siting methods. These methods range from water divining to intuition based on local experience.

According to their location on the photogeologic map, boreholes were classified into six geologic categories related to observed structural features: in the vicinity of a dolerite intrusion (Dolerite), a fault (Faults), a fold axis (Folds), an increase or decrease in dip along the dip (Dd), an increase or decrease in dip along the strike (Ds), or no observable structural deformations (Nsd). Statistical tests were conducted to determine whether the yield distributions of these structural categories were significantly different. Further tests were carried out to test the influence of saturated depth of the aquifer penetrated, bedding dip, and Strahler catchment order which was used as an index of a borehole's potential catchment area. Yield-probability relationships were then derived for each of the groupings identified as being statistically significant. These were compared to the results achieved by drillers in order to quantify whether probable yields could be increased.

**Yields and geological influences**

A cumulative distribution curve of borehole yields for each of the six defined structural categories is shown in figure 3. The summary statistics of these distributions are presented in table 1. These distributions were compared using the Kolmogorov-Smirnov non-parametric test to identify wether they were statistically different at the 5% level. These results, shown in table 2, suggest that yields from boreholes located in the vicinity of fold axes and faults are not significantly greater than those located in non-deformed beds, although this may not be conclusive since too few boreholes were located near faults. Any fracturing of the aquifer which arises from these deformation processes is therefore not likely to significantly affect the permeability of the aquifer. Boreholes located in the vicinity of dolerite, or where there is an observable change in bedding dip, have significantly higher yields than non-deformed beds. Furthermore, except for those located directly on dolerite, boreholes in these categories always struck water. These features are therefore associated with significant fracturing or structural weaknesses which increase aquifer permeabilities. Dip changes along the strike and along the dip do not appear to produce significantly different yield distributions, hence they probably result in a similar intensity of fracturing.

To determine whether differences in the mean saturated depth of the aquifer penetrated by boreholes in each category could have influenced these yield distributions, student's t difference of mean tests were performed. The mean saturated depths (table 3) of the six categories were not statistically significant at the 5% level. Furthermore, neither borehole depth nor saturated depth were significantly correlated to yields (table 4) when all boreholes were considered or when structural effects were neutralised by only considering boreholes where no deformation has occurred. The low correlations suggest that borehole depths do not affect yields, implying that massive blocks of the aquifer do not transmit any water. Productivity is therefore dependent on the permeability of discrete fracture zones intercepted by boreholes and not on the area of the saturated seepage face.

To determine whether bedding dip influences yields, yields from boreholes in each of the three dip categories and near no observable structural deformations were compared (table 5). A K-S analysis determined that there was no significant difference in the cumulative yield distributions. Variations in the uplifting of these beds has therefore not resulted in an increased intensity of fracturing.

The summary statistics of yield distributions according to catchment order for boreholes near no structural deformations are shown in table 6. A K-S analysis of these distributions showed that, in general, there were significant differences in yield at the 5% level (table 7). The results suggest that the variability between the distributions of the first order and second order catchments is not significant, however, yields from these catchment orders are significantly lower than boreholes in higher catchment orders. The fact that boreholes in fourth order catchments are significantly higher than those in third order catchments while those in fifth order ones are not, may be attributed to too few observations from catchments above a third order. In general, however, higher yields can be expected from boreholes as the potential catchment area increases. This increase might also reflect the fact that increasing stream order could be an index of the erodability and potential fracturing of the rock, since streams tend to develop along the axes of structural weaknesses in the underlying geology.

To determine whether yield variations related to catchment order could have contributed to the observed differences in the yield distributions between different structural groups, catchment order frequencies for each group were tabulated (table 8) and compared using Chi-squared tests (table 9). Except for the dolerite and Ds category, there was little deviation in the catchment order composition between the structural classes. This suggests that yield variations due to catchment order differences did not greatly bias the structural yield distributions. Therefore, the differences in yield distribution pertaining to the effects of structural deformation previously identified remain valid. The large percentage of boreholes in higher catchment orders in category Ds may explain the unexpectedly high mean yields in that category (table 1 and Fig. 3).

**Yield-probability assessment**

Statistical analyses has suggested that structural influences have resulted in three significant yield distributions, with yields from boreholes in the vicinity of dolerite differing from those in the vicinity of bedding dip changes and from those where little fracturing has occurred. The probability of obtaining a required yield would therefore be different in each of these structural categories. It can also be expected that catchment order would further affect these yield probabilities.

Theoretical probability curves of expected yield were derived for each of the three statistically different structural distributions. These curves were derived from theoretical log-normal distributions based on the statistics of observed yields (table 1). A sub-division of each category by catchment order was limited to two classes due to the limited number of observations. By comparing these curves to the yield probabilities achieved by drillers, represented by the yield distribution of existing boreholes, the potential to increase the probability of achieving successful boreholes were quantified.

The yield probabilities for first and second order catchments are shown in figure 4 and those for higher order catchments in figure 5. There does not appear to be a higher yield probability by locating boreholes next to dolerite in lower order catchments. This may be due to the risk of drilling into dolerite, since dolerite boundaries may be difficult to detect in headwater regions where weathering has not exposed its configuration or when the direction of the dyke's dip is unknown. In addition, the country rock of such regions may consist of rocks which have been baked during the intrusion of the dyke, thereby reducing the intensity of fracturing and causing the rock to be more resistant to weathering. Furthermore, if the direction of the dyke's dip is not known, boreholes may not penetrate the weathered zone or may be located so that the impermeable dyke cuts off the borehole's potential recharge area. In comparison, siting a borehole in the vicinity of a change in dip increases the yield probability relative to other features. The fracturing present in these regions reduces the chance of striking a dry hole ($< 0.02\ l\ s^{-1}$) to less than 2%, compared to about 18% in other areas. The probability of a successful domestic borehole ($> 0.14\ l\ s^{-1}$) increases from 60% to 93%, whereas that of striking a high-yielding municipal production borehole ($> 5\ l\ s^{-1}$) increases from 13% to 24%. The identification of regions where bedding dip changes can, therefore, greatly increase the potential yield of a borehole and reduce the risk of borehole failure.

The siting of boreholes in higher order catchments further increases the yield probability and can result in a higher success rate than that currently achieved by drillers. The probability of striking a dry hole in these areas is less than 10%, and less than 1% in the vicinity of dip changes. This represents a slight improvement over the approximately 4% failure rate by drillers in these catchments. Successful domestic boreholes may be achieved with a minimum probability of 70%, rising to 90% and 97% in the vicinity of dolerite and dip changes respectively. The probability of success for a production boreholes is between 20% and 31%. For higher yields, siting boreholes adjacent to dolerite intrusions produces only a marginally higher yield probability.

**Conclusions**

Boreholes located in the catchment were classified according to structural geologic features identified by photogeologic survey and hypothesised as being potential fracture zones. The influence of borehole depth, saturated depth, bedding dip and catchment order on yield distributions were also examined. Several of these parameters were found to be associated with high yielding boreholes:

1) Boreholes adjacent to dolerite intrusions and regions of changes in the bedding dip angle identifiable from air photos have significantly higher yields than boreholes located in fold axes or were no structural deformation was observed. Furthermore, these boreholes always struck water, whereas many dry holes were encountered in non-deformed beds, along folds or faults. This confirms that air photos can be used to identify regions were higher yielding boreholes can be expected.

2) Borehole yields showed no correlation with depth or saturated depth penetrated. Yields are therefore not dependent on the seepage face, but rather on the permeabilities of intercepted fractures. Since fractures tend to decrease with depth, this suggests that the practice of drilling to great depths to increase yield is uneconomical.

3) Differences in bedding dip did not result in any significant variations in yield distribution.

4) Boreholes located along channels of increasing catchment order were found to be associated with higher borehole yields. This may attributed to the increasing contributing area or to the structural weaknesses followed by larger order stream channels.

5) Higher yield probabilities than those achieved by drillers and lower probabilities of a dry hole can be achieved by siting boreholes in the vicinity of changes in bedding dip, or in the vicinity of dolerite in higher order catchments where its configuration can be defined and recharge to the borehole is not cut off by the intrusion. The identification of these regions from aerial photographs as preferential drilling sites will therefore result in a higher yield probability than that currently achieved by drillers.

**Acknowledgements**

Funds for the research were provided by the Water Research Commission of South Africa as part of a research contract to the Institute for Water Research. The survey of local landowners was conducted by C. Langton and A. Murdoch. Helpful editorial comments were provided by Dr. D.A Hughes.

## References

Department of Water Affairs (1986). Management of the Water Resources of the Republic of South Africa. CTP Book Printers, Cape Town.

Geomap SA Geneve (1966). Photogeologic Map 3226C.

Hughes, D.A. and Sami, K. (1991). The Bedford Catchments. An Introduction to Their Physical and Hydrological Characteristics. WRC Report No. 138/1/91. Water Research Commission, Pretoria, South Africa.

Johnson, M.R. (1976). Stratigraphy and Sedimentology of the Cape and Karoo Sequences in the Eastern Cape Province. Unpubl. PhD thesis, Geology Department, Rhodes University, Grahamstown.

Kirchner, J. and Van Tonder, G.J. (1990). Exploitation Potential of Karoo Aquifers. WRC Report 170/1/91. Water Research Commission, Pretoria, South Africa.

LeGrand, H.E. (1967). Groundwater of the Piedmont and Blue Ridge Provinces of the southeastern States. U.S. Geologic Survey. Circular 538.

Reynders, A.G., Moolman, J.H. and Stone, A.W. (1985). Water level response in fractured rock aquifers underlying irrigated lands - a study in the lower Great Fish river valley. Water SA, 11 (2): 93-98.

Sami, K. (1992). Recharge mechanisms and geochemical processes in a semi-arid sedimentary basin, eastern Cape, South Africa. J. Hydrol., (In press).

Tordiffe, E.A.W. (1978). Aspects of the Hydrochemistry of the Karoo sequence in the Great Fish River Basin, Eastern Cape Province, with Special Reference to the Groundwater Quality. Unpubl. Ph.D. thesis. Department of Geology, University of the Orange Free State.

Truswell, J.F. (1977). The Geological Evolution of South Africa. Purnell, Cape Town.

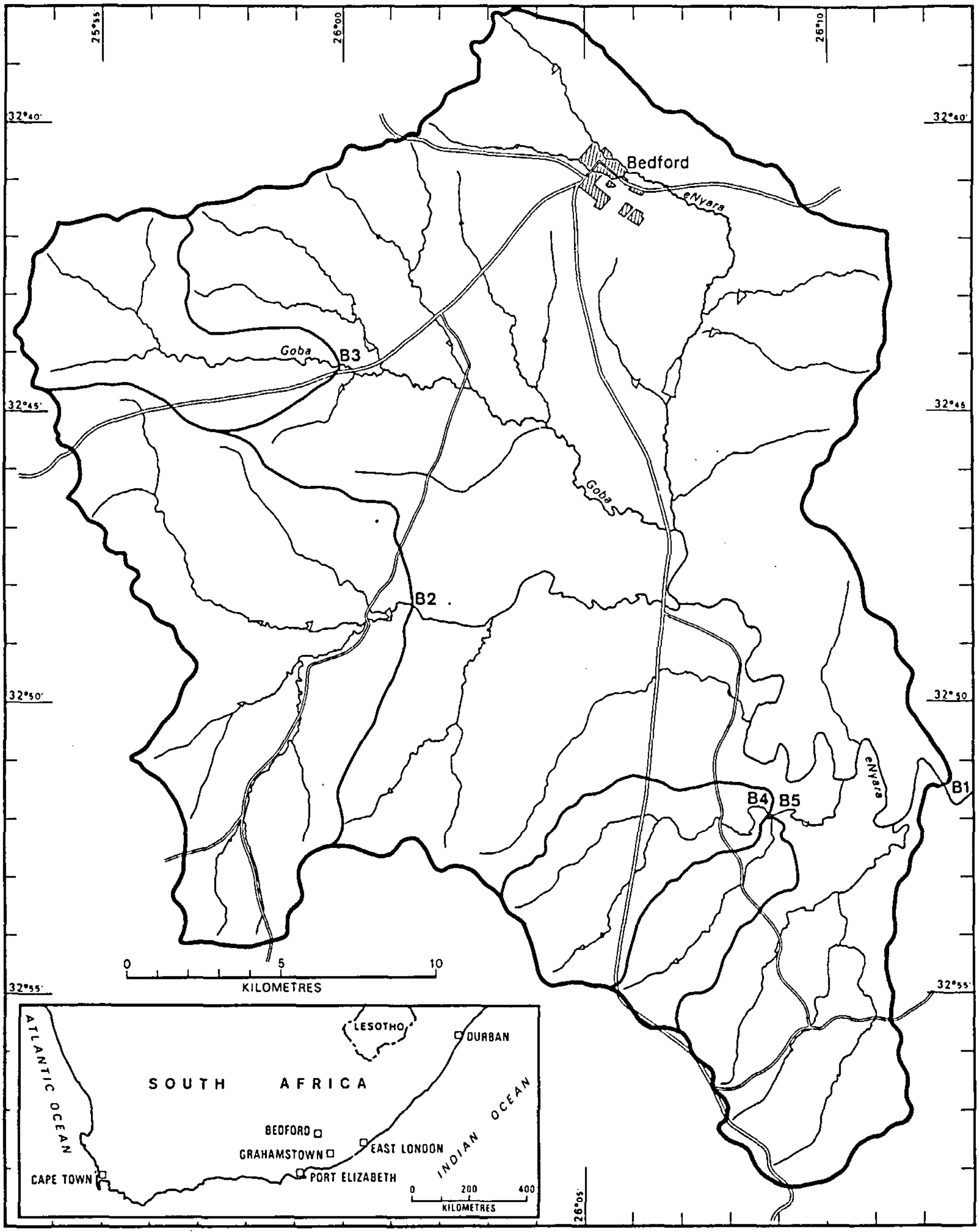


Figure 1. Location of the Bedford research catchment.

Table 1. Summary statistics of borehole yields in l $s^{-1}$ according to their photogeologic classification.

| | Dolerite | Folds | Dd | Ds | Faults | Nsd | Total |
|---|---|---|---|---|---|---|---|
| Sample size | 49 | 28 | 21 | 23 | 10 | 108 | 240 |
| Mean | 4.452 | 1.493 | 3.980 | 6.521 | 1.681 | 1.375 | 2.756 |
| Median | 1.135 | 0.378 | 3.783 | 3.783 | 0.694 | 0.504 | 0.631 |
| Std. deviation | 7.986 | 2.494 | 3.996 | 8.089 | 2.180 | 2.277 | 5.153 |
| Std. error | 1.141 | 0.471 | 0.872 | 1.687 | 0.689 | 0.219 | 0.333 |
| Minimum | 0 | 0 | 0.063 | 0.189 | 0.252 | 0 | 0 |
| Maximum | 27.744 | 7.567 | 12.611 | 27.744 | 6.306 | 12.611 | 27.744 |
| Lower quartile | 0.278 | 0 | 0.63i | 0.757 | 0.353 | 0.178 | 0.252 |
| Upper quartile | 3.153 | 1.513 | 5.297 | 10.089 | 1.892 | 1.261 | 2.522 |

Table 2. Significance of the difference between the yield distributions of the six structural categories at the 5% level.

| | Dolerite | Folds | Dd | Ds | Faults |
|---|---|---|---|---|---|
| Folds | Yes | | | | |
| Dd | Yes | Yes | | | |
| Ds | No | Yes | No | | |
| Faults | No | No | No | No | |
| Nsd | Yes | No | Yes | Yes | No |

Table 3. Summary of the saturated depths (meters) of boreholes in each of the structural categories.

| | Dolerite | Folds | Dd | Ds | Faults | Nsd | Total |
|---|---|---|---|---|---|---|---|
| Sample size | 36 | 18 | 18 | 17 | 8 | 66 | 163 |
| Mean | 94.646 | 93.278 | 90.000 | 69.059 | 84.5 | 83.856 | 86.446 |
| Median | 95 | 60 | 80 | 60 | 73 | 79 | 80 |
| Std. deviation | 30.263 | 122.755 | 43.718 | 28.519 | 44.776 | 48.098 | 55.956 |

Table 4. Correlation coefficients between yields and depths when structural influences are neglected by considering all boreholes when they are neutralised by only considering boreholes near no near no structural deformations.

| All boreholes | Depth | Sat. depth |
|---|---|---|
| Cor. coeff. | -0.156 | 0.060 |
| Sample size | 194 | 163 |
| Sig. level | 0.315 | 0.446 |
| No observed deformations | | |
| Cor. coeff. | 0.237 | 0.146 |
| Sample size | 86 | 66 |
| Sig level | 0.028 | 0.244 |

Table 5. Borehole yields ($l\ s^{-1}$) in each of the defined bedding dip categories.

| Bedding dip | 0-$3^0$ | 4-$10^0$ | 11-$25^0$ |
|---|---|---|---|
| Sample size | 28 | 60 | 20 |
| Mean | 0.990 | 1.258 | 2.073 |
| Median | 0.504 | 0.441 | 0.694 |
| Std. deviation | 1.400 | 2.349 | 2.703 |
| Lower quartile | 0.189 | 0.126 | 0.328 |
| Upper quartile | 0.946 | 1.009 | 3.684 |

Table 6. Borehole yields ($l\ s^{-1}$) by catchment order.

| Order | 1 | 2 | 3 | 4 | 5 |
|---|---|---|---|---|---|
| Sample size | 31 | 43 | 21 | 7 | 7 |
| Mean | 0.525 | 1.257 | 1.415 | 3.891 | 3.387 |
| Median | 0.252 | 0.504 | 0.757 | 3.783 | 1.892 |
| Std. deviation | 1.012 | 2.146 | 1.857 | 2.936 | 4.388 |
| Lower quartile | 0 | 0.189 | 0.378 | 0.378 | 0.631 |
| Upper quartile | 5.555 | 0.757 | 1.513 | 6.306 | 5.044 |

Table 7. Significance of the difference between yield distributions in each catchment order at the 5% level.

| Order | 1 | 2 | 3 | 4 |
|---|---|---|---|---|
| 2 | No | | | |
| 3 | Yes | Yes | | |
| 4 | Yes | Yes | Yes | |
| 5 | Yes | Yes | No | No |

Table 8. Number of boreholes in each in each structural and catchment order category.

| Order | 1 | 2 | 3 | 4 | 5 |
|---|---|---|---|---|---|
| Dolerite | 12 | 13 | 6 | 16 | 2 |
| Folds | 12 | 5 | 7 | 4 | 0 |
| Dd | 5 | 8 | 6 | 1 | 1 |
| Ds | 3 | 4 | 6 | 8 | 2 |
| Faults | 3 | 2 | 5 | 0 | 0 |
| Nsd | 31 | 43 | 21 | 7 | 7 |
| Total | 66 | 75 | 51 | 36 | 12 |

Table 9. Significance of the difference of the catchment order distribution between structural groups at the 5% level.

| | Dolerite | Folds | Dd | Ds | Faults |
|---|---|---|---|---|---|
| Folds | No | | | | |
| Dd | No | No | | | |
| Ds | No | No | Yes | | |
| Faults | No | No | No | No | |
| Nsd | Yes | No | No | Yes | No |

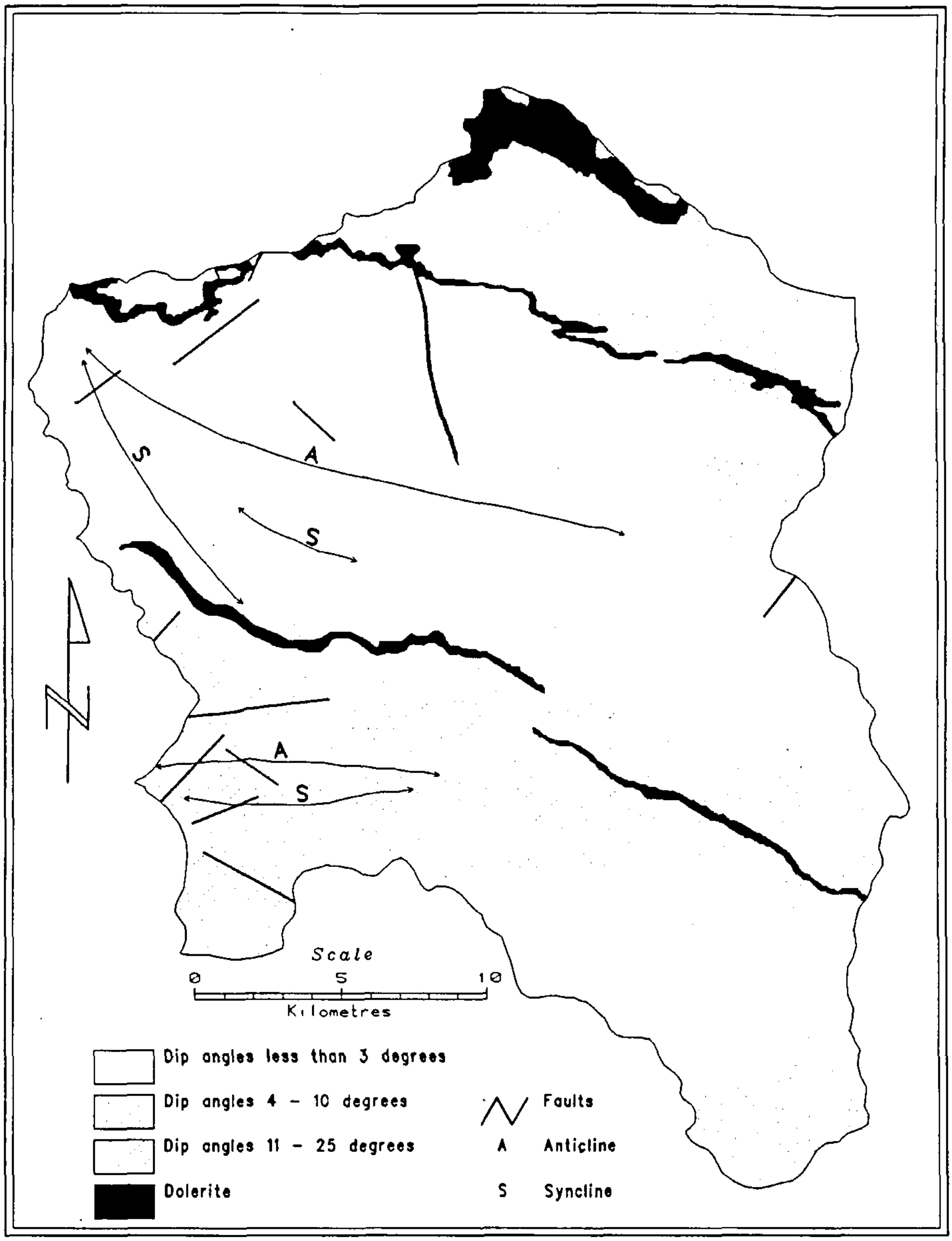


Figure 2. Structural geological map of the Bedford catchment.

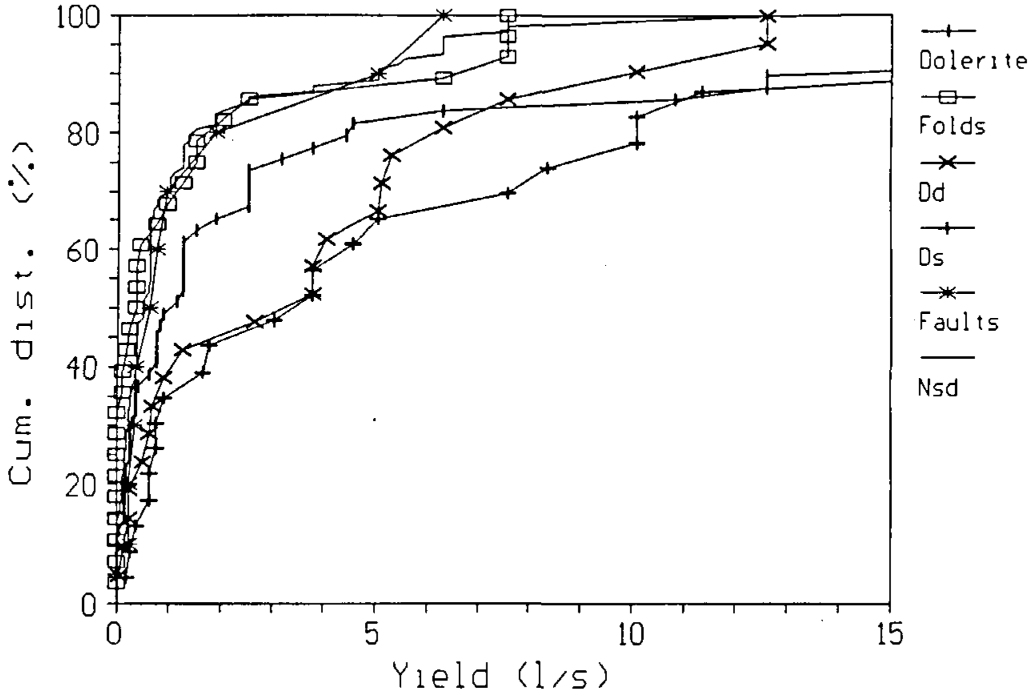


**Figure 3. Cumulative distribution curves of borehole yields in the six identified structural categories.**

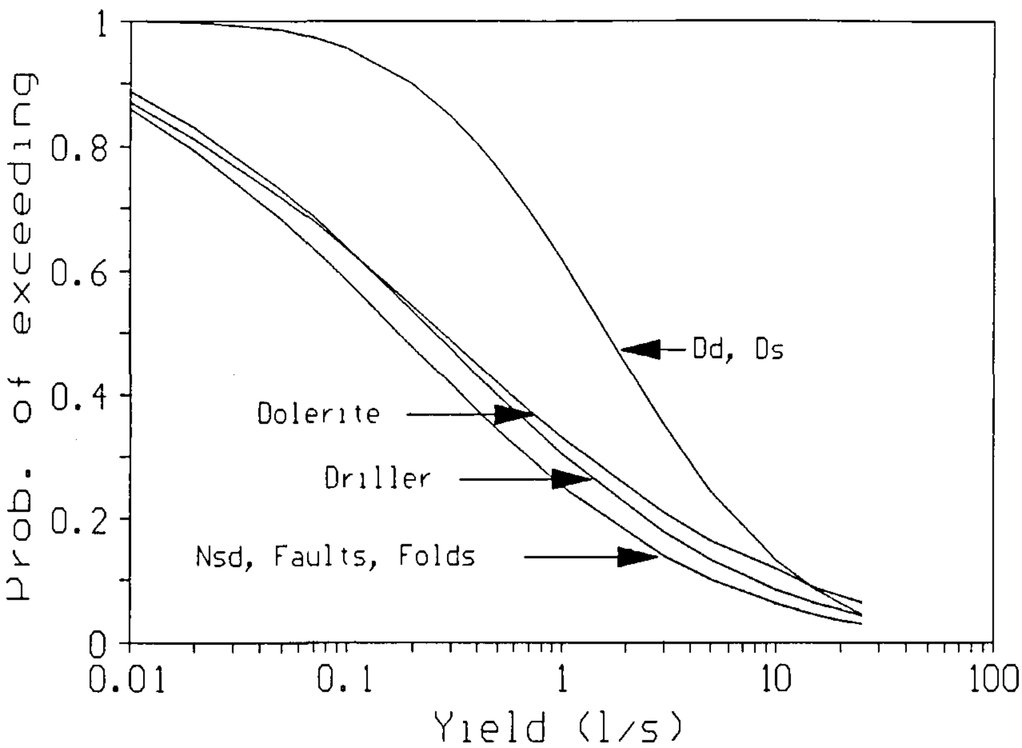


**Figure 4. Yield probability curves for first and second order catchments.**

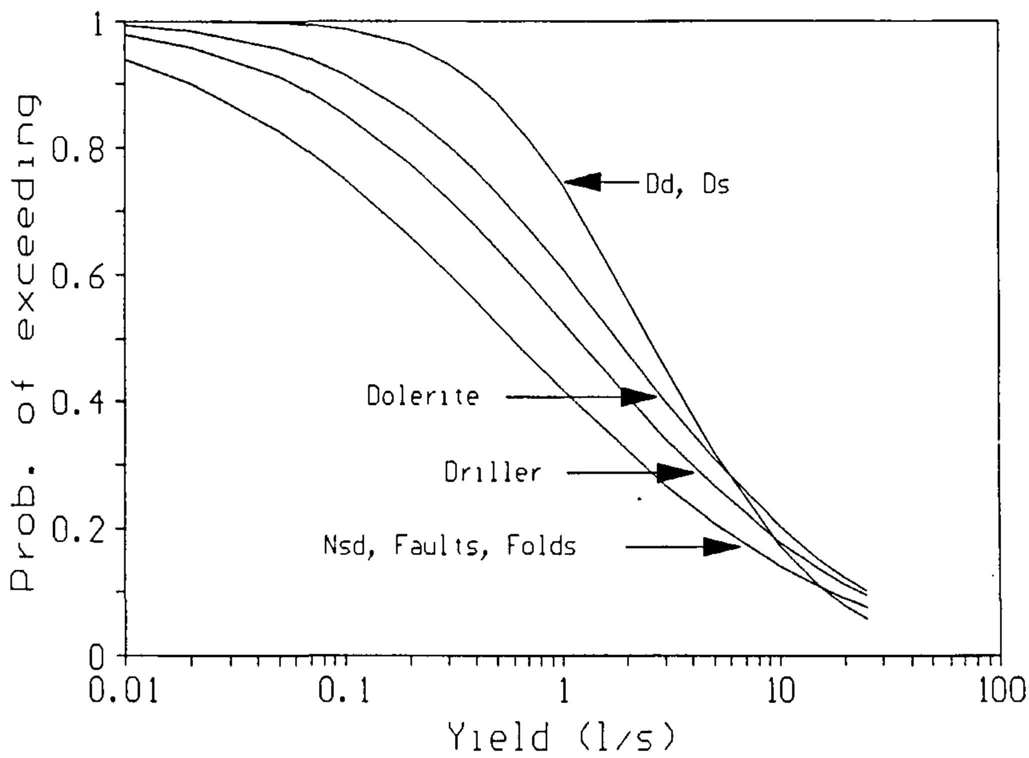


**Figure 5. Yield probability curves for third, fourth and fifth order catchments.**

## APPENDIX B : List of vegetation species found in Bedford catchments.

Table B1.1 Species expected to occur under natural conditions.

| | Botanical Name | Common Name |
|---|---|---|
| Grasses | *Themeda triandra* | Rooigras |
| | *Eragrostis chloromelas* | |
| | *Digitaria argyrograpta* | |
| | *Microchloa caffra* | |
| | *Heteropogon contortus* | Spear grass |
| | *Erigrostus obtusa* | |
| | *Tragus koelerioides* | |
| | *Cymbopogon plurinodis* | Turpentine grass |
| | *Sporobolis fimbriatus* | Dropseed grass |
| | *Cynodon incompletus* | |
| | *Panicum stapfianum* | Stap's Buffalo grass |
| | *Eustachyus paspaloides* | |
| | *E. capensis* | |
| | *E. curvula* | |
| Karoo Forbes | *Felicia muricata* | |
| | *Pelargonium sidifolium* | |
| | *Helichrysum rugulosum* | |
| | *H. dregeanum* | |
| | *Anthericum sp.* | |
| | *Blepharis integrifolia* | |
| | *Mariscus dregeanus* | |
| | *Argyrolobium pauciflorum* | |
| | *Crassula capitella* | |
| | *M. capensis* | |
| | *Cyanotis speciosa* | |
| | *Cyperus usitatus* | |
| | *Hermannia incana* | |
| | *Selago triquetra* | |
| | *Hibiscus pusillus* | |
| | *Sutera pinnatifida* | |
| Trees | *Acacia karoo* | |

Table B1.2 Species under selective grazing.

| | Botanical Name | Common name |
|---|---|---|
| Grasses | *Digitaria argyrograpta* | |
| | *Erigrostus obtusa* | |
| | *Erigrostus chloromelas* | |
| | *Sporobolis fimbriatus* | Dropseed grass |
| | *Tragus koelerioides* | |
| Karoo Forbes | *Nenax microphylla* | |
| | *Sutera pinnatifida* | |
| | *Rosenia humilis* | |
| | *Euryops anthemoides* | |
| | *Selago triquetra* | |
| | *Pelargonium abrotanifolium* | |
| | *Walafrida saxatilis* | |
| | *Pentzia incana* | |
| Trees | *Acacia karoo* | |

Table B1.3 Species under continuous heavy grazing.

| | Botanical Name | Common Name |
|---|---|---|
| Grasses | *Microchloa caffra* | |
| | *Sporobolis discosporis* | |
| | *Aristida conjesta* | |
| Karoo Forbes | *Felicia muricata* | |
| | *Hermannia incana* | |
| | *Helichrysum dregeanum* | |
| Trees | *Acacia karoo* | |